The Pennsylvania State University

The Graduate School

College of Engineering

CRITICAL MEMBER REMOVAL AND LOAD REDISTRIBUTION OF A DETERIORATED TRUSS BRIDGE

A Thesis in

Civil Engineering

by

Lynsey D. Reese

Submitted in Partial Fulfillment
of the Requirements
for the Degree of

Master of Science

August 2009

The thesis of Lynsey Reese was reviewed and approved* by the following:

Daniel G. Linzell
Associate Professor of Civil Engineering
Thesis Advisor

Andrew Scanlon
Professor of Civil Engineering

Thomas E. Boothby
Professor of Architectural Engineering

Peggy A. Johnson
Professor of Civil Engineering
Head of the Department of Civil and Environmental Engineering

*Signatures are on file in the Graduate School

ABSTRACT

Serious questions surrounding the strength and stability of truss bridges and the adequacy of the aging infrastructure have arisen due to the collapses of the I-35W Bridge in Minneapolis, Minnesota and the Dysart Bridge in Cambria County, Pennsylvania. The behavior of truss bridges when a critical member is removed is at the forefront of research. Being able to understand the load redistribution as well as the global response of deteriorated truss bridges when critical members are removed needs to be fully understood to prevent any further collapses from occurring. A pristine and deteriorated model was created to determine the effects of aging and deterioration on the critical member removal and load redistribution response of a truss bridge. Key information in the analysis was the critical member (assumed to fail when it reached its yield capacity or critical buckling load), the critical load that caused the member to yield, the location of the critical load, and the failure sequence once the critical member was removed from the structure. Eight stacked side-by-side HS-20 trucks caused the pristine model to fail while a loading of seven stacked side-by-side HS-20 trucks caused the deteriorated model to fail. The member failure sequence also was different for the pristine model compared to the deteriorated model. Deterioration and aging was found to have a direct impact on the load redistribution and global failure pattern of the truss bridge.

TABLE OF CONTENTS

LIST OF FIGURES v

LIST OF TABLES vi

ACKNOWLEDGEMENTS vii

Chapter 1 Introduction 1

1.1 Background 1
1.2 Problem Statement 5
1.3 Objectives 5
1.4 Scope and Task List 6
1.5 Summary 8

Chapter 2 Literature Review 10

2.1 Truss Types 10
2.2 Progressive Collapse 12
2.2.1 Zipper-Type Progressive Collapse 12
2.2.2 Instability-Type Progressive Collapse 17
2.3 Truss Bridge Experiments 18
2.4 Modeling 21
2.4.1 General Modeling Considerations 22
2.4.2 Progressive Collapse Modeling 24
2.5 Condition Evaluation 30
2.6 Summary 32

Chapter 3 Structure Description 33

3.1 Introduction 33
3.2 Rock Creek Bridge 33
3.3 Beech Creek Veterans Memorial Bridge 37
3.4 Beech Creek Veterans Memorial Bridge Condition Evaluation 42
3.4.1 Bearings 42
3.4.2 Floor System 43
3.4.3 Truss 46
3.5 Summary 52

Chapter 4 Modeling Procedure 53

4.1 Rock Creek Bridge Pristine Model 53
4.2 Model Validation 56
4.3 Beech Creek Veterans Memorial Bridge Pristine Model 65
4.4 Examination 68
4.5 Summary 72

Chapter 5 Critical Member Analysis and Discussion 73

5.1 Introduction 73
5.2 Pristine Model 75
5.2.1 Loading 75
5.2.2 Critical Member Identification 80
5.2.3 Critical Load Location 93
5.2.4 Critical Member Removal and Load Redistribution Analysis 101
5.3 Deteriorated Model 118
5.3.1 Loading 122
5.3.2 Critical Member Identification 122
5.3.3 Critical Load Location 133
5.3.4 Critical Member Removal and Load Redistribution Analysis 137
5.4 Comparison of Pristine and Deteriorated Model 145
5.5 Conclusions 150

Chapter 6 Summary and Conclusions 152

6.1 Summary 152
6.2 Conclusions 153
6.3 Future Research 157

Bibliography 158

Appendix A Figures 161

Appendix B Tables 167

LIST OF FIGURES

Figure **1-1.** Examples of Truss Bridge Configurations: (a) Warren Truss, (b) Howe Truss, (c) Pratt Truss 2

Figure **1-2.** Pratt Truss Idealized Force Diagram 3

Figure **2-1.** Subtypes of Pratt Trusses..... 11

Figure **2-2.** Typical Detail of Eyebar Chain and Hanger Connection 14

Figure **2-3.** Mianus River Bridge Collapse..... 15

Figure **2-4**. Schematic of Pin-and-Hanger Assembly of the Mianus River Bridge 16

Figure **2-5.** Loading Pattern for Truss Bridge 28

Figure **2-6.** Schematic of Multiple HS-20 Trucks 29

Figure **3-1.** Rock Creek Bridge 34

Figure **3-2.** Typical Truss Elevation and Framing Plan, Rock Creek Bridge..... 35

Figure **3-3.** Member Cross Sections, Rock Creek Bridge 36

Figure **3-4.** Beech Creek Veterans Memorial Bridge..... 38

Figure **3-5.** Typical Truss Elevation and Framing Plan, Beech Creek Veterans Memorial Bridge 39

Figure **3-6.** Member Cross Sections, Beech Creek Veterans Memorial Bridge..... 40

Figure **3-7.** Beech Creek Veterans Memorial Bridge Condition Evaluation Identification 42

Figure **3-8.** Framing Plan, Beech Creek Veterans Memorial Bridge 44

Figure **4-1.** Truss Components 54

Figure **4-2.** Analytical Model, Rock Creek Bridge 55

Figure **4-3.** Concrete Block Geometry, Rock Creek Bridge (Azizinamini 1997) 57

Figure **4-4.** Dead Load Configuration, Elevation and Plan View, Rock Creek Bridge (Azizinamini 1997)..... 58

Figure **4-5**. Dead Load Concentrated Loads, Rock Creek Bridge..... 59

Figure **4-6.** Validation Member Designation..... 59

Figure **4-7.** Axial Force in Member 1, Rock Creek Bridge 60

Figure **4-8.** Components of Beech Creek Veterans Memorial Bridge..... 66

Figure **4-9.** Beech Creek Veterans Memorial Bridge Pristine SAP2000 Model 67

Figure **4-10.** Member Identification, Beech Creek Veterans Memorial Bridge 69

Figure **4-11.** Influence Line for Member 1004, Beech Creek Veterans Memorial Bridge..... 69

Figure **4-12.** Influence Line for Member 1012, Beech Creek Veterans Memorial Bridge..... 70

Figure **4-13.** Influence Line for Member 1021, Beech Creek Veterans Memorial Bridge..... 70

Figure **5-1**. Flowchart of Process for Evaluation of Beech Creek Veterans Memorial Bridge 74

Figure **5-2**. Standard AASHTO HS-20 Truck 76

Figure **5-3**. Minimum Side-by-Side HS20 Truck Spacing 76

Figure **5-4**. Schematic of Side-by-Side HS-20 Trucks 78

Figure **5-5**. HS-20 Trucks Traversing East to West 79

Figure **5-6**. Lane Designations 80

Figure **5-7**. North Truss Member Identification 83

Figure **5-8**. South Truss Member Identification 84

Figure **5-9**. Axial Force in Member 1012 Due to Incrementing West to East HS-20 94

Figure **5-10**. Axial Force in Member 1012 Due to Incrementing East to West HS-20 95

Figure **5-11**. Axial Force in Member 1021 Due to Incrementing West to East HS-20 95

Figure **5-12**. Axial Force in Member 1021 Due to Incrementing East to West HS-20 96

Figure **5-13**. Axial Force in Member 1040 Due to Incrementing West to East HS-20 96

Figure **5-14**. Axial Force in Member 1040 Due to Incrementing East to West HS-20 97

Figure **5-15**. Axial Force in Member 1049 Due to Incrementing West to East HS-20 97

Figure **5-16**. Axial Force in Member 1049 Due to Incrementing East to West HS-20 98

Figure **5-17**. Typical Wheel Load Distribution to Joints for HS-20 Truck 101

Figure **5-18**. Failed Members in North Truss, Critical Member 1012..... 105

Figure **5-19**. Deflected Shape, Critical Member 1012 105

Figure **5-20**. Failed Members, Critical Member 1021, North Truss 108

Figure **5-21**. Deflected Shape, Critical Member 1021 108

Figure **5-22**. Failed Member, Critical Member 1040, South Truss 111

Figure **5-23**. Deflected Shape, Critical Member 1040 111

Figure **5-24**. Failed Members, Critical Member 1049, South Truss 113

Figure **5-25**. Deflected Shape, Critical Member 1049 114

Figure **5-26**. Axial Force in Member 1012 Due to Incementing West to East HS-20 Truck .. 134

Figure **5-27**. Axial Force in Member 1012 Due to Incrementing East to West HS-20 Truck 134

Figure **5-28**. Axial Force in Member 1019 Due to Incrementing West to East HS-20 Trucks 135

Figure **5-29**. Axial Force in Member 1019 Due to Incrementing East to West HS-20 Trucks 135

Figure **5-30**. Failed Members, Deteriorated Critical Member 1012 138

Figure **5-31**. Deflected Shape, Deteriorated Critical Member 1012 138

Figure **5-32**. Failed Members, Deteriorated Critical Member 1019 141

Figure **5-33**. Deflected Shape, Deteriorated Critical Member 1019 142

Figure **5-34**. Failure Members of the Pristine Model, Critical Member 1012 148

Figure **5-35**. Failure Members of the Deteriorated Model, Critical Member 1012 148

Figure **5-36**. Failure Members of the Pristine Model, Critical Member 1021 149

Figure **5-37**. Failure Members of the Deteriorated Model, Critical Member 1019 150

Figure **A4.1** – Axial Force in Member 1, Rock Creek Bridge 161

Figure **A4.2** – Axial Force in Member 2, Rock Creek Bridge 162

Figure **A4.3** – Axial Force in Member 3, Rock Creek Bridge 162

Figure **A4.4** –Axial Force in Member 4, Rock Creek Bridge 163

Figure **A4.5** –Axial Force in Member 5, Rock Creek Bridge 163

Figure **A4.6** – Axial Force in Member 6, Rock Creek Bridge 164

Figure **A4.7** –Axial Force in Member 7, Rock Creek Bridge 164

Figure **A4.8** – Axial Force in Member 8, Rock Creek Bridge 165

Figure **A4.9** –Axial Force in Member 9, Rock Creek Bridge 165

Figure **A4.10** –Axial Force in Member 10, Rock Creek Bridge 166

LIST OF TABLES

Table **3-1**. Truss Member Cross Sectional Properties, Rock Creek Bridge 37

Table **3-2.** Member Types, Beech Creek Veterans Memorial Bridge 41

Table **3-3.** Stringer Section Loss Properties – Member W24 x 55 44

Table **3-4.** End Floorbeam Section Loss Properties – Member 36 x 150 46

Table **3-5.** Interior Floorbeam Section Loss Properties – Member 36 x 260 46

Table **3-6.** North Truss Member Properties, Section Loss of End Posts and Upper Chord Members 48

Table **3-7.** North Truss Member Properties, Section Loss of Vertical Members 49

Table **3-8.** North Truss Member Properties, Section Loss of Diagonal Members 50

Table **3-9.** North Truss Member Properties, Section Loss of Lower Chord Members 51

Table **4-1.** Material and Geometric Properties, Rock Creek Bridge (Azizinamini et al. 1997) 56

Table **4-2.** Comparison of SAP2000 and Test Results, Members 1 – 5, Rock Creek Bridge 62

Table **4-3.** Comparison of SAP2000 and Test Results, Members 6 – 10, Rock Creek Bridge 63

Table **4-4.** Percentage Error Between SAP2000 and Hand Calculations 71

Table **5-1**. Tensile Capacity of Members 83

Table **5-2**. Total Stress in North Truss Members Due to Self Weight and HS-20 Trucks 86

Table **5-3**. Total Stress in North Truss Members Due to Self Weight and HS-20 Trucks 87

Table **5-4**. Total Stress in North Truss Members Due to Self Weight and HS-20 Trucks 88

Table **5-5**. Critical Axial Tensile Force and Stress for North and South Truss Members 89

Table **5-6**. Critical Buckling Load for Compression Members 90

Table **5-7**. Combined Axial and Bending Stresses for Top and Bottom Chord, North Truss 92

Table **5-8**. Critical Location, Distance From West Abutment 100

Table **5-9**. Combined Axial and Bending Stress for Top and Bottom Chord, Critical Member 1012 106

Table **5-10**. Combined Axial and Bending Stress for Top and Bottom Chord, Critical Member 1021 109

Table **5-11**. Combined Axial and Bending Stress for Top and Bottom Chord, Critical Member 1040 112

Table **5-12**. Combined Axial and Bending Stress for Top and Bottom Chord, Critical Member 1049 115

Table **5-13**. Section Loss, North Truss End Posts, Beech Creek Veterans Memorial Bridge 118

Table **5-14**. Section Loss, North Truss Verticals, Beech Creek Veterans Memorial Bridge .. 119

Table **5-15**. Section Loss, North Truss Bottom Chord, Beech Creek Veterans Memorial Bridge 120

Table **5-16**. Section Loss, North Truss Diagonals, Beech Creek Veterans Memorial Bridge 121

Table **5-17**. Tensile Capacity of Deteriorated Members 124

Table **5-18**. Stresses in Deteriorated North Truss for Self Weight and HS-20 Trucks..... 126

Table **5-19**. Stresses in Deteriorated North Truss for Self Weight and HS-20 Trucks..... 127

Table **5-20**. Stresses in Deteriorated North Truss for Self Weight and HS-20 Trucks..... 128

Table **5-21**. Critical Axial Tensile Force and Stress for North Truss Members 129

Table **5-22**. Critical Buckling Load for Deteriorated Compression Members 130

Table **5-23**. Combined Axial and Bending Stresses for Top and Bottom Chord, Deteriorated North Truss 132

Table **5-24**. Combined Axial and Bending Stress for Top and Bottom Chord, Deteriorated Critical Member 1012 140

Table **5-25**. Combined Axial and Bending Stress for Top and Bottom Chord, Deteriorated Critical Member 1019 143

Table **5-26**. Critical Locations, Pristine and Deteriorated Bridge 146

Table **6-1**. Member Failure Sequence, Pristine and Deteriorated Model 154

Table **B5-1**. Axial Force in North Truss Members for Self Weight and Truck Loading 167

Table **B5-2**. Axial Force in North Truss Members for Self Weight and Truck Loading 168

Table **B5-3**. Axial Force in North Truss Members for Self Weight and Truck Loading 169

Table **B5-4**. Axial Force in South Truss Members for Self Weight and Truck Loading 170

Table **B5-5**. Axial Force in South Truss Members for Self Weight and Truck Loading 171

Table **B5-6**. Axial Force in South Truss Members for Self Weight and Truck Loading 172

Table **B5-7**. Total Stress in South Truss Members Due to Self Weight and HS-20 Trucks.... 173

Table **B5-8**. Total Stress in South Truss Members Due to Self Weight and HS-20 Trucks.... 174

Table **B5-9**. Total Stress in South Truss Members Due to Self Weight and HS-20 Trucks.... 175

Table **B5-10**. Axial Force in Deteriorated North Truss for Self Weight and HS-20 Trucks... 176

Table **B5-11**. Axial Force in Deteriorated North Truss for Self Weight and HS-20 Trucks... 177

Table **B5-12**. Axial Force in Deteriorated North Truss for Self Weight and HS-20 Trucks... 178

Table **B5-13**. Axial Force in Deteriorated South Truss for Self Weight and HS-20 Trucks... 179

Table **B5-14**. Axial Force in Deteriorated South Truss for Self Weight and HS-20 Trucks... 180

Table **B5-15**. Axial Force in Deteriorated South Truss for Self Weight and HS-20 Trucks... 181

Table **B5-16**. Stresses in Deteriorated South Truss for Self Weight and HS-20 Trucks..... 182

Table **B5-17**. Stresses in Deteriorated South Truss for Self Weight and HS-20 Trucks..... 183

Table **B5-18**. Stresses in Deteriorated South Truss for Self Weight and HS-20 Trucks..... 184

ACKNOWLEDGEMENTS

I would first like to thank Pennsylvania Department of Transportation District 2-0 for providing key information and lending their resources for the completion of this research.

I would like to thank my thesis advisor Dr. Daniel Linzell for his time, guidance, and support. I would also like to thank my committee members Dr. Andrew Scanlon and Dr. Thomas Boothby for their comments and revisions.

I would also like to thank my family and friends for their support, patience, and motivation throughout the process of completing my thesis. Without them this thesis would have never been completed.

Chapter 1

Introduction

1.1 Background

The failures of the I-35W Bridge in Minneapolis, Minnesota (NTSB 2008) and the Dysart Bridge in Cambria County, Pennsylvania (Grata 2007) had led to serious questions surrounding the strength and stability of truss bridges and the adequacy of aging infrastructure in the United States. The Research and Innovative Technology Administration (RITA) published the 2007 Condition of U.S. Highway Bridges by State (RITA 2008) and reported that Pennsylvania had approximately 23,500 bridges and of those bridges 44% were structurally deficient or functionally obsolete. Given the aging infrastructure, the need to understand the behavior and load distribution in truss bridges as deterioration increases is imperative. Understanding the behavior of aging truss bridges may help remediation efforts and prevent catastrophic collapses.

Truss bridges were the primary choice in bridge design from the 1870s through the 1930s and were constructed using timber, wrought iron, and steel. Trusses are comprised of many small members that together can support a large amount of weight and span great distances. In theory, the individual members of a simple truss are only subject to tension and compression forces and not bending. Trusses are also classified by the basic design used (Tennessee Department of Transportation 2008). Shown in Figure 1-1 are the most common trusses: the Warren Truss; the Howe Truss; and the Pratt Truss.

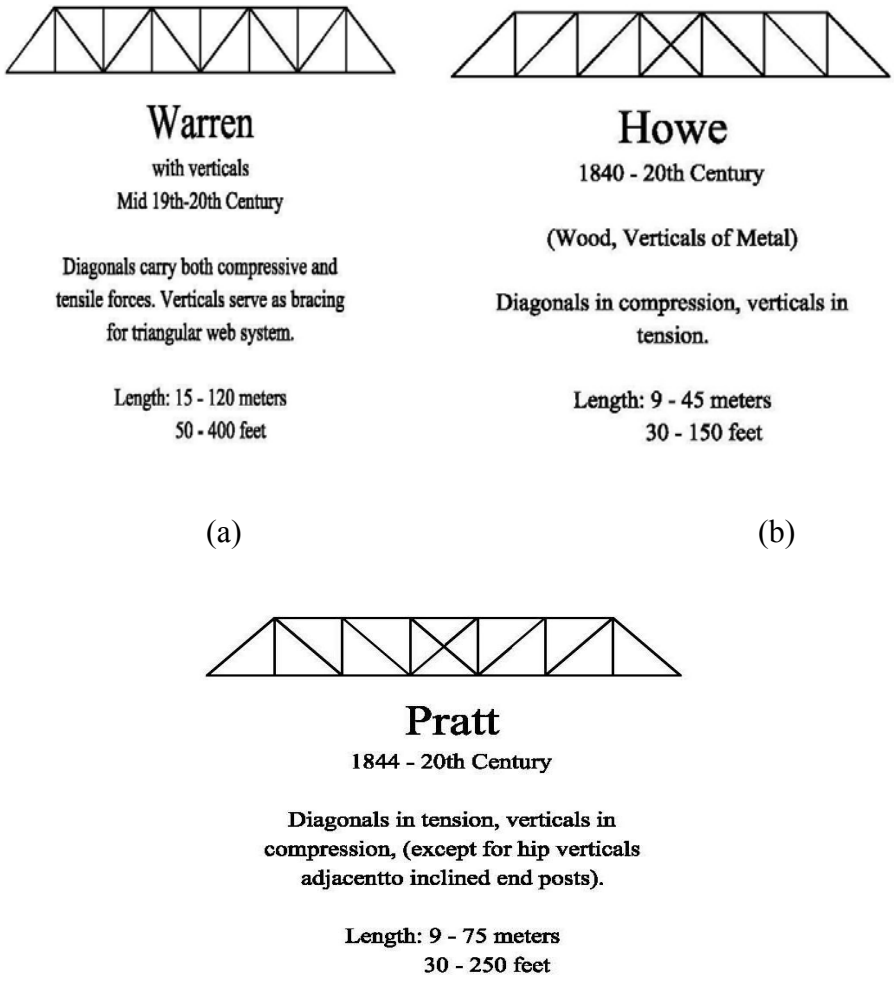

Figure **1-1.** Examples of Truss Bridge Configurations: (a) Warren Truss, (b) Howe Truss, (c) Pratt Truss

The Warren Truss shown in Figure 1-1a is the most common truss for both simple and continuous truss bridges because of its ease of construction. For smaller spans, no vertical members are used while for longer spans, vertical members are added to provide extra strength. Warren Trusses are typically used for spans between 50 – 100 meters (160 – 330 feet). The Howe Truss shown in Figure 1-1b has all of the diagonals sloped towards the center of the bridge. In theory the diagonal members handle the compressive forces while the vertical members carry the tensile forces. Howe Trusses are typically used for spans between 9 – 45 meters (30 – 150 feet). The Pratt Truss (Figure 1-1c) is identified by its diagonal members who, except for the end panels, all sloped toward the center of the span. All the diagonal members, except for those in the end panel, are theoretically subjected to tension forces only while the shorter vertical members in the center of the span and the top chords handle the compressive forces. Figure 1-2 displays the forces in a typical Pratt Truss. This thesis will focus specifically on Pratt Trusses because the representative area, Pennsylvania Department of Transportation (PennDOT) District 2-0 in Clearfield, PA, has a large amount of Pratt Truss bridges.

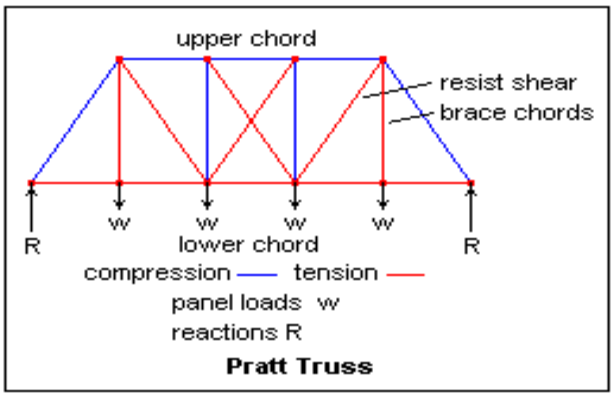

Figure **1-2.** Pratt Truss Idealized Force Diagram

Pratt Trusses, and the majority of all other truss bridges, are classified as fracture critical structures and are composed of fracture critical members. A fracture critical member is an element in tension that if fractured would probably cause a portion or the entire bridge to collapse (Dexter et al. 2005). Fracture critical members fail in a brittle manner, which can be characterized as instantaneous and does not allow for a response and remediation of the problem prior to the failure event. This is unlike ductile behavior which takes some time to occur and, subsequently, can provide some warning signs of impending failure.

A serious problem with fracture critical elements and bridges is the resulting vulnerability the problems create for progressive collapse. Progressive collapse of truss bridges can be initiated by either a rupture (tensile failure) or a buckling (compressive failure) of truss members. Progressive collapse is the collapse of all or a large part of a structure precipitated by damage or failure of a relatively small part of that structure (Nair 2003). The phenomenon is of particular concern since progressive collapse is often (though not always) disproportionate, i.e., the collapse is out of proportion (rupture or buckling of one member can lead to the collapse of the entire span of the truss) to the event that triggers it. Thus, in structures or bridges susceptible to progressive collapse, small events can have catastrophic consequences.

1.2 Problem Statement

The load redistribution in truss bridges when a critical member is removed has come to the forefront of research since the failure of the Minnesota I-35 Bridge. The load redistribution as well as the response of deteriorated truss structures that are susceptible to progressive collapse needs to be fully understood to prevent any further collapses from occurring. This study evaluates the response and load redistribution of pristine and deteriorated Pratt Truss bridges. It will provide a methodology for agencies to create a simple model of a Pratt Truss bridge to obtain information on the current condition of the bridge and the ability to determine the critical member in the bridge.

1.3 Objectives

The primary objectives of this study were to: (1) understand the behavior of Pratt Trusses when a critical member is removed; (2) investigate load redistribution to remaining members; and (3) observe their behavior and the susceptibility of the entire structure to collapse. Lower chord members and their connections, located in the "splash zone" and, more susceptible to deterioration through contact with water and deicing salts, were selected as the members that were studied. A secondary objective was to determine if aging and deterioration affected the load redistribution of truss members and global behavior of the truss bridge by studying bridges built in the early 1930s.

1.4 Scope and Task List

This study investigated the performance of a Pratt Truss when a critical member is removed. The study also examined load redistribution that occurred when the critical member was removed and also if aging and deterioration played a role in the global failure mode of the truss bridge. The behavior of the connections was also explored by creating a sub-model of deteriorated connections to determine if deterioration played a role in the global load distribution in the truss. This study did not look at the influence of fatigue on the members of the truss.

This investigation included both analytical and field evaluation components. The analytical component developed models using SAP2000 that accurately predicted the response of a Pratt Truss bridge as well as modeled the progressive collapse and deterioration of an actual Pratt Truss Bridge located in central Pennsylvania. The first bridge, the Rock Creek Bridge, was from a previous project and had reported experimental and analytical results (Azizinamini et al. 1997). The other Pratt Truss Bridge modeled was chosen from a group of representative structures in central Pennsylvania.

The field evaluation component involved condition evaluations of the Pennsylvania Bridge to determine the amount of deterioration that had occurred. Condition evaluations followed the *NCHRP Synthesis Report 354: Inspection and Management of Bridges with Fracture-Critical Details* (2005a) and the American Association of State Highway and Transportation Officials (AASHTO) *Manual for Condition Evaluation of Bridges* (AASHTO 2003). Previous rehabilitation and the extent

of deterioration were provided from old inspection reports. Truss members were evaluated for deterioration and connections were inspected to determine their level of deterioration and actual level of restraint. Computer models were updated to represent each bridge's current condition and modeled to determine if deterioration plays a role in the final behavior of truss bridges.

Tasks completed in association with the research project included:

- Literature search of all relevant material pertaining to this study. The search included: Pratt Trusses, modeling trusses and progressive collapse, dynamic response of truss members due to the initial progressive collapse, and condition evaluations to account for aging and deterioration.
- Modeled two truss bridges, the Rock Creek Bridge and a selected Pennsylvania Pratt Truss using SAP2000. The models were initially to be constructed from design plans and, as such, will not account for deterioration. All computer models were three dimensional and incorporated material and geometric nonlinearities.
- Validated the Rock Creek Bridge analytical model by comparing it to laboratory test results reported by Azizinamini et al. (1997).
- Based on research by Ghosn and Moses (1998) determined the critical member by applying an incremental analysis load until a member reached its failure point or buckles. This member was then considered the most critical member and was removed from the model. The analysis was rerun using same incremental approach, to determine where the load was being

redistributed. Removal of the member simulated the member being incapable of carrying any additional load.

- Completion of a condition evaluation of the selected Pennsylvania Pratt Truss. The condition evaluation followed procedures outlined in *NCHRP Synthesis Report 354: Inspection and Management of Bridges with Fracture-Critical Details* (2005a) and the American Association of State Highway and Transportation Officials *Manual for Condition Evaluation of Bridges* (AASHTO 2003).
- From the condition evaluation aging and deterioration were accounted for, in the models, by changing cross sectional properties along the length of the members and by changing connections to realistically model the behavior of the bridge.
- Compared how the pristine models behaved with respect to the deteriorated models by examining critical members and load redistribution. Also compared the final failure mode of the pristine model to the deteriorated model.

1.5 Summary

Since trusses are one of the oldest types of bridges in the United States, understanding the behavior of this aging infrastructure can help determine the need for rehabilitation and assess the risk of failure. Recent collapses of the I-35W Bridge and the Dysart Bridge have highlighted the importance of understanding how loads are

redistributed when critical members are removed by either deterioration, an extreme loading event or from a collision. This investigation studied the progressive collapse behavior of two Pratt Truss bridges and the effects of aging and deterioration on each bridge's collapse load and mode.

Chapter 2

Literature Review

This section examines literature topics relevant to this research, such as truss types; progressive collapse; modeling; and steel member deterioration and aging. Truss types are first discussed and then types of progressive collapse. Case studies of relevant progressive collapse types will be discussed as well as how researchers model truss bridges and progressive collapse. Finally, approaches commonly used for measuring and modeling deterioration and aging are outlined.

2.1 Truss Types

The Pratt Truss was first developed in 1844 under the patent of Thomas and Caleb Pratt (TDOT 2008). Prevalent from the 1849s through the early twentieth century, the idealized Pratt has diagonals in tension, verticals in compression except for the hip verticals immediately adjacent to the inclined end posts of the bridge (Barker and Puckett 2007). Figure 1-2 shows the idealized force diagram for a Pratt Truss. Pratt Trusses were initially built as a combination of wood and iron members, but were soon constructed using only iron and, eventually, using only steel. The Pratt Truss inspired a large number of variations and modified subtypes during the nineteenth and early twentieth centuries (TDOT 2008). Major subtypes of the Pratt design include Pratt Half-Hip Truss, Whipple Truss, Parker Truss, Baltimore (Petit) Truss, and Pennsylvania (Petit) Truss. Figure 2-1 shows examples of the subtypes of the Pratt design.

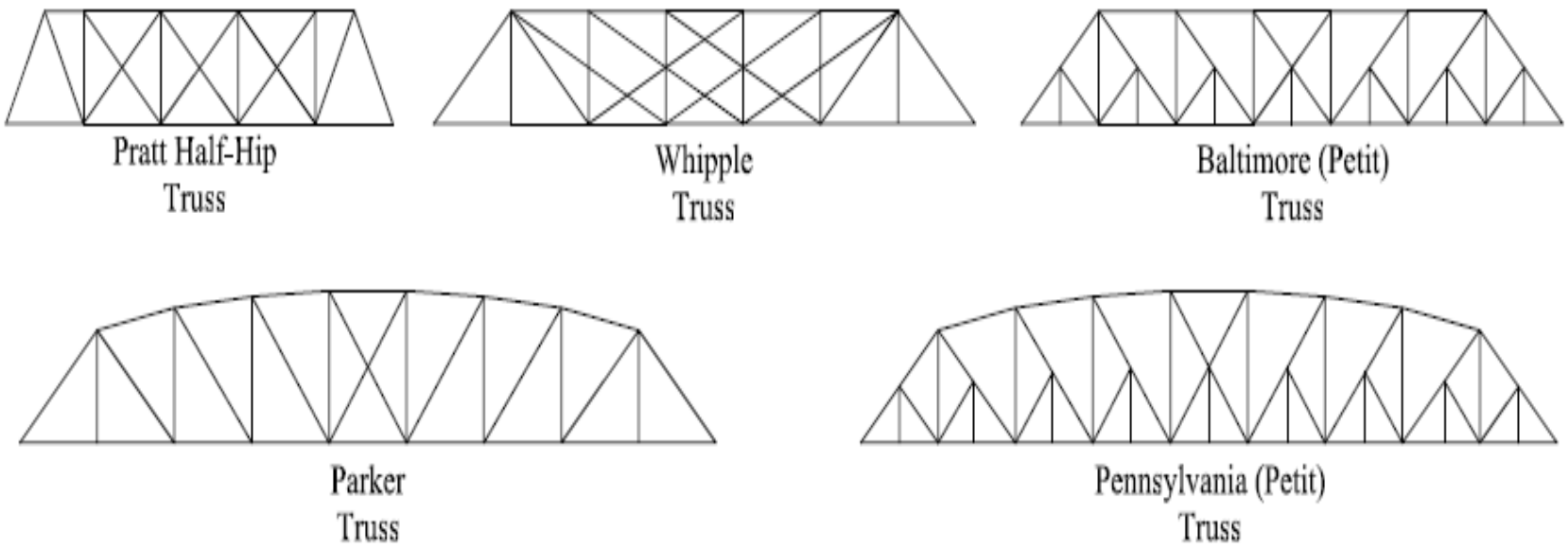

Figure **2-1.** Subtypes of Pratt Trusses.

2.2 Progressive Collapse

Progressive collapse is defined as the collapse of all or a large part of a structure precipitated by damage or failure of a relatively small part of it (Nair 2003). Progressive collapse includes two types of loading: the load that causes the structural element to fail (primary load) and the loads that are generated due to the structural motions caused by sudden collapse of the element (secondary loads). In a truss bridge two types of failure mechanisms can cause progressive collapse of the bridge. The first type, zipper-type collapse, is related to the failure of a member while in tension. The second type, instability-type collapse, is the compressive buckling of a member (Starossek 2007).

2.2.1 Zipper-Type Progressive Collapse

Zipper-type collapse is the sudden rupture of a member that leads to structural instability that propagates by overloading other members. A zipper-type collapse exhibits initial failure of one or a few structural elements, in this case a diagonal tension member of the truss. There is redistribution of the forces to the remaining structure. This redistribution of forces leads to impulsive loading and a dynamic response of the remaining structure due to the impulse. The combined static and dynamic effects cause a force concentration to members in the vicinity of the initially failing member (Starossek 2007), leading to collapse of the structure.

Zipper-type collapse can be related to removal of a critical member in a fracture critical bridge. A fracture critical member is a steel member in tension, or with a tension

element, whose failure would probably cause a portion of or an entire bridge to collapse (Nagavi and Atkan 2003). A fracture critical bridge is a steel structure that is designed with little or no load path redundancy that typically fails with the failure of a tension member. Load path redundancy is a characteristic of the design that allows loads in the bridge to redistribute to other structural members on the bridge if any one member loses capacity (Ghosn and Moses 1998).

The *AASHTO Manual for Condition Evaluation of Bridges* (2004) defines two-truss systems as fracture critical bridges. On the other hand, the *Inspection of Fracture-Critical Bridge, Members Report FHWA-IP-86-26* (2004) defines multiple truss systems (simple and continuous) including eyebar trusses, welded trusses, trusses with suspended span, and riveted trusses as fracture critical bridges. Although the definition of fracture critical trusses differs between publications there is an understanding that removing a critical member from a truss can lead to the collapse of the structure.

The failure of the Point Pleasant Bridge between Point Pleasant, West Virginia and Kanauga, Ohio in 1967 is one example of a zipper-type collapse (NTSB 1968). The bridge was an eyebar chain suspension bridge.

The failure was attributed to a fracture of one of the nonredundant eyebars supporting the main span (Fisher 1984). The fracture of the eyebar was determined to be a combination of stress-corrosion cracking and corrosion-fatigue (Dicker 1971). Failure of the eyebar (Shown in Figure 2-2) created a zipper-type collapse by redistributing the load to other members causing overloads on those members. The bridge collapsed in a progressive fashion from the initial failure of the eyebar and the entire main span fell into the Ohio River.

Figure **2-2.** Typical Detail of Eyebar Chain and Hanger Connection

Another example of a zipper-type collapse was the Mianus River Bridge collapse, Figure 2-3, in 1983 on I-95 in Connecticut (built in 1957). It was the result of a faulty pin-and-hanger assembly (NTSB 1984) shown in Figure 2-4(a) and Figure 2-4(b). The figure shows a typical schematic of a pin-and-hanger assembly that was in place at the time of the collapse. The hanger in the assembly experienced tensile forces and when it failed it lead to a zipper-type collapse similar to that of a tension member in a truss bridge. It was a zipper-type collapse because the tension member (the hanger) failed causing an entire section of the bridge to collapse.

Figure **2-3.** Mianus River Bridge Collapse

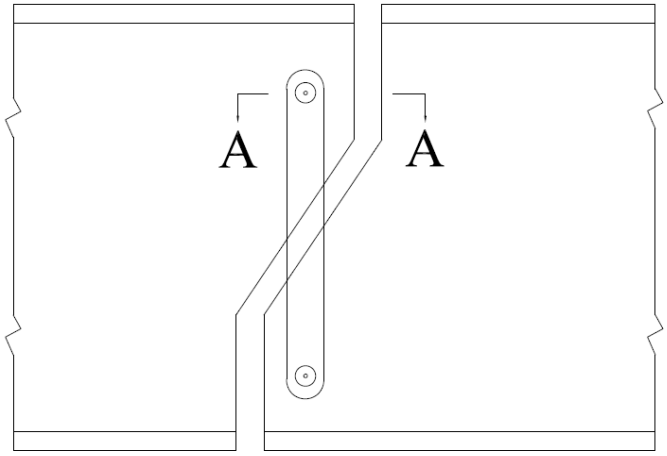

(a)

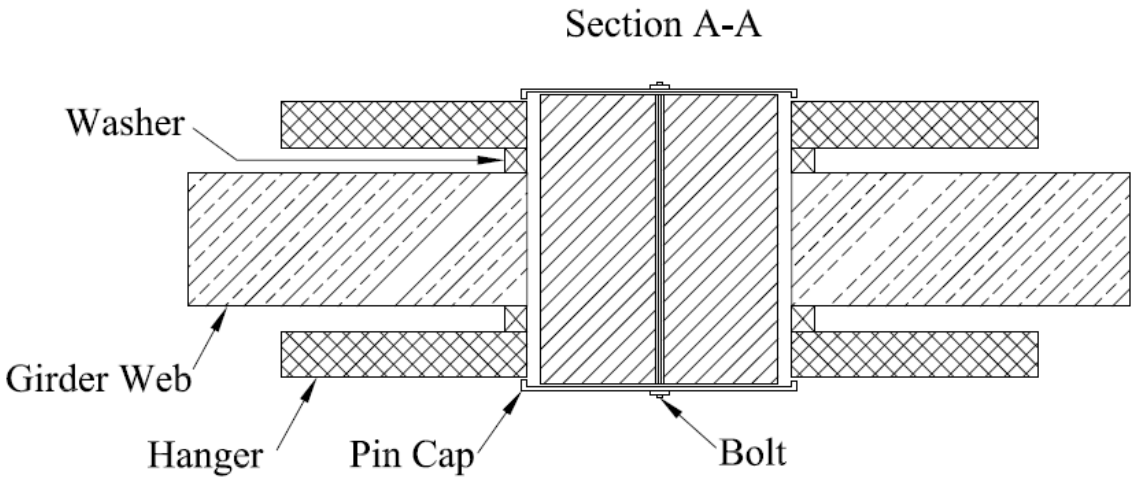

(b)

Figure **2-4**. Schematic of Pin-and-Hanger Assembly of the Mianus River Bridge

Before the collapse of the suspended span, the hanger in the southeast corner of the span came off the inside end of the lower pin. When the hanger came off the lower pin, the entire weight of the southeast corner of the span was shifted onto the outside hanger. The shift of the hanger created a disproportionate load on the southeast corner of

the span. The load gradually worked the outside hanger farther outward on the pin, and over a period of time, a fatigue crack developed in the upper pin. The fatigue crack caused the shoulder of the pin to fracture causing the pin and hanger assembly to fail. The span collapsed after the pin and hanger assembly failed (Dexter et al. 2005a). The ladder part of the collapse can be classified as a zipper-type collapse, but the initial failure was an instability-type collapse because there was a disproportionate load on the remaining members due to the loss of a structural member.

2.2.2 Instability-Type Progressive Collapse

Instability-type collapse is characterized by small vibrations due to imperfections and loading leading to large deformations or collapse. The failure of an element due to some small triggering event can make a system unstable and result in a collapse (Smith 2006). An instability-type collapse has an initial failure of a member which stabilizes the load carrying elements. The sudden failure of the stabilizing member creates a disproportionate load on the remaining members overloading them to failure (Starossek 2007).

The Mianus River Bridge collapse was caused by an instability-type progressive collapse. The small movements of the hanger caused the hanger the slip from the pin. This action caused a disproportional load on the other pin in the assembly. The instability eventually fractured the pin holding the assembly together leading to the collapse of the span.

2.3 Truss Bridge Experiments

Major research projects have been completed on truss bridges that included destructive testing and analytical modeling of the bridges. The first experiment was conducted by Aktan et al. (1994) and the second experimental study was conducted by Azizinamini et al. (1997). Both studies are summarized below and discuss the objectives of their studies as well as their findings.

Destructive testing was completed on a recently decommissioned Pratt Truss by Aktan et al. (1994) to determine if (1) bridges remaining from the early 1900s pose a public safety hazard because of the amount of deterioration present; (2) if there are any cost-effective and unobtrusive methods of upgrading deteriorated steel truss bridges; and (3) answering problems associated with condition evaluations: (a) limitations in detecting damage and deterioration in hidden elements and (b) the lack of a rational procedure for reliable analytical modeling.

An arms-length condition evaluation was completed on the Pratt Truss and it was found to be in fair to poor condition. The rollers appeared not to have functioned for many years because of accumulated rust. Bottom chords and gusset plates had considerable rust at connections to bearings. Several interior stringers were not bearing on the abutment walls at both ends. Exterior stringers suffered from extensive rust and deterioration. Damage was caused by atmospheric effects accelerated by poor slope and deicing salts. Beyond the condition evaluation, coupon samples were collected to determine the mechanical characteristics of the pre-A7 truss material. Average values for the yield stress (Fy = 248 MPa (36 ksi)), the modulus of elasticity (E = 207 GPa (30,000

ksi)), as well as the yield plateau, strain-hardening characteristics, and the elongation capacity were found to be comparable to those for A7 steel (Aktan et al. 1994).

In situ testing was completed using four double-action actuators. The tests concluded that even though some members and connections experienced corrosion and deterioration, the truss capacity was not adversely affected by this deterioration at the serviceability, damageability, and failure limit states. The tests confirmed that the important parameters that affect the capacity of the bridge are far more complex than just local deterioration. The connection behavior as well as modeling the frozen bearing correctly played a role in the behavior of the bridge (Aktan et al. 1994).

The response of the bearings indicated that the roller bearings had not been functioning for some time as ideal rollers. Because of this, the trusses were acting as arches, a phenomenon that altered the bridge behavior. The frozen rollers did not transfer tension to the lower chords particularly close to the supports. This mechanism stiffened the trusses and accumulated more energy in the upper chord than if the rollers could move freely. When the applied load reached a critical level, the rollers of the Pratt Truss started to move freely, and some of the energy that accumulated in the upper chord was suddenly released. This mechanism caused brittle failure of the Pratt Truss (Aktan et al. 1994).

The third objective of the research was to try to create a rational procedure to analytically model the Pratt Truss Bridge. The authors were unable to model the actual behavior and limit states of the deteriorated truss bridge. Although some of the forces could be estimated in truck load tests, forces in the lower chord elements were overestimated and the predicted deflections were off by 15%. The stiffnesses were off

because of the frozen rollers, from effects of the floor and portal bracing systems, and by the gusset plates, that reduced the effective length of the members. The authors concluded that the capacities of the bridge could not be predicted without conducting the experimental studies and the failure modes (the brittle failure of the Pratt Truss) and some important mechanisms (variations in the strain field within a cross section, variation of post-yielding strains along the deteriorated members, post-yield hardening in built-up latticed members caused by lattice yielding) could not be predicted without additional destructive testing (Aktan et al. 1994).

The second study was conducted by Azizinamini et al. (1997) at the University of Nebraska-Lincoln laboratory. The bridge was a Pratt-Pony Truss built in 1920. Destructive testing was completed to (1) study the global behavior of the bridge and identify the critical members; (2) study the behavior of selected details in the bridge such as member connections; (3) study applicable retrofit and strengthening schemes; and (4) develop experimental data for the validation of finite element analysis models.

Two ultimate load tests were conducted on the Pratt-Pony Truss. The first ultimate load test was of the original bridge while the second test was after the failed member and other key members were retrofitted. The global behavior of the bridge during the first ultimate load test was brittle and one of the diagonal tension braces failed with a capacity of 51710 kg (114 kips) (Azizinamini et al. 1997).

Following the first ultimate load test the bridge was retrofitted to (1) increase the ultimate capacity of the bridge; and (2) prevent a brittle mode of failure. A retrofitting scheme using a cable tensioning system was used. Post-tensioned cables parallel to the critical tension members were used for the bridge strengthening. The cables reduced the

forces developed in the tension members. Test results indicated considerable increase in ductility and an overall increase in strength to 69855 kg (154 kips). The global failure mode was ductile and the retrofitting scheme increased strength and provided a more ductile failure (Azizinamini et al. 1997).

The last objective of the study was to validate an analytical model from the experimental data collected. Azizinamini used a three dimensional analysis, SAP90, for modeling the bridge because a two dimensional model resulted in approximately a 13% lower axial force than the three dimensional analysis. The authors were able to validate a three dimensional model to accurately represent the response of the bridge under live loading (Azizinamini et al. 1997).

2.4 Modeling

First, general computer modeling considerations for truss bridges will be presented. This will include discussion of; two-dimensional versus three-dimensional models; and the influence of selecting different finite elements on truss models. This section will be followed by a detailed discussion of different methodologies for modeling progressive collapse from tension yielding and compressive buckling. The last section will discuss the incorporation of deterioration into computer models.

2.4.1 General Modeling Considerations

Trautner and Frangopol (1990) chose a Pratt-Through Truss for analysis and modeling comparison. Part of their research was to determine the appropriate time to use a more complex 3D computer model versus a more simplistic 2D model. Another objective of the study was to compare 2D models, one composed entirely of truss elements and one containing beam and truss elements, to determine which was more accurate.

Four different models were developed to compare the accuracy of each model for predicting the behavior of a truss bridge. The four included; a two-dimensional model with all truss elements; a two-dimensional model with beam and truss elements; a three dimensional model with beam and truss elements; and a three-dimensional model with beam and truss elements including the floor system (Trautner and Frangopol 1990).

The 2D model with beam elements generated slightly less stress in the truss elements (diagonals) than the model with truss elements only. However, the members converted to bending elements (posts and chords) in the 2D mixed element model usually exhibited higher stresses (Trautner and Frangopol 1990).

Nagavi and Aktan (2003) modeled the nonlinear behavior of heavy class steel truss bridges using a three-dimensional static collapse analysis (3DSCAS) program. Heavy class steel truss bridges are composed of rolled shape members and gusset plates and rivets creating rigid connections. The research was completed to examine structural reliability in heavy class steel truss bridges. Two elements from 3DSCAS were utilized for modeling heavy class steel trusses:

A three-dimensional inelastic truss finite element that considered yielding in tension/compression, yielding in tension, buckling in compression, and a bilinear material model (Mondkar and Powell 1975); and a three-dimensional inelastic beam finite element that considered a "lumped plasticity" approach, straight geometry, and a tri-linear material model. Inelastic behavior is confined to plastic subhinges lumped at each end of the element with a rigid-plastic strain-hardening behavior. Inelastic behavior begins when the first subhinge reaches it yield surface and with an increasing load the second and third yield surfaces are reached at the other plastic hinges (Chen and Powell 1982).

The researchers were able to evaluate the critical elements and connections that govern postyielding behavior, possible failure modes, and the number of plastic hinges that are formed before the structure may reach its postyield capacity. An appropriate mix of truss and beam elements was recommended for feasible nonlinear analysis of bridges. Inelastic beam elements were recommended to represent the rigidly connected members of the upper chord and the compression verticals. Using truss elements was recommended for simulating slender members at the bottom chord and tension diagonals.

A condition assessment and retrofit of a historic steel-truss railway bridge was completed by Spyrakos et al. (2004). The researchers developed a dynamic analytical model of the railway bridge using three-dimensional beam elements. All of the joints were modeled as rigid connections even though the structure was a truss system. The researchers assumed that moments transferred through joints were of interest only for the top and bottom beams of the trusses and the floor deck beams. Moments that develop in the vertical members and diagonal ties were assumed to be negligible.

The dynamic analysis of the system was based on a lumped mass formulation. The development of the finite element model was based on the following assumptions: (1) pinned at its vertical supports; (2) the loads and reactions are applied only at joints; and (3) additional masses due to the deck loads are introduced to the deck beams while lumped masses are generated at the nodes (Spyrakos et al. 2004). From the analytical model and the dynamic analysis, Spyrakos et al. (2004) was able to accurately predict the response of a historic steel-truss railway bridge.

Along with progressively modeling the structure with more complexity, level of discretization needs to be considered. Rutz and Rens (2004) conducted a study comparing a truss bridge modeled using a traditional skeleton frame and increasing the precision of the model by adding additional members to the model to represent the stringers, deck and diaphragms. By increasing the models robustness the authors were able to introduce alternative load paths: stringers supplementing the bottom chords, the stiffening of the deck, and the deck as a lateral diaphragm. It was concluded that the combination of the skeleton model plus stringers and a deck system reduced the axial forces by 13% in the bottom chord members.

2.4.2 Progressive Collapse Modeling

Progressive collapse modeling has been extensively researched by the Department of Defense (DoD 2005) and the U.S. General Services Administration (GSA 2003). Both have published documents advising designers and engineers the best practices for reducing the likelihood of progressive collapse in existing buildings and new

construction, however this research has not been extended to bridges. The manuals published discuss indirect and direct design and analysis approaches to understand the inherent redundancy in a structure. One method introduced is the alternate load path analysis by the National Institute of Standards Technology (NIST 2007).

The alternate load path direct design approach considers the resistance to progressive collapse when the amount of damage is predetermined. This is interpreted as the removal of one load bearing element, and assessing local and global structural stability (NIST 2007). Large rotation and ductility values are permitted when the resistance to progressive collapse is achieved. The load carried by the lost element must find an alternate load path to the supports without precipitating structural collapse. An important aspect of this method is the transition from the original structural configuration to the damaged state is assumed to be instantaneous, exposing the structure to a dynamic effect (DoD 2005). This approach does not specify a threat or a cause for the damaged state, it is only postulated.

Depending on the type and importance of the structure and the consequences of structural failure, the analysis techniques used can vary from simple linear-elastic static computations to sophisticated non-linear, dynamic computer analysis. In general, more complex modeling provides more realistic results, but typically requires a greater time investment and aptitude of the engineer to obtain accurate results (GSA 2003). Accurately modeling a structure is also based on the selection of the constitutive models that relate the stresses and strains, at the material level, and forces and displacements at the structural level. Four different analytical methods are presented in the manual ranging from simplistic to complex (NIST 2007).

Marjanishvili (2004) also describes four different methods for analytically modeling the progressive collapse of structures similar to GSA (2003) and DoD (2005). The four methods include linear elastic static analysis, nonlinear static analysis (inelastic static analysis used by GSA (2003)), linear elastic time history analysis (dynamic) (elastic dynamic analysis used by GSA (2003)), and nonlinear time history analysis (dynamic) (inelastic dynamic analysis). The complexity of the models developed for each of these methods can vary greatly from a simple two-dimensional linear elastic static procedure to complex three-dimensional nonlinear time history analysis. The loss of the load carrying elements (initiating damage) is modeled as a sudden dynamic or quasi-static removal of the element, depending on the method used.

In progressive collapse analysis there is no external load applied unlike in most dynamic analysis situations. Inertia forces from the removal of several elements introduce internal dynamic loads to the structure from an "at rest" structure. The "at rest" condition of the structure is before initiating damage and includes all normal loads. Since the dynamic analysis is dependent on the load sequence it is imperative to have the sequence in order to accurately capture the structural response of the structure. The structure is loaded with normal loads (i.e. dead and live load) and then a load carrying member is removed from the structure. The removal of the member could be represented by a change in the stiffness matrix. The equilibrium of the structure after the removal of the member is the redistribution of the load that the lost member was carrying. An internal force or reaction is applied to other members equal to the load to the load the removed member was carrying. (Marjanishvili 2004).

Marjanishvili's (2004) preferred method for progressive analysis is described as the *progressive analysis method*. This method requires an evaluation of a structure through an increasingly precise analysis. The process begins with a basic linear-elastic static analysis. If the analysis passes this step, whose evaluation requirements are the most conservative, and then the analysis is complete. If the structure fails, then the analysis proceeds to more complex linear and nonlinear analyses. At each step, the structure's performance against increasingly less conservative criteria is tested.

Identifying critical members from a progressive collapse perspective was discussed in a report published by Azizinamini et al. (1997) that focused on the behavior of historic Pratt Trusses. The report stated that the overall strength of a bridge is controlled by members requiring the lowest applied load to reach their ultimate strength. Such members would be the first members to fail in the course of loading the bridge. Azizinamini identified the most critical members in a truss bridge by utilizing a three-dimensional linear model of a bridge using SAP90 program. Monotonically increasing point loads were applied that corresponded to a loading configuration used for ultimate load testing of an actual structure, assuming an arbitrary value of 4540 kg (10 kips) per ram. Through the ultimate load testing failure was a very brittle and occurred in one of the tension braces in the third panel of the bridge. The fracture took place near the pin where the straight portion of the brace was connected to the pin using a forging technique. It was stated that special attention should be given to tension members and especially to forged areas (Azizinamini et al. 1997).

Ghosn and Moses (1998) developed a methodology for determining the residual capacity of fractured bridges and understanding post-fracture behavior of fracture critical

bridges. For their approach, load factors LF_1 and LF_d, are used to help establish the redundancy of bride structures and were calculated using a three-dimensional finite element analysis. LF_1 is the multiple of side-by-side HS-20 trucks that the structure can carry in addition to unfactored dead loads (using elastic analysis) before the first member reaches the resistance predicted by design specifications (Dexter et al. 2005). Figure 2-5 shows a representative example of a loading pattern to determine LF_1. In addition to the loading pattern shown other patterns would be analyzed to determine any other critical members in the structure.

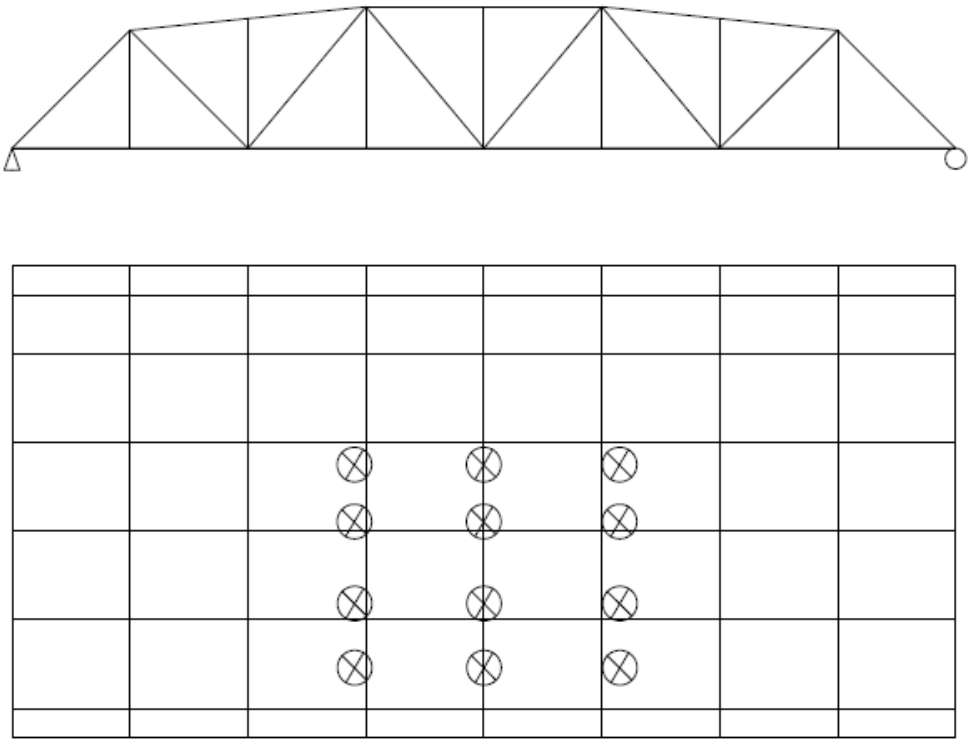

Figure **2-5.** Loading Pattern for Truss Bridge

LF_d is the residual capacity of the damaged structure and is calculated by performing a nonlinear analysis of the damaged structure (with critical member removed) under the effect of unfactored dead load and incrementally applied multiples of side-by-side HS-20 truck loads until the system collapses. LF_d gives a measure of the capacity of the structure for the damaged condition limit state. Using LF_1 and LF_d provide a measure of the level of redundancy in the bridge. Figure 2-6 shows a schematic of multiples of side-by-side HS-20 trucks (Ghosn and Moses 1998).

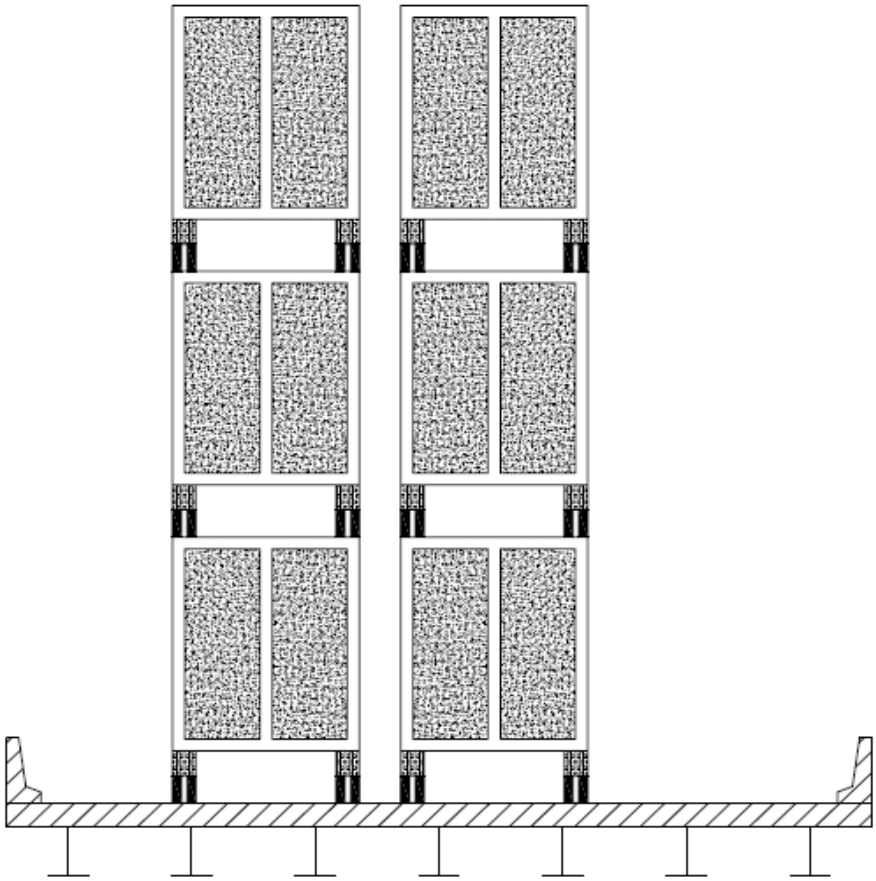

Figure **2-6.** Schematic of Multiple HS-20 Trucks

2.5 Condition Evaluation

The collapse of the Point Pleasant Bridge mentioned in Section 2.2.1 was the catalyst for many changes in specifications, design, fabrication, shop inspection, in-service inspection, and maintenance of steel bridges (Dexter et al. 2005a). As a result of the collapse, mandatory Charpy V-notch (CVN) toughness requirements were initiated for welds and base metal to ensure adequate resistance to fracture (Fisher 1984). However, many older steel bridges built before the implementation of these design provisions in the mid-1970s possess poor materials and design. Other factors that make older bridges more susceptible to fracture include: (1) marginal fracture toughness of the steel; (2) detailing, fabrication quality, and shop inspection; (3) severe corrosion problems; and (4) higher traffic volumes and truck weights than the bridge was originally designed to handle (Scheffey 1971). In light of these factors, periodic in-service inspection is required for older bridges to provide an opportunity to detect cracks and corrosion before they grow to a critical size (NTSB 1968).

To evaluate the condition of existing bridges, states may implement their own specifications, but commonly the AASHTO *Manual for Condition Evaluation of Bridges* (2004) is used. This manual serves as a standard and provides uniformity in the procedures and policies for determining the physical condition, maintenance needs and load capacity of national highway bridges. Section 3.8.3.6 and 3.12 of the manual outline the procedure for inspecting and evaluating truss bridges and critical members (AASHTO 2003).

The following list gives the procedure for evaluating existing truss bridges from AASHTO:

1. Sight along the roadway and truss chord members to determine any misalignment either horizontal or vertical. Check for sag which may indicate partial failure in joints or improper adjustments of the steel vertical or counters.
2. Check each truss member.
3. Compression members should be examined to see if they are straight with no kinks or bows. Check to ensure connections are intact. Check for any evidence of crushing at the ends of compression chord.
4. Tension members in truss should be identified as to whether or not they are fracture critical members. All fracture critical members should be inspected closely in accordance with the provisions of Section 3.12. Each component, if a tension member consists of more than one component, should be checked to see that the stresses are being divided equally.
5. Check truss and bracing members for traffic damage.
6. Check all upper and lower lateral bracing members for damage and observe if they are properly adjusted and functioning satisfactorily.
7. Check the conditions of the pins at the connections and see that the nuts and keys are in place. Also, see that spacers on the pins are holding eye-bars and looped rods in their proper position.
8. Check rivets and bolts to see that none are loose, worn, or sheared.

The provisions of Section 3.12 define fracture critical members (FCMs) or member components as steel tension members or steel tension components of members whose failure would be expected to result in collapse of the bridge. FCMs have all or part of their cross section in tension. Most cracks in steel members occur in tension zones, generally at a flaw or defect in the material. Cracks also occur at the connections. Once a crack appears in a tension member, the failure could be sudden and may lead to the collapse of the bridge. Along with the above procedure, the *Manual for Condition Evaluation of Bridges* states that a plan for inspecting such members must be developed as well. The FCM inspection plan should identify the inspection frequency and procedures to be used. A very detailed, close visual "hands-on" inspection in the field is the primary method of detecting cracks for the inspection.

2.6 Summary

The previous sections have outlined the topics applicable to this research, including progressive collapse types and bridge failure examples, analytical modeling, and aging and deterioration. The following chapters will present the structures used for this research and analytical modeling to accomplish the objectives of this study.

Chapter 3

Structure Description

3.1 Introduction

Two Pratt Truss bridges were analyzed for this investigation. The first bridge, the Rock Creek Bridge, was the control structure to determine if the analytical model was accurately representing the existing test data (Azizinamini et al. 1997). The other truss bridge was built in 1935 and is located in Central Pennsylvania. This structure was analyzed to determine the critical members and determine if aging and deterioration played a role in the structure's final collapse mechanism.

3.2 Rock Creek Bridge

The Rock Creek Bridge, the control bridge for this study, is a Pratt-Pony Truss bridge built in 1920 in central Nebraska. The bridge is a 5-panel, 27.4 meter (90 foot) span, with a road width of approximately 4.7 meters (15.5 feet). Like most of the historic bridges, some of the members in each truss (i.e., vertical posts, inclined posts, and top chords) are built up members consisting of channel and angle sections connected with lacing. Figure 3-1 depicts the Rock Creek Bridge before being removed and relocated to the University of Nebraska-Lincoln lab (Azizinamini et al. 1997).

Figure **3-1.** Rock Creek Bridge

The overall geometry of the bridge is shown in the typical truss elevation and structure framing plan drawings in Figure 3-2. Member cross sections and sizes are shown in Figure 3-3, and are summarized, along with relevant properties in Table 3-1.

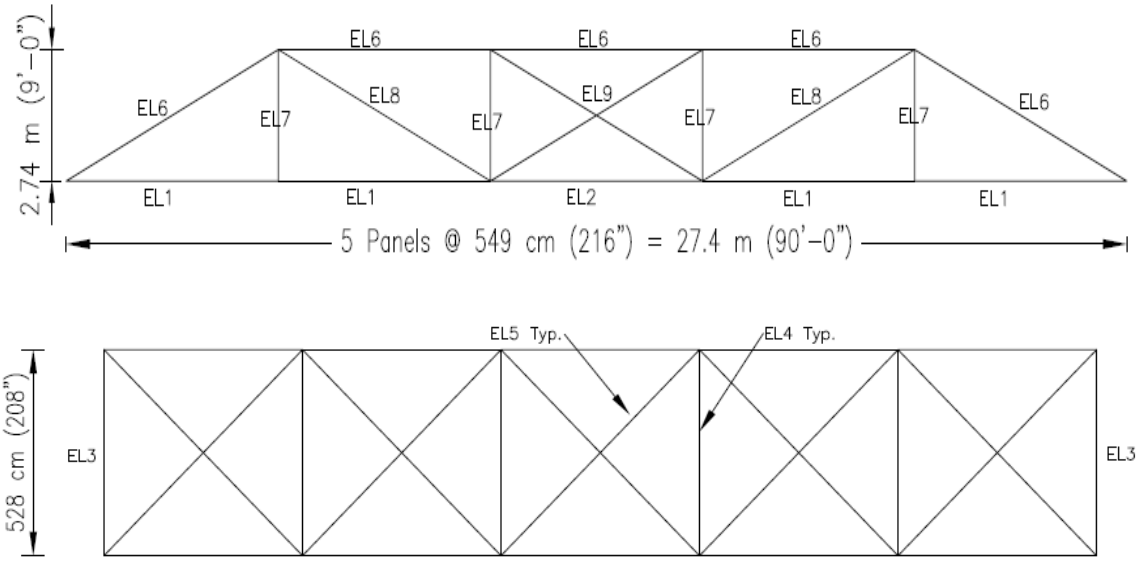

Figure **3-2.** Typical Truss Elevation and Framing Plan, Rock Creek Bridge

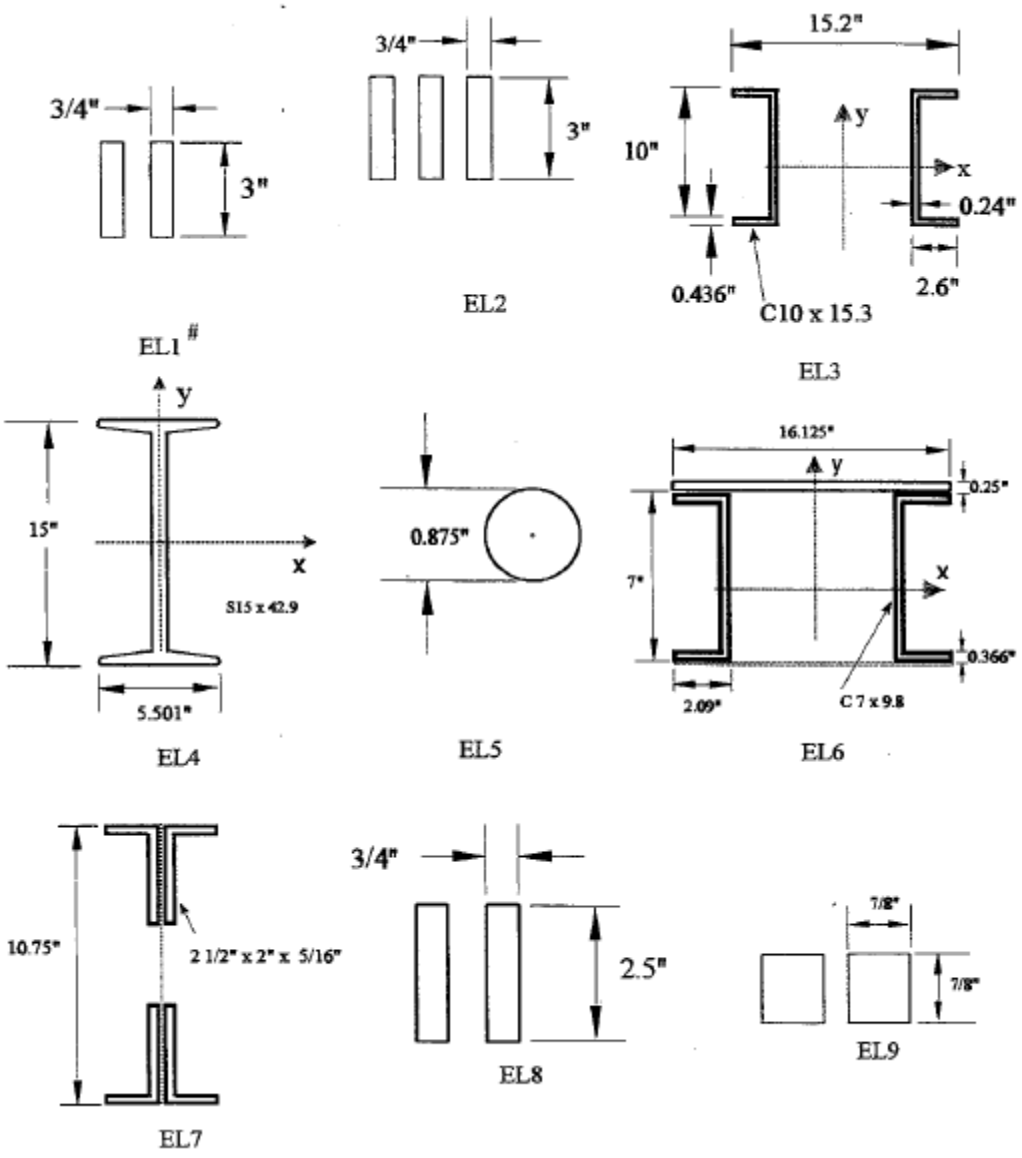

See Figure 3-2 for Member Identification

Figure **3-3.** Member Cross Sections, Rock Creek Bridge

Element Type	Location	Area in^2	I_x in^4	I_y in^4	J in^4
EL1	Bottom Chord, Panels 1,2	4.50	-	-	-
EL2	Vertical Post	6.75	-	-	-
EL3	End Cross Beams	8.98	134.80	4.56	139.36
EL4	Cross Beams	12.60	447.00	14.40	461.40
EL5	Floor Bracing	0.60	-	-	-
EL6	Top Chord, Inclined Post	9.77	73.74	239.17	312.91
EL7	Vertical Post	5.24	3.15	1.78	4.94
EL8	Side Bracing Panel 2	3.75	-	-	-
EL9	Side Bracing Panel 3	1.53	-	-	-

Table **3-1**. Truss Member Cross Sectional Properties, Rock Creek Bridge

3.3 Beech Creek Veterans Memorial Bridge

The central Pennsylvania bridge is located in Clinton County and is an example of a Pratt Through Truss bridge. This bridge was constructed in 1935 and is a 7 panel, 43.9 meter (144 foot) span that crosses Beech Creek. The bridge has a roadway width of approximately 11.0 meters (36 feet) with a 0.66 meter (2.167 feet) sidewalk on one side that was installed during rehabilitation in 1993. A majority of the members in this truss

are built up sections consisting of channels and plates. Figure 3-4 shows a picture of the Beech Creek Veterans Memorial Bridge.

Figure **3-4.** Beech Creek Veterans Memorial Bridge

In 1993 major rehabilitation was completed on the truss structure. The backwalls were removed and replaced. The existing wingwalls were raised and concrete safety barriers were added. To assist with drainage, 15.24 centimeter (6 inches) foundation drains were installed behind the backwalls. The rocker bearings were replaced with pot bearings. The concrete deck was removed and replaced and the sidewalk and barriers were installed. Shear connectors were added to the stringers and floorbeams to make the

floor system composite. Structural steel below the deck level was sandblasted and repainted while structural steel above the deck was overcoated and existing paint was not removed (PennDOT District 2-0 2008). Completed steel repairs included; replacement of all deck stringers; replacement of all bottom lateral bracing including angles and connection plates; repair of the sidewalk brackets; replacement of connection plates between the bottom of the sidewalk bracket and the truss; and installation of cantilevered W12x40s at the third points under the sidewalk.

The overall geometry of the bridge is shown in Figure 3-5. The sizes and types of the truss members are summarized in Table 3-2. Figure 3-6 details the member cross sections and is referenced in Figure 3-5.

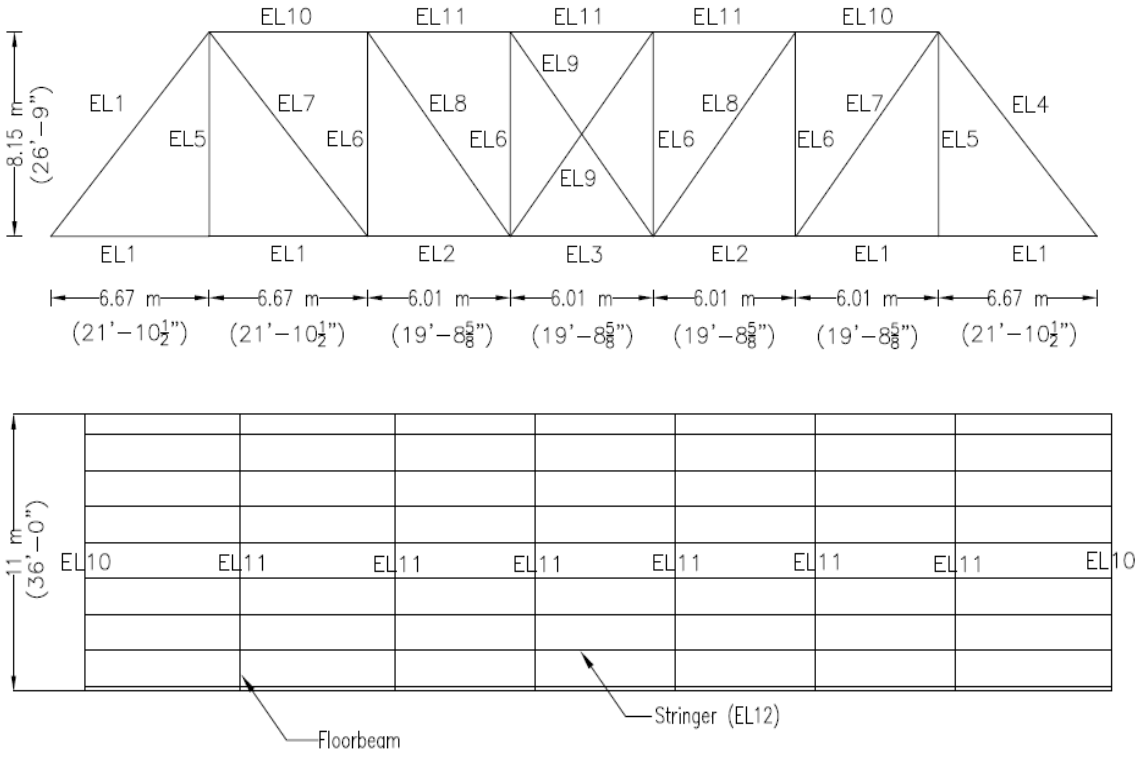

Figure **3-5.** Typical Truss Elevation and Framing Plan, Beech Creek Veterans Memorial Bridge

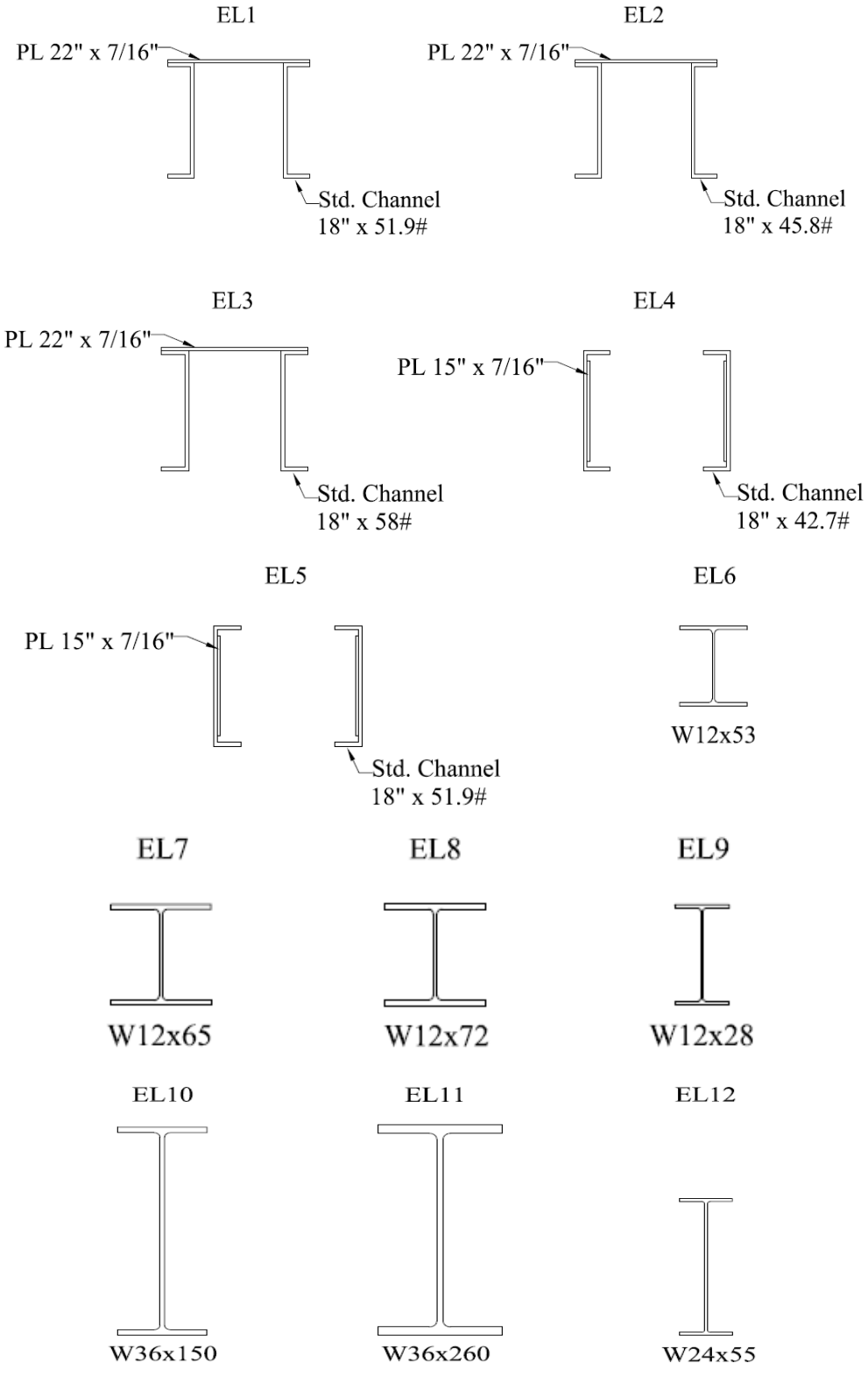

Figure **3-6.** Member Cross Sections, Beech Creek Veterans Memorial Bridge

Element Type	Location	Area cm^2 (in^2)	y bar cm (in)	I_x cm^4 (in^4)	I_y cm^4 (in^4)
EL1	L0 - U1 L7 - U6	257.97 (39.98)	28.5 (11.22)	$7.76x10^4$ (1865.6)	$9.39x10^4$ (2255.3)
EL2	U1 - U2 U5 - U6	234.68 (36.375)	29.06 (11.44)	$7.28x10^4$ (1748.9)	$8.68x10^4$ (2085.7)
EL3	U2 - U3 U3 - U4 U4 - U5	281.19 (43.58)	28.04 (11.04)	$8.24x10^4$ (1979.07)	$1.01x10^5$ (2428.3)
EL4	L0 - L1 L1 - L2 L2 - L3 L4 - L5 L5 - L6 L6 - L7	250.35 (38.8)	22.86 (9.0)	$7.80x10^4$ (1874.82)	$1.65x10^5$ (3977.2)
EL5	L3 - L4	280.58 (43.49)	22.86 (9.0)	$6.20x10^4$ (1490.29)	$1.88x10^5$ 4510.37
EL6	L1 - U1 L3 - U2 L4 - U5 L6 - U6	100.58 (15.59)	15.32 (6.03)	$1.77x10^4$ (426.2)	$4.00x10^3$ (96.1)
EL7	L2 - U2 L3 - U3 L4 - U4 L5 - U5	123.29 (19.11)	15.39 (6.06)	$2.22x10^4$ (533.4)	$7.27x10^3$ (174.6)
EL8	L2 - U1 L5 - U6	136.52 (21.16)	15.54 (6.12)	$2.49x10^4$ (597.4)	$8.13x10^3$ (195.3)
EL9	L3 - U4 L4 - U3	53.10 (8.23)	15.24 (6.0)	$8.89x10^3$ (213.5)	799.16 (19.2)
EL10	End Floorbeam	284.52 (44.1)	45.57 (17.94)	$3.80x10^5$ (9118.7)	$1.15x10^4$ (275.4)
EL11	Interior Floorbeam	439.29 (76.46)	46.03 (18.12)	$7.17x10^5$ (17230.8)	$4.54x10^4$ (1090.5)
EL12	Stringer	104.52 (16.2)	29.93 (11.79)	$5.62x10^4$ (1350.0)	$1.21x10^3$ (29.1)

Table **3-2.** Member Types, Beech Creek Veterans Memorial Bridge

3.4 Beech Creek Veterans Memorial Bridge Condition Evaluation

Prior to the 1993 rehabilitation of the Beech Creek Veterans Memorial Bridge an in-depth condition evaluation was completed by the Pennsylvania Department of Transportation District 2-0 (1993). The information gathered from the condition evaluation will be used in the following chapters to create a deteriorated model of the Beech Creek Veterans Memorial Bridge. The condition evaluation used a member designation as shown in Figure 3-7 for the entire inspection. The following is pertinent information collected from the superstructure condition evaluation.

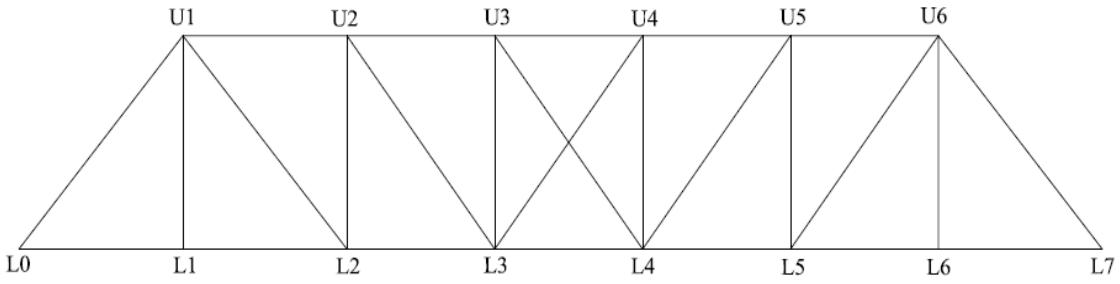

Figure **3-7.** Beech Creek Veterans Memorial Bridge Condition Evaluation Identification

3.4.1 Bearings

The bearings were cast steel shoes with 15.2 cm (6") diameter pins. There was slight corrosion on the outboard side of the fixed bearings of the west abutment, primarily on the pin plate immediately below the pin. Corrosion was more severe on the inboard side of both bearings. The expansion bearings at the east abutment were in poor condition. Both the outboard and inboard sides of the bearing exhibited corrosion around

the pin plate and nut. The roller nest was severely corroded along the lower keeper bar, with section loss and heavy debris buildup between the rollers. The exposed surface of the rear roller, nearest the backwall, was heavily pitted. A large amount of debris was removed from around the bearing revealing a heavily corroded masonry plate with severely deteriorated anchor bolt nuts. The bearings appeared to be frozen with no evidence of rotation or translation.

3.4.2 Floor System

The stringers were in fair to poor condition, primarily due to deterioration of the end regions and connections. The west end of each stringer bay, shown in Figure 3-8, typically exhibited extensive deck leakage resulting in considerable deterioration of the ends of the stringers and their connections to the floorbeams. Figure 3-8 shows a typical framing plan for the Beech Creek Veterans Memorial Bridge. Cross section A-A shows where the deterioration occurred for the stringers. Each bay had similar deterioration within 0.305 m (1 ft) of the connection to the floorbeam. At the ends of most stringers, the top and bottom flange were heavily pitted and delaminated, with section loss. Web deterioration was also widespread at the ends of the members, particularly at the lower portions. Section losses up to 0.16 cm (1/16”) in web thickness were observed in many locations, with localized spots of up to 0.32 cm (1/8”) loss. Many stringer connection angles and rivets were severely rusted and pitted. Severe deck leakage left a heavy buildup of efflorescence with rust stains on many connections. The first and last quarter of each stringer exhibited the same amount deterioration. Rivet heads at these heavily

deteriorated locations were often pitted and severely corroded. When struck with a hammer, significant portions of the rivet heads broke off. From the condition evaluation, the section loss in the stringers near the connections was calculated and new section properties were tabulated. A reduced moment of inertia, centroid, and section modulus was calculated and shown in Table 3-3.

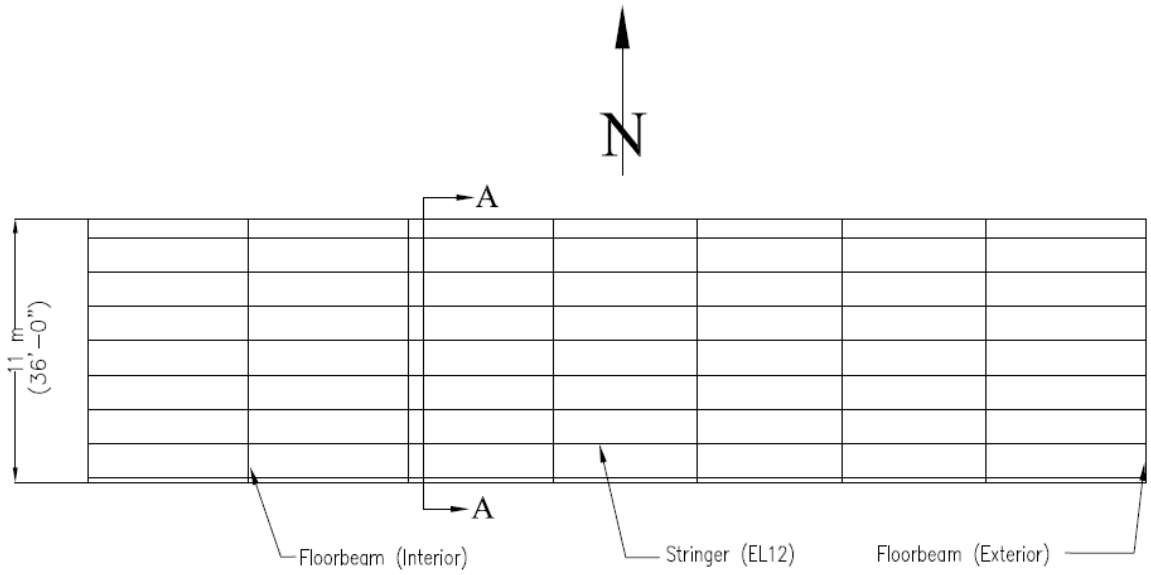

Figure **3-8.** Framing Plan, Beech Creek Veterans Memorial Bridge

I_{xx} =	48888.9 cm^4 (1175.8 in^4)
S_{xbot} =	1792.5 cm^3 (109.5 in^3)
S_{xtop} =	1892.2 cm^3 (115.6 in^3)
y_{bar} =	27.3 cm (10.7 in)

Table **3-3.** Stringer Section Loss Properties – Member W24 x 55

The floor beams were in fair to poor condition according to the condition evaluation. There were many areas of severe corrosion with stratified rust, heavy pitting, and section loss. In general, section losses were moderate and localized. The top flanges were typically corroded along the exposed underside due to deck leakage. The extent of this deterioration varied from mild corrosion along the outer edges of the flange to severe corrosion of the entire flange, resulting in heavy pitting, layered rust and section loss. The more severe corrosion occurred near the ends of the floor beams. The floorbeam webs also exhibited varying degrees of corrosion, primarily along the lower portion near the bottom flange and beneath the stringers. At the end connections, the webs commonly showed pitting and rust for the full depth along the connection angle. Section loss was evident on all webs to a moderate extent, primarily at the stringer connections, the lower web, and end connections. Section loss of 0.16 – 0.32 cm (1/6" – 1/8") was observed in the web of the floor beams. Severe rust stratification and heavy pitting were typical on the top surface of the bottom flanges. The stratification extended the entire length of the floor beams with section losses of 0.32 cm (1/8"). Since the deterioration was constant through the length of the floorbeam, the section loss calculated applied to the entire floorbeam. Reduced section properties based on the condition evaluation were calculated for the end floorbeam and interior floor beams. Tables 3-4 and 3-5 show the reduced section properties for each floorbeam in the bridge. Figure 3-8 shows the layout of the floor beams in the floor system. The condition of the floorbeam end connections was poor. The rivets at the top and bottom of the connection were in poor condition and deteriorated.

I_{xx} =	357145.3 cm^4 (8601.2 in^4)
S_{xbot} =	7843.1 cm^3 (479.9 in^3)
S_{xtop} =	7843.1 cm^3 (479.9 in^3)
y_{bar} =	45.5 cm (17.9 in)

Table **3-4.** End Floorbeam Section Loss Properties – Member 36 x 150

I_{xx} =	702221.7 cm^4 (16888.1 in^4)
S_{xbot} =	15122.2 cm^3 (923.7 in^3)
S_{xtop} =	15395.0 cm^3 (940.4 in^3)
y_{bar} =	46.4 cm (18.3 in)

Table **3-5.** Interior Floorbeam Section Loss Properties – Member 36 x 260

3.4.3 Truss

The north truss exhibited the greatest deterioration due to extensive leakage of the deck and sidewalk above the lower chord. The lower chord members were characterized by light to moderate corrosion and staining along their lengths, primarily along the tops of the flanges. Minor packrust was observed between the channel flanges and the lacing plates. More severe deterioration had occurred at the lower truss joints. The presence of bird nests and debris led to deterioration of the lower parts of the truss joints and lower chord members. Delamination of the steel, with some section loss, was present in the

members. Typical section loss was observed to be 0.32 cm (1/8”). The lower portions of the gusset plates also exhibited corrosion with some pitting. At each joint, several rivets were substantially deteriorated.

The upper portions of the lower truss joints exhibited significant corrosion and deterioration where the diagonal and vertical truss members pass through the sidewalk. The sidewalk concrete was originally cast against the truss members using joint filler to seal the perimeter of each member. At many joints this seal failed, allowing water to seep along the vertical or diagonal member to the joint below. As a result, vertical and diagonal members exhibited considerable corrosion, scaling, and pitting where they pass through the sidewalk. Section loss of varying degrees has occurred at most of the verticals and diagonals. The condition of the truss members and joints above the sidewalk was very good. No significant deterioration was observed. Tables 3-6 through Table 3-9 summarize the section loss present in all of the truss members and calculate the amount of area that has been lost through corrosion and deterioration. The tables refer to Figure 3-7 for the member identification.

Member		Location	With No Section Loss					With Section Loss			
			Gross Area, A_g	Effective Gross, A_{ge}	Net Area, A_n	Gross I_g	Net I_n	Loss Area, AL	% Loss of Age	Effective Age	Net An
			cm^2 (in^2)	cm^2 (in^2)	cm^2 (in^2)	cm^4 (in^4)	cm^4 (in^4)	cm^2 (in^2)		cm^2 (in^2)	cm^2 (in^2)
End Posts	L0 - U1	Inbd Channel @ Sidewalk	257.9 (39.99)	257.9 (39.99)	N/A	77625.6 (1866)	N/A	6.1 (0.94)	2.4%	251.9 (39.05)	N/A
	L7 - U6	@ Sidewalk	257.9 (39.99)	257.9 (39.99)	N/A	77625.6 (1866)	N/A	9.6 (1.49)	3.7%	248.3 (38.5)	N/A
Upper Chord	U1-U2		234.7 (36.39)	234.7 (36.39)	N/A	72800 (1750)	N/A	0	0.0%	234.7 (36.39)	N/A
	U2-U3		281.2 (43.59)	281.2 (43.59)	N/A	82368 (1980)	N/A	0	0.0%	281.2 (43.59)	N/A
	U3-U4		281.2 (43.59)	281.2 (43.59)	N/A	82368 (1980)	N/A	0	0.0%	281.2 (43.59)	N/A
	U4-U5		281.2 (43.59)	281.2 (43.59)	N/A	82368 (1980)	N/A	0	0.0%	281.2 (43.59)	N/A
	U5-U6		234.7 (36.39)	281.2 (43.59)	N/A	72800 (1750)	N/A	0	0.0%	281.2 (43.59)	N/A

Table **3-6.** North Truss Member Properties, Section Loss of End Posts and Upper Chord Members

Member		Location	With No Section Loss					With Section Loss			
			Gross Area, A_g	Effective Gross, A_{ge}	Net Area, A_n	Gross I_g	Net I_n	Loss Area, AL	% Loss of Age	Effective Age	Net An
			cm^2 (in^2)	cm^2 (in^2)	cm^2 (in^2)	cm^4 (in^4)	cm^4 (in^4)	cm^2 (in^2)		cm^2 (in^2)	cm^2 (in^2)
Verticals	L1-U1	Top of Sidewalk	100.6 (15.6)	100.6 (15.6)	100.6 (15.6)	3997.8 (96.1)	3997.8 (96.1)	12.4 (1.9)	12.3%	88.2 (13.7)	88.2 (13.7)
	L2-U2	Top and bottom of sidewalk	123.3 (19.1)	123.3 (19.1)	123.3 (19.1)	7280.0 (175.0)	7280.0 (175.0)	9.1 (1.4)	7.4%	114.2 (17.7)	114.2 (17.7)
	L3-U3	At sidewalk	123.3 (19.1)	123.3 (19.1)	123.3 (19.1)	7280.0 (175.0)	7280.0 (175.0)	1.2 (0.2)	1.0%	122.0 (18.9)	122.0 (18.9)
	L4-U4	At sidewalk	123.3 (19.1)	123.3 (19.1)	123.3 (19.1)	7280.0 (175.0)	7280.0 (175.0)	1.6 (0.3)	8.4%	121.6 (18.9)	121.6 (18.9)
	L5-U5	At sidewalk	123.3 (19.1)	123.3 (19.1)	123.3 (19.1)	7280.0 (175.0)	7280.0 (175.0)	11.3 (1.8)	9.2%	112.0 (17.4)	112.0 (17.4)
	L6-U6	At sidewalk	100.6 (15.6)	100.6 (15.6)	100.6 (15.6)	3997.8 (96.1)	3997.8 (96.1)	6.1 (1.0)	6.1%	94.4 (14.6)	94.4 (14.6)

Table **3-7.** North Truss Member Properties, Section Loss of Vertical Members

Member		Location	With No Section Loss					With Section Loss			
			Gross Area, A_g	Effective Gross, A_{ge}	Net Area, A_n	Gross I_g	Net I_n	Loss Area, AL	% Loss of Age	Effective Age	Net An
			cm^2 (in^2)	cm^2 (in^2)	cm^2 (in^2)	cm^4 (in^4)	cm^4 (in^4)	cm^2 (in^2)		cm^2 (in^2)	cm^2 (in^2)
Diagonals	L2-U1	At sidewalk, underside	136.5 (21.2)	136.5 (21.2)	136.5 (21.2)	8112.0 (195.0)	8112.0 (195.0)	9.1 (1.4)	6.7%	127.4 (19.8)	127.38 (19.75)
	L3-U2	At sidewalk, top	100.6 (15.6)	100.6 (15.6)	85.7 (13.3)	3997.8 (96.1)	3997.8 (96.1)	11.2 (1.7)	11.2%	89.3 (13.9)	89.3 (13.9)
	L3-U4	At sidewalk	53.1 (8.2)	53.1 (8.2)	53.1 (8.2)	728.0 (17.5)	728.0 (17.5)	3.5 (0.5)	6.6%	49.6 (7.7)	49.6 (7.7)
	L4-U3	At sidewalk, underside	53.1 (8.2)	53.1 (8.2)	53.1 (8.2)	728.0 (17.5)	728.0 (17.5)	10.5 (1.6)	19.8%	42.6 (6.6)	42.6 (6.6)
	L4-U5	At sidewalk, top	100.6 (15.59)	100.6 (15.59)	100.6 (15.59)	3997.8 (96.1)	3997.8 (96.1)	16.1 (2.5)	16.0%	84.4 (13.09)	84.4 (13.09)
	L5-U6	At sidewalk	136.5 (21.16)	136.5 (21.16)	136.5 (21.16)	8112.0 (195)	8112.0 (195)	1.1 (0.17)	0.8%	135.4 (20.99)	135.4 (20.99)

Table **3-8.** North Truss Member Properties, Section Loss of Diagonal Members

Member		Location	With No Section Loss					With Section Loss			
			Gross Area, A_g	Effective Gross, A_{ge}	Net Area, A_n	Gross I_g	Net I_n	Loss Area, AL	% Loss of Age	Effective Age	Net An
			cm^2 (in^2)	cm^2 (in^2)	cm^2 (in^2)	cm^4 (in^4)	cm^4 (in^4)	cm^2 (in^2)		cm^2 (in^2)	cm^2 (in^2)
Lower Chord	L0-L1	At L1	161.0 (24.96)	156.3 (24.24)	132.2 (20.5)	29577.6 (711)	24294.4 (584)	8.4 (1.31)	5.2%	147.9 (22.93)	123.8 (19.19)
	L1-L2	Near L1	161.0 (24.96)	161.0 (24.96)	161.0 (24.96)	29577.6 (711)	29577.6 (711)	10.4 (1.62)	6.5%	150.5 (23.34)	150.5 (23.34)
	L2-L3	Near L2	245.7 (38.09)	235.7 (36.54)	198.9 (30.84)	45843.2 (1102)	37315.2 (897)	9.0 (1.4)	3.7%	226.7 (35.14)	189.9 (29.44)
	L3-L4	Near L4	280.5 (43.49)	274.5 (42.56)	232.5 (36.04)	51667.2 (1242)	42182.4 (1014)	6.8 (1.06)	2.4%	267.7 (41.5)	225.6 (34.98)
	L4-L5	Near L5	245.7 (38.09)	235.7 (36.54)	198.9 (30.84)	45843.2 (1102)	37315.2 (897)	3.0 (0.47)	1.2%	232.7 (36.07)	195.9 (30.37)
	L5-L6	At critical section	161.0 (24.96)	156.3 (24.24)	132.2 (20.5)	2953.6 (71)	24294.4 (584)	0.0 (0)	0.0%	156.3 (24.24)	132.2 (20.5)
	L6-L7	At critical section	161.0 (24.96)	156.3 (24.24)	132.2 (20.5)	2953.6 (71)	24294.4 (584)	0.0 (0)	0.0%	156.3 (24.24)	132.2 (20.5)

Table **3-9.** North Truss Member Properties, Section Loss of Lower Chord Members

The south truss was in good condition. The lower chord members support an abandoned steel utility pipe along the outside face of the south truss. The chord members exhibited slight packrust between the tie plates and the channel flanges at the outer edges of the plates. Up to 0.16 cm (1/16") of section loss was observed on the channel sections at the lower 2.54 cm (1") of the inside web surface. The lower chord joints were in good condition except for occasional light corrosion of the gusset plates and ends of the truss member, and a few deteriorated rivet heads.

The verticals and diagonals of the South Truss were in very good condition. The members exhibited slight paint pitting with light rusting. The most severe corrosion occurred at the connections of the railing to the verticals and diagonals. The degree of that corrosion varies, with the greatest deterioration at Joints L4, L5, and L6. The upper chord members and joints were in good condition as well.

3.5 Summary

This section gives structural descriptions of the bridges that are being examined for this study as well as a condition evaluation of the Beech Creek Veterans Memorial Bridge. This information will be used for the remainder of the research to determine if deterioration plays a role in the global response of the bridge.

Chapter 4

Modeling Procedure

A computational study was carried out using SAP2000 finite element models of the Rock Creek Bridge and the Beech Creek Veterans Memorial Bridge. After validation using the Rock Creek Bridge model, models of the Beech Creek Veterans Memorial Bridge assuming no deterioration, termed "pristine", were examined along with models that included deterioration. These models were used to study global failure mode of the bridge to determine if deterioration plays a role in the final failure mode. The following sections describe the pristine model and loading scheme for the Rock Creek Bridge and then describe the validation completed on the Rock Creek Bridge. The sections following the validation of the Rock Creek Bridge include model description and loading scheme for the Beech Creek Veterans Memorial Bridge and the examination using classical methods of influence lines.

4.1 Rock Creek Bridge Pristine Model

The bridge was modeled in SAP2000 using truss and beam elements. The truss elements are formulated assuming that the truss element can only carry axial forces and cannot sustain shear force or bending moment. The beam elements were used for members subjected to significant bending effects as opposed to twisting or axial forces. Members in the model were given the same cross sectional properties as shown in Table

3-1 and are based on field measurements of the bridge members. Figure 4-1 shows a model of a truss bridge. The floor system, including the stringers and the floorbeams, were modeled with beam elements. The truss members, including end posts, vertical posts, top chords, bottom chords and the lateral bracings in the floor system were also modeled using beam elements. Diagonal members in the truss were modeled using truss elements. The modeling technique used in the Rock Creek Bridge model was based on work completed by Azizinamini et al. (1997).

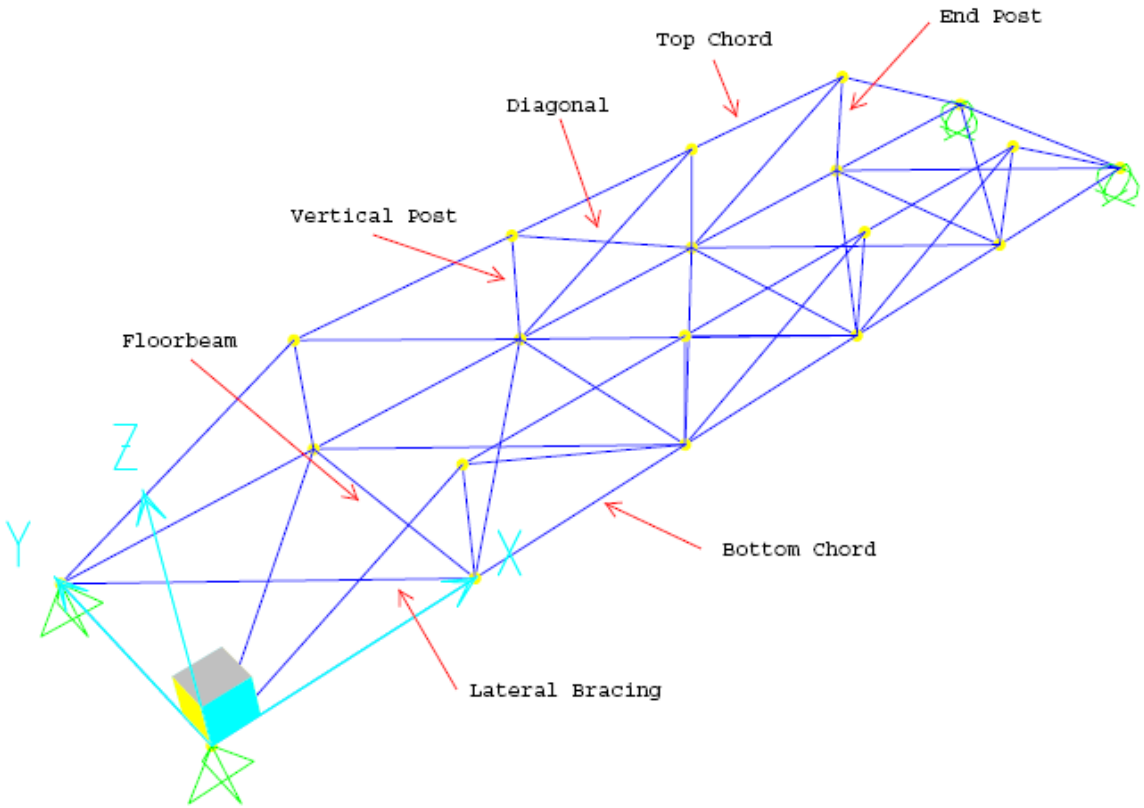

Figure **4-1.** Truss Components

Other important modeling considerations included the connections between the floor beams and the vertical posts. Connections were modeled as pins because of the pin

and eyebar connection present in the Rock Creek Bridge. Boundary conditions were also of importance and initially consisted of simply supported conditions with pins at one end of the bridge and rollers at the opposite end. Based on the work by Azizinamini the hinges and rollers provided in the truss and supports were assumed to function properly even though they were rusted and corroded. Material properties for the model were based on coupon tests completed on selected compression members as shown in Table 4-1 (Azizinamini et al. 1997). An elastic, small deformation analysis was completed. Figure 4-2 shows the Rock Creek Bridge pristine model.

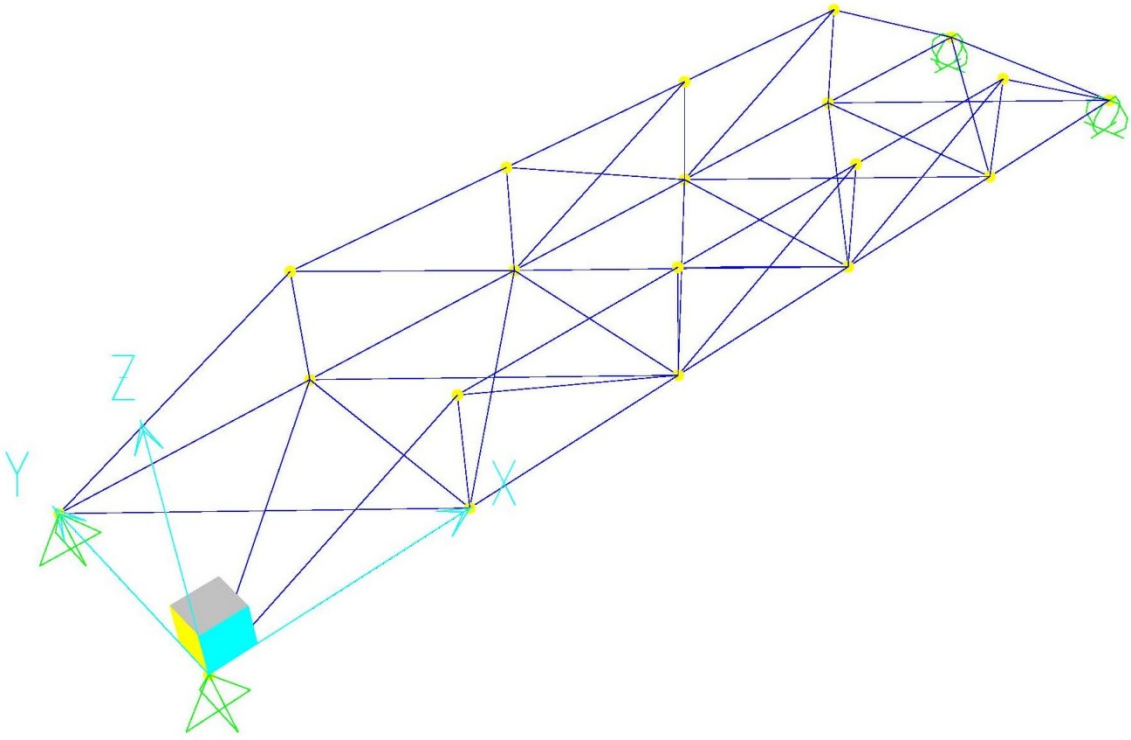

Figure **4-2.** Analytical Model, Rock Creek Bridge

Samples	Dimensions		Tensile			Modulus
	T x W cm (in)	Area cm^2 (in^2)	Ultimate 0.2% Offset	Yield Mpa (ksi)	% Elongation (in 2")	MPa x 10^3 (ksi x 10^3)
C1	0.538 x 1.293 (0.212 x 0.509)	0.697 -0.108	-414.1 -60.1	-283.2 -41.1	31	-248.7 -36.1
C2	0.549 x 1.293 (0.216 x 0.509)	0.71 -0.11	-408.6 -59.3	-287.3 -41.7	35	-262.5 -38.1
C5	0.541 x 1.293 (0.213 x 0.509)	0.697 -0.108	-423.0 -61.4	-340.4 -49.4	29	-199.1 -28.9
D3	0.635 x 1.293 (0.250 x 0.509)	0.819 -0.127	-441.6 -64.1	-299.7 -43.5	31	-203.9 -29.6
D4	0.635 x 1.293 (0.250 x 0.509)	0.819 -0.127	-403.8 -58.6	-264.6 -38.4	36	-201.9 -29.3
T6	0.622 x 1.293 (0.245 x 0.509)	0.793 -0.123	-401.7 -58.3	-261.8 -38	37	-227.4 -33
T7	0.599 x 1.293 (0.236 x 0.509)	0.774 -0.12	-398.9 -57.9	-261.8 -38	39	-220.5 -32

Table **4-1.** Material and Geometric Properties, Rock Creek Bridge (Azizinamini et al. 1997)

Concentrated loads were placed on nodes to simulate field tests conducted by Azizinamini et al. (1997). The loads located along or between the elements were transferred to the nodes using the lever rule.

4.2 Model Validation

Validation of the model was completed by comparing results to the test results compiled by Azizinamini et al. (1997). The following section describes the loading scheme used to simulate the field tests, the method used to compare the results, and modifications made to the model to improve.

A dead load equivalent to approximately 1.1 kN/m^2 (23 psf) was applied to the bridge for the test. To simulate the dead load, two large concrete blocks were lowered onto the bridge in the second and fourth panels. The weight of each block was 57.9 kN (13 kips). To ensure equal distribution of the dead load, the lever rule was used to distribute the load to the surrounding nodes of the model. Figure 4-3 and Figure 4-4 show concrete block details and the load configuration used in the field tests and simulated in the model. Three stages resulted corresponding to the placement of each concrete block on the bridge structure. Load stage 1 corresponds to zero dead load. Load stages 2 and 3 correspond to placing the first and second concrete blocks on the bridge, respectively (Azizinamini et al. 1997).

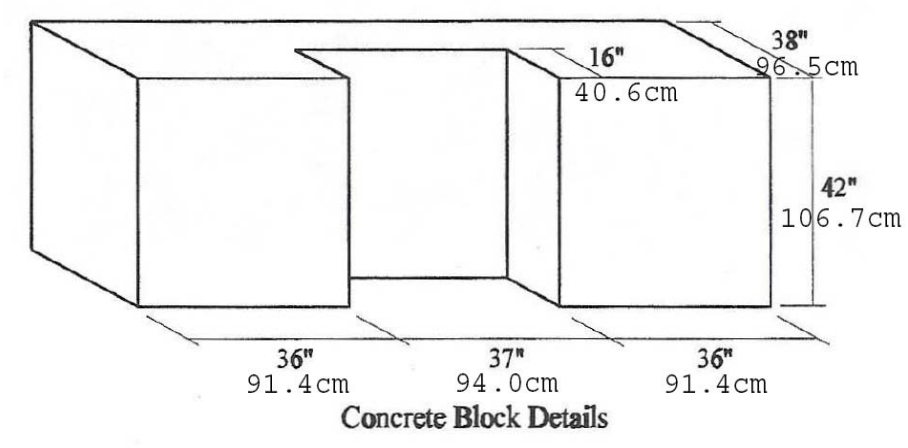

Figure **4-3.** Concrete Block Geometry, Rock Creek Bridge

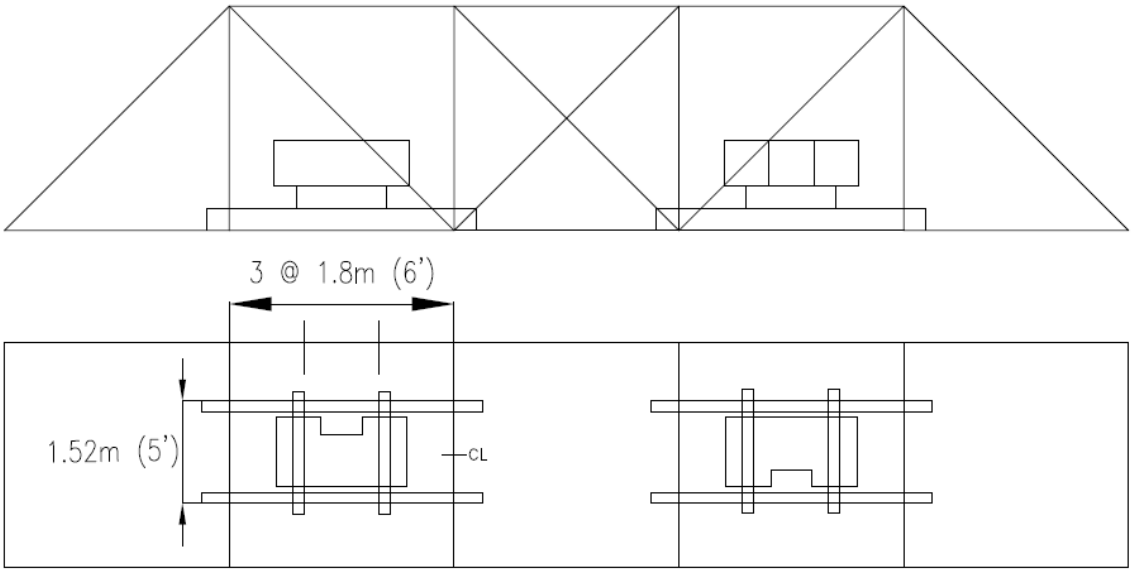

Figure **4-4.** Dead Load Configuration, Elevation and Plan View, Rock Creek Bridge

The concentrated loads for the model were determined using the geometry of the concrete block and the unit weight of concrete 23.6 N/m^3 (150 pcf). Figure 4-5 shows the point loads used for the model.

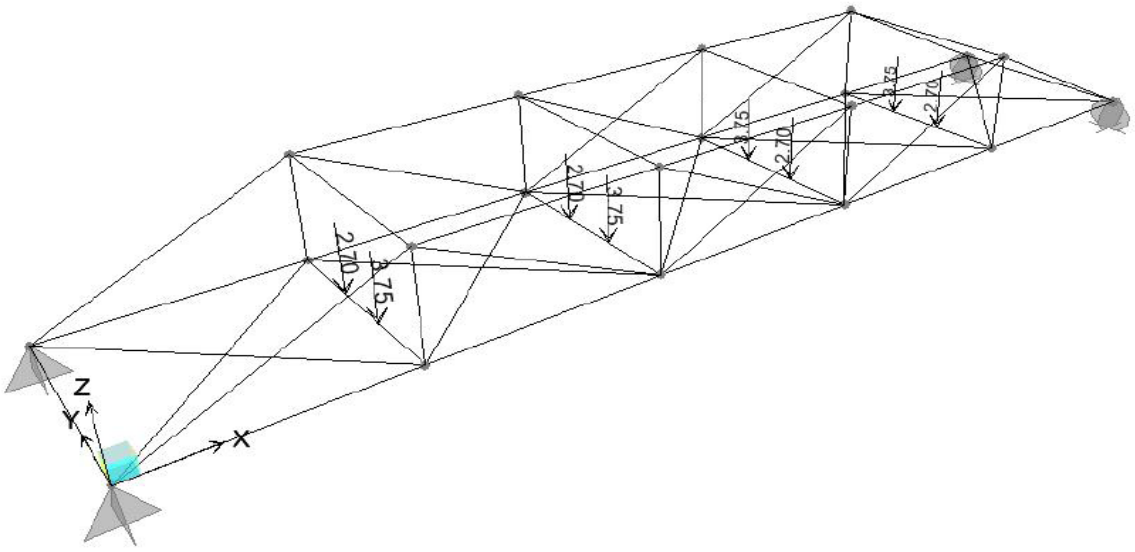

Figure **4-5**. Dead Load Concentrated Loads, Rock Creek Bridge

Figure 4-6 shows members selected for the validation. Selected members were those that were instrumented by Azizinamini during field testing (Azizinamini 1997). Axial forces were determined for each of these ten members to validate the Rock Creek Bridge model.

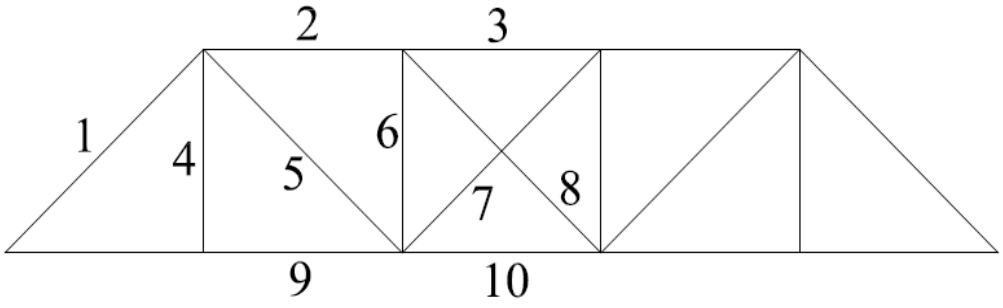

Figure **4-6.** Validation Member Designation

Figure 4-7 shows representative axial forces in Member 1 of the model of Rock Creek Bridge. The results are reported at two stages corresponding to the placement of each concrete block on the bridge structure. The horizontal axis in this figure indentifies each loading stage with Stage 1 corresponding to zero dead load and Stages 2 and 3 corresponding to placement of the first and second concrete blocks onto the bridge ignoring the self weight of the bridge. The vertical axis in the figure represents the axial force. Azizinamini and SAP90 results were compiled from previous research (Azizinamini 1997) while the SAP2000 results were from the current analytical model described in previous sections. Results for the other instrumented members are shown in Appendix A - Figures A4.1 to A4.10.

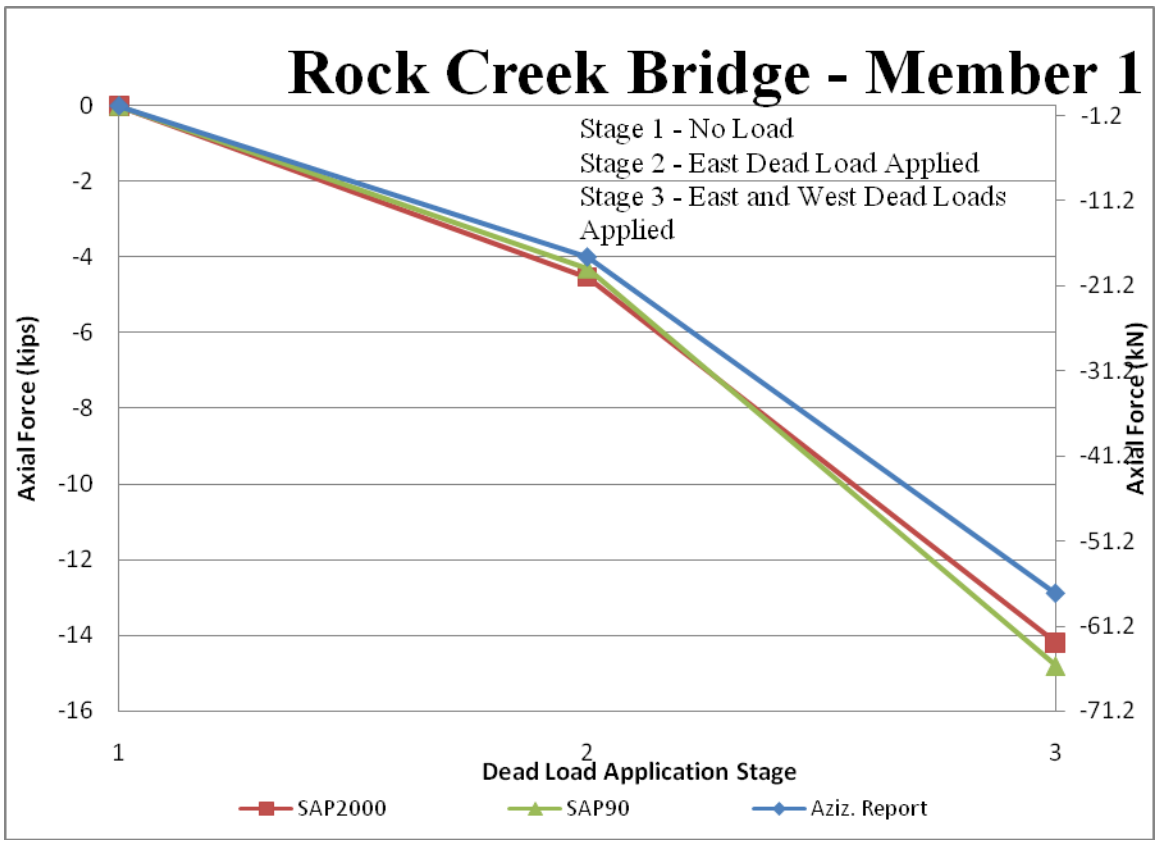

Figure **4-7.** Axial Force in Member 1, Rock Creek Bridge

Tables 4-2 and 4-3 provide a numerical comparison of the field data results, the SAP90 results, and the SAP2000 results for each stage of loading in each member. The first two columns designate the member identification and the stage number, the next three are the results from the field results and the analytical model and the last two columns are the percentage error for the field results compared to each of the analytical models.

Member	Stage	Axial Force kN (kips) - Azizinamini Field Results	Axial Force kN (kips) - SAP90	Axial Force kN (kips) - SAP2000	Field Results vs. SAP90	Field Results vs. SAP2000
1	1	0 0	0 0	0 0	0.00%	0.00%
	2	-17.79 (-4)	-19.13 (-4.3)	-20.2 (-4.53)	7.50%	13.30%
	3	-57.38 (-12.9)	-65.83 (-14.8)	-63.2 (-14.2)	14.73%	10.10%
2	1	0 0	0 0	0 0	0.00%	0.00%
	2	-31.14 (-7)	-21.35 (-4.8)	-39 (-8.76)	-31.43%	25.20%
	3	-77.84 (-17.5)	-64.5 (-14.5)	-83 (-18.6)	-17.14%	6.60%
3	1	0 0	0 0	0 0	0.00%	0.00%
	2	-48.04 (-10.8)	-46.7 (-10.5)	-47.1 (-10.59)	-2.78%	-1.91%
	3	-84.96 (-19.1)	-88.96 (-20)	-95.5 (-21.47)	4.71%	12.41%
4	1	0.067 -0.015	0 0	0 0	-100.00%	-100.00%
	2	0.089 -0.02	0.089 -0.02	0.089 -0.02	0.00%	0.00%
	3	1.02 -0.23	14.7 -3.3	15.5 -3.49	1334.78%	1417.39%
5	1	0 0	0 0	0 0	0.00%	0.00%
	2	19.57 -4.4	19.57 -4.4	21.6 -4.85	0.00%	10.20%
	3	30.69 -6.9	32.47 -7.3	36 -8.1	5.80%	17.40%

Table **4-2.** Comparison of SAP2000 and Test Results, Members 1 – 5, Rock Creek Bridge

Member	Stage	Axial Force kN (kip) - Azizinamini Field Results	Axial Force kN (kip) - SAP90	Axial Force kN (kip) - SAP2000	Field Results vs. SAP90	Field Results vs. SAP2000
6	1	0 0	0 0	0 0	0.00%	0.00%
	2	-7.12 (-1.6)	-4.45 (-1)	-6.98 (-1.57)	-37.50%	-1.88%
	3	-2.22 (-0.5)	-1.11 (-0.25)	-2.8 (-0.626)	-50.00%	-25.20%
7	1	0 0	0 0	0 0	0.00%	0.00%
	2	-7.12 (-1.6)	-8.45 (-1.9)	-7.43 (-1.67)	18.75%	4.37%
	3	-4.67 (-1.05)	-1.78 (-0.4)	-3.74 (-0.84)	-61.90%	-19.90%
8	1	0 0	0 0	0 0	0.00%	0.00%
	2	-12.37 (-2.78)	-10.68 (-2.4)	-11.1 (-2.5)	-13.67%	-10.10%
	3	-6.23 (-1.4)	-1.33 (-0.3)	-2.7 (-0.61)	-78.57%	-56.40%
9	1	0 0	0 0	0 0	0.00%	0.00%
	2	12.01 -2.7	17.79 -4	16.03 -3.6	48.15%	33.48%
	3	-37.81 (-8.5)	-60.05 (-13.5)	-51.5 (-11.57)	58.82%	36.10%
10	1	0 0	0 0	0 0	0.00%	0.00%
	2	-31.14 (-7)	-42.26 (-9.5)	-38.4 (-8.64)	35.71%	23.40%
	3	-60.05 (-13.5)	-79.17 (-17.8)	-77 (-17.3)	31.85%	28.10%

Table **4-3.** Comparison of SAP2000 and Test Results, Members 6 – 10, Rock Creek Bridge

From Table 4-2 and Figures A4.1 through A4.10 the analytical models give a good representation of the bridge behavior under the prescribed dead load. The average percent error of Stage 2 and 3 for SAP2000 compared to field results was 12.4% and 23.6%, respectively. (It should be noted that, for Stage 3 – Member 4 was eliminated from the error calculations due to the large amount of error present.) Possible causes for this Member 4 error are given below. The percentage error in the SAP2000 analytical model is relatively small because the axial forces in the members are very small. The largest axial force is 95.5 kN (21.5 kip) and any small discrepancy will lead to large error calculations. The average percent error of Stage 2 and 3 for SAP90 compared to field results was 19.6% and 32.4%, respectively. This average does not include values for Member 4 in Stage 3. Member 4 is the only member in which the analytical results do not correspond with the test results. For Stage 3, Member 4 has a 1334.8% error compared to SAP90 and a 1417.4% error compared to SAP2000. Member 4 is a vertical post which is composed of channels laced together. Studies have shown that built up members can have one or two members carry a considerable amount of the weight and an analytical model is not capable of picking up the unequal load distribution among one member. Other possibilities for the discrepancy in the test results to the model results could be due to inaccurate field data. The SAP90 and SAP2000 models predict the same response for the member while the test results are significantly off suggesting that the test data was inaccurate. The other members in the Rock Creek Bridge exemplify the same response as found in the field.

Modifications were made to the analytical model to improve its the accuracy. The first modification was the elimination of self-weight of the members in the model.

Azizinamini only wanted to see the effects of the dead load due to the concrete blocks and analyzed the SAP90 model without incorporating the self-weight of the members. With the removal of the self-weight of the bridge the response in the members was similar to the SAP90 and test results. The behavior and response of each member, with the exception of Member 4 at Stage 3, mimicked the results obtained from Azizinamini once the self weight was removed from the analytical model.

4.3 Beech Creek Veterans Memorial Bridge Pristine Model

The Beech Creek Veterans Memorial Bridge was modeled using truss and beam elements. The Section Designer in SAP2000 was used to define each member's cross sectional properties and geometry. Cross sectional properties are given in Table 3-2 and Figure 3-6 shows bridge geometry. The floor system, including floorbeams and stringers, were modeled using beam elements. The vertical posts, bottom and top chord, and end posts of the truss were modeled as beam elements. The diagonals of the truss, the lateral bracing and the end panel bracing were modeled as truss elements. Figure 4-8 shows the components in the Beech Creek Veterans Memorial Bridge.

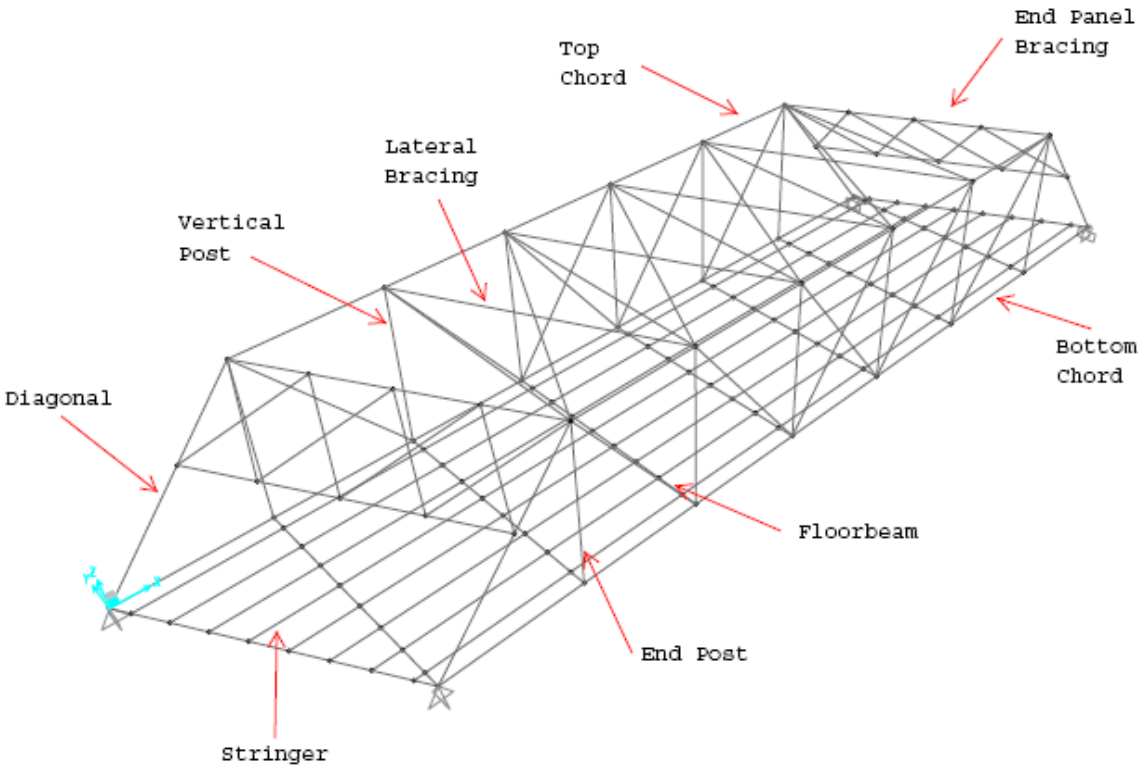

Figure **4-8.** Components of Beech Creek Veterans Memorial Bridge

Material properties were based on nominal values from the original bridge plans. The plans specified the yield stress was F_y = 207 MPa (30 ksi) and the ultimate stress was F_u = 400 MPa (58 ksi). The modulus of elasticity was assumed to be 207 GPa (30,000 ksi).

Other general modeling considerations included the connections between the floor beams and vertical posts. Connections were modeled as pinned connections following the Rock Creek Bridge approach. Boundary conditions were simply supported with pins at one end of the bridge and rollers at the opposite end. An elastic, small deformation

analysis was completed. Figure 4-9 shows the finite element model of the Beech Creek Veterans Memorial Bridge.

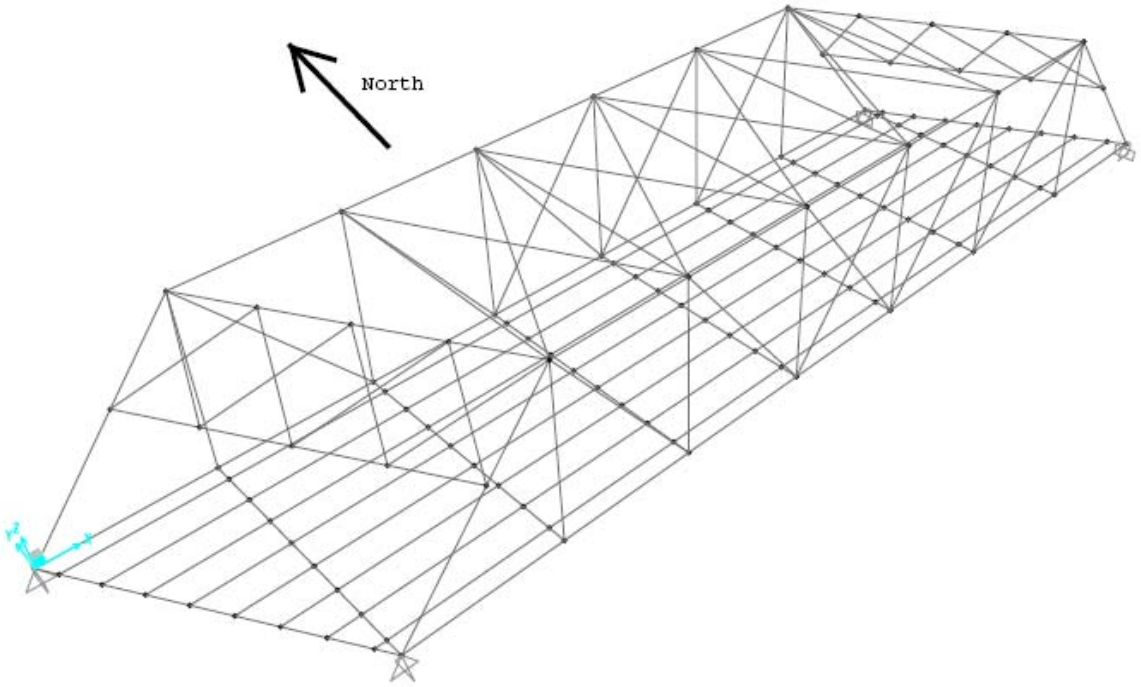

Figure **4-9.** Beech Creek Veterans Memorial Bridge Pristine SAP2000 Model

The pristine model ignored corrosion and section properties were not reduced. It was examined to determine the critical member as well as the global failure mode. All connections and supports were assumed to function properly. The connection between the floor beams and bottom chords was assumed to be rigid, following Azizinamini (1997), and the floor beams were modeled as beam elements.

Examination of the pristine model consisted of completing an elastic analysis with a single point load traversing the structure. Results from the analysis were compared to hand calculations to determine the accuracy of the model. Influence lines were used to compare the results of the hand calculations and the analysis.

4.4 Examination

Examination of the model for the Beech Creek Veterans Memorial Bridge consisted of comparing hand calculated influence lines for members of the truss to influence lines created by running a linear elastic analysis in SAP2000. The verification used a 4.45 kN (1 kip) moving load.

An upper chord member (member 1004 in Figure 4-10) and two diagonal members (members 1012 and 1021) were chosen for comparison. These members were chosen because they provided a representative sample of the members in the truss and tension members were of particular interest in this research. Tension members were of particular interest because the research focused on critical member removal and critical members are classified as tension members. Figures 4-11 through 4-13 compare hand calculated and SAP2000 influence lines for these members.

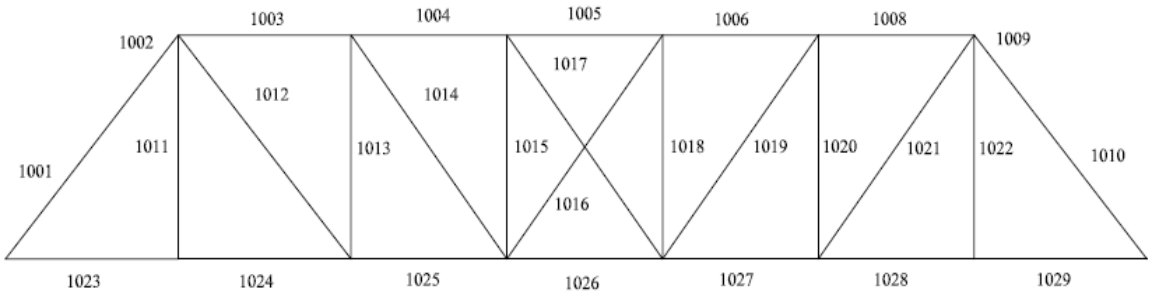

Figure **4-10.** Member Identification, Beech Creek Veterans Memorial Bridge

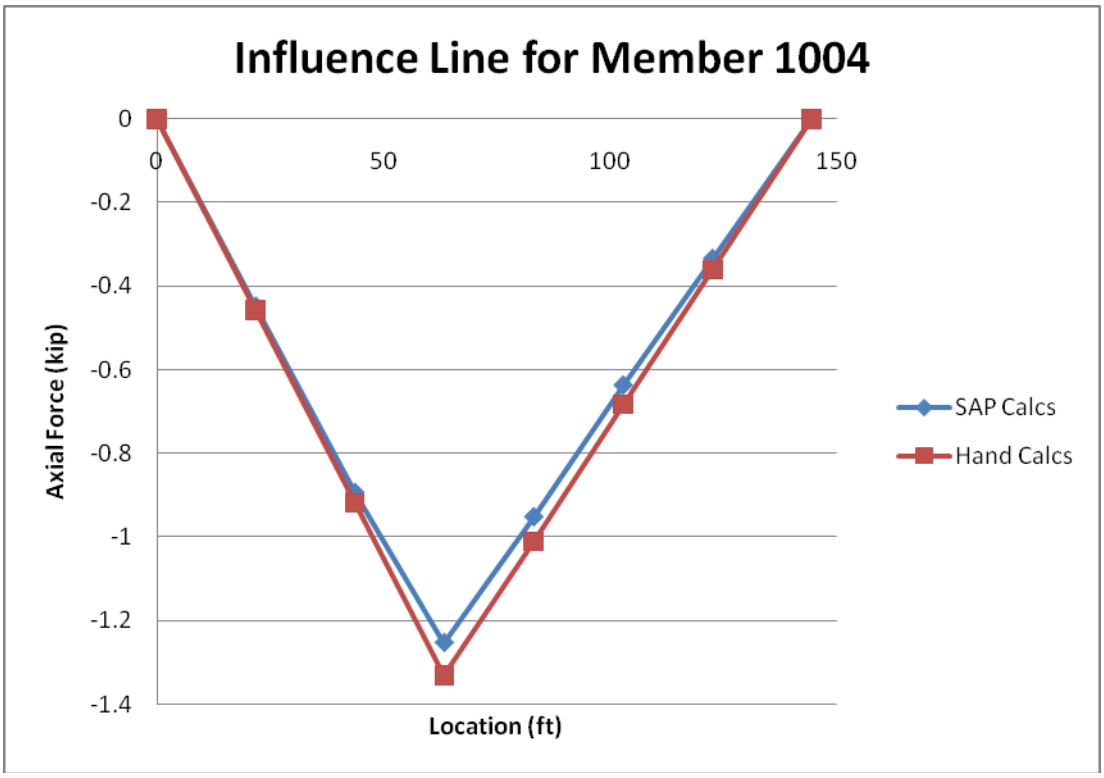

Figure **4-11.** Influence Line for Member 1004, Beech Creek Veterans Memorial Bridge

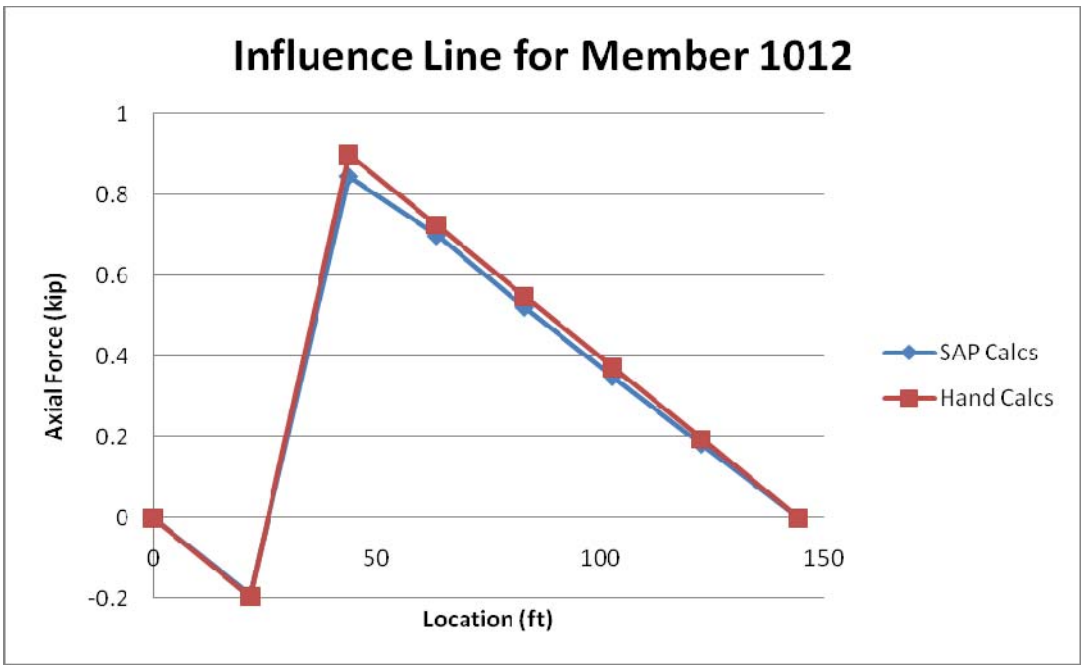

Figure **4-12.** Influence Line for Member 1012, Beech Creek Veterans Memorial Bridge

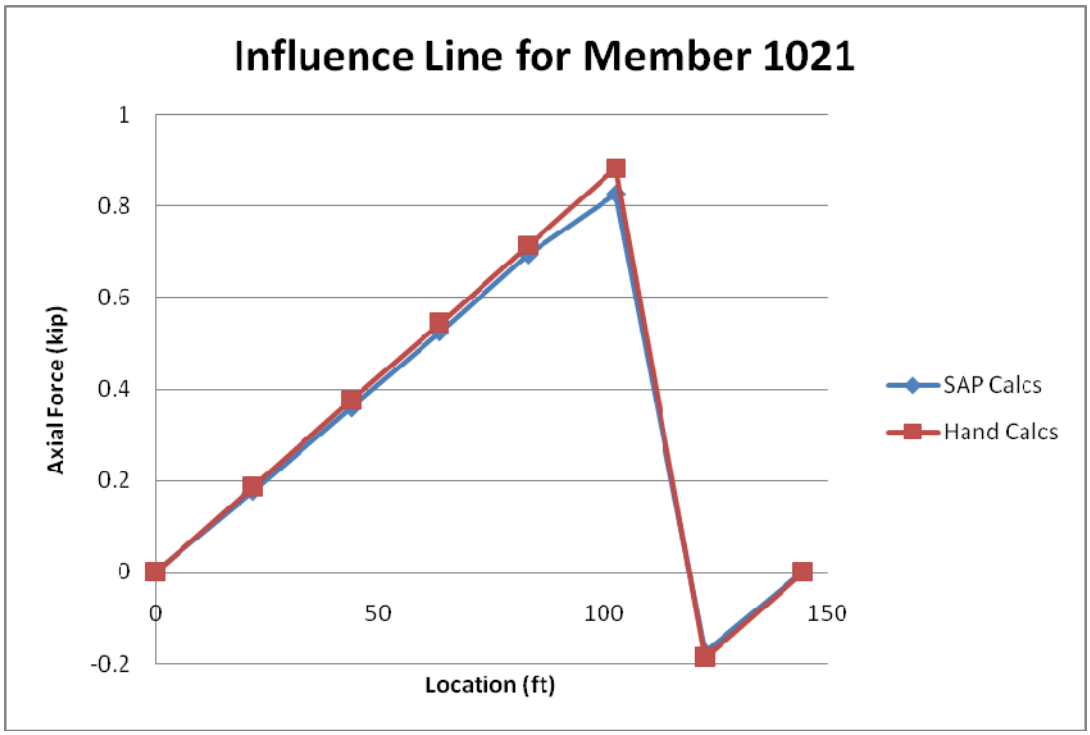

Figure **4-13.** Influence Line for Member 1021, Beech Creek Veterans Memorial Bridge

Table 4-4 shows the percentage error between the SAP analysis and the hand calculations. The location is measured from the west abutment. The largest error of -7.2% occurs in Member 1004, which is an upper chord member, at 37.40 m (122.626 ft) from the west abutment. Average errors of -3.74%, -3.84%, and -3.65% for each respective member was calculated. Overall, the validations of the SAP2000 pristine model compared to the hand calculations of the influence lines for the bridge were in good agreement.

Location m (ft)	Member 1004	Member 1012	Member 1021
0 (0)	0.0%	0.0%	0.0%
6.67 (21.875)	-2.0%	-3.1%	-5.3%
13.34 (43.75)	-2.6%	-6.1%	-4.5%
19.34 (63.469)	-5.8%	-3.7%	-3.7%
25.34 (83.188)	-5.7%	-4.9%	-2.9%
31.34 (102.907)	-6.6%	-6.2%	-6.4%
37.38 (122.626)	-7.2%	-6.7%	-6.4%
44.04 (144.5)	0.0%	0.0%	0.0%

Table **4-4.** Percentage Error Between SAP2000 and Hand Calculations

4.5 Summary

This chapter outlined the finite element models analyzed using SAP2000. Each analysis was a linear elastic analysis. Each model was described along with any validation or examination that was performed.

Chapter 5

Critical Member Analysis and Discussion

5.1 Introduction

This chapter discusses the analysis and results for the Beech Creek Veterans Bridge analytical model. Linear and plastic analyses were performed on two analytical models, pristine and deteriorated, to determine the critical member, the critical truck location that caused the highest force in certain truss members, and the load redistribution when critical members were removed. The global failure sequence of the members was also compared between the pristine and deteriorated models. Figure 5-1 shows a flowchart that details the steps used to complete the critical member analysis and critical member removal. The flowchart will be referred to throughout the chapter and detailed explanations for each process will follow.

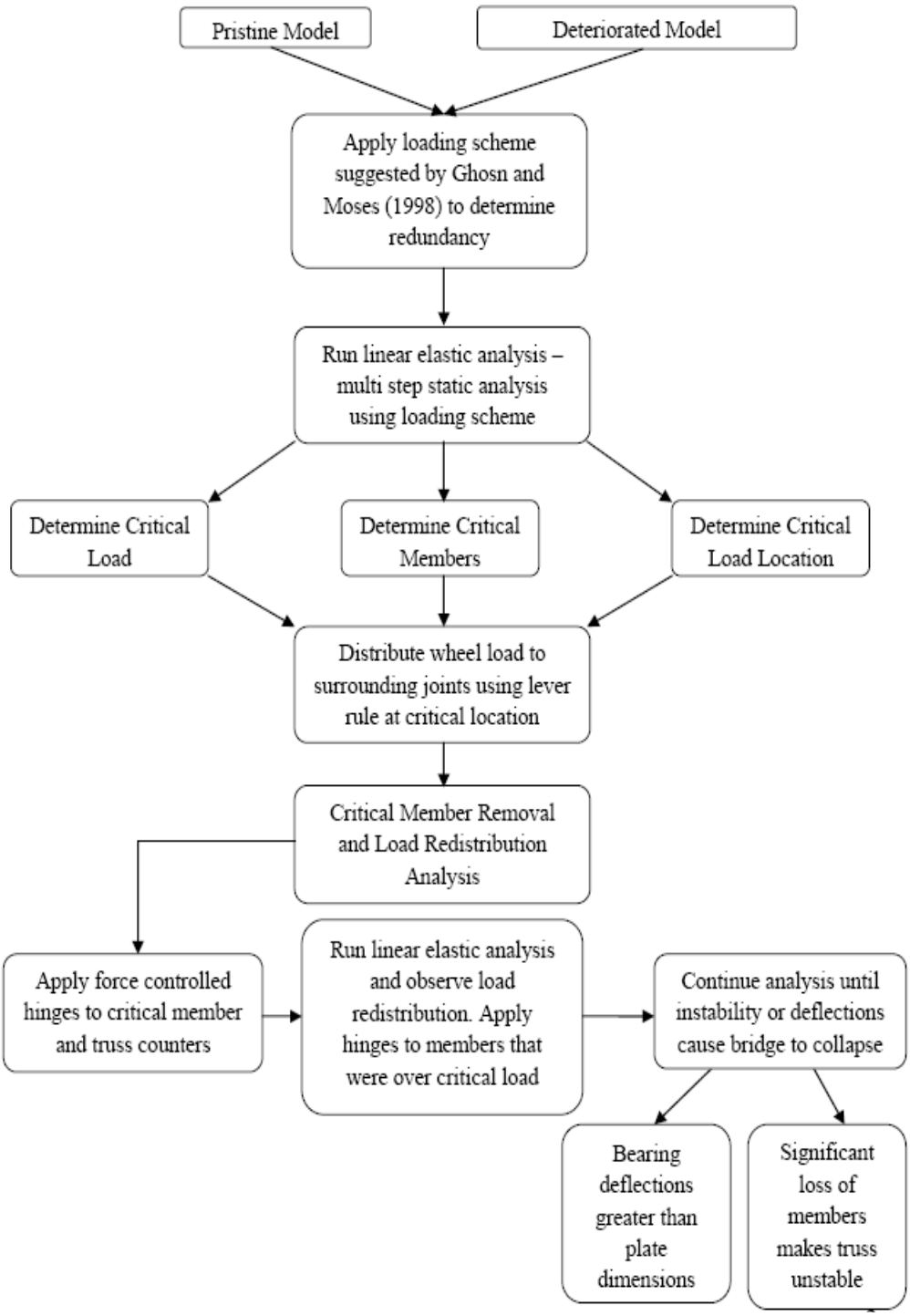

Figure **5-1**. Flowchart of Process for Evaluation of Beech Creek Veterans Memorial Bridge

5.2 Pristine Model

As discussed previously in Chapter 4, the pristine model of the Beech Creek Veterans Memorial Bridge used the original bridge plans and assumed there was no deterioration or section loss present in the model. The pristine model was created following recommendations and techniques used by Azizinamini et al. (1997). Section and geometric properties for the pristine bridge were referenced in Chapter 3. The following sections detail the steps outlined in Figure 5-1 for the pristine model.

5.2.1 Loading

The loading scheme used for the analysis was an approach proposed by Ghosn and Moses (1998) to determine the amount of redundancy in a structure. They recognized that redundancy was a function of the system behavior and not the individual component behavior. Their approach used two side-by-side AASHTO HS-20 trucks traversing the length of the bridge. Figure 5-2 shows the standard HS-20 truck with the axle loading and spacing and Figure 5-3 shows the minimum spacing for two side-by-side trucks. Their approach was created to permit analysis of a bridge without the use of complex structural models using finite element packages capable of elastic and inelastic analyses to determine the amount of redundancy in a structure.

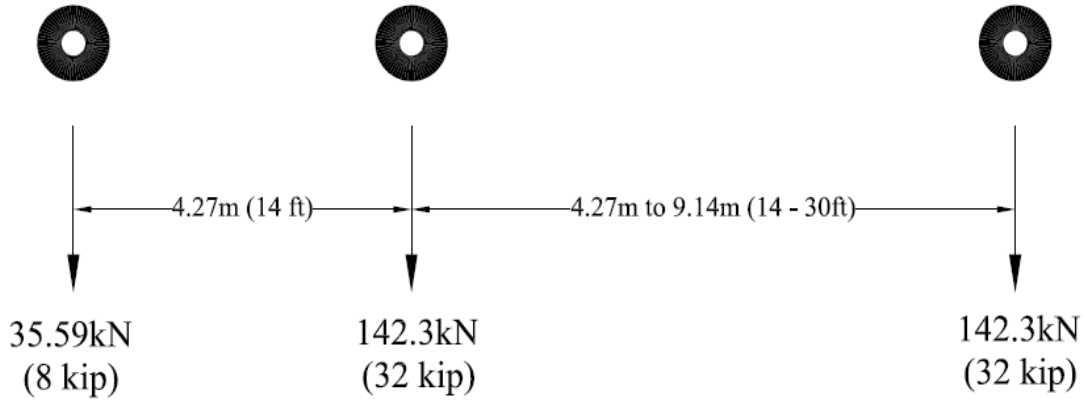

Figure **5-2**. Standard AASHTO HS-20 Truck

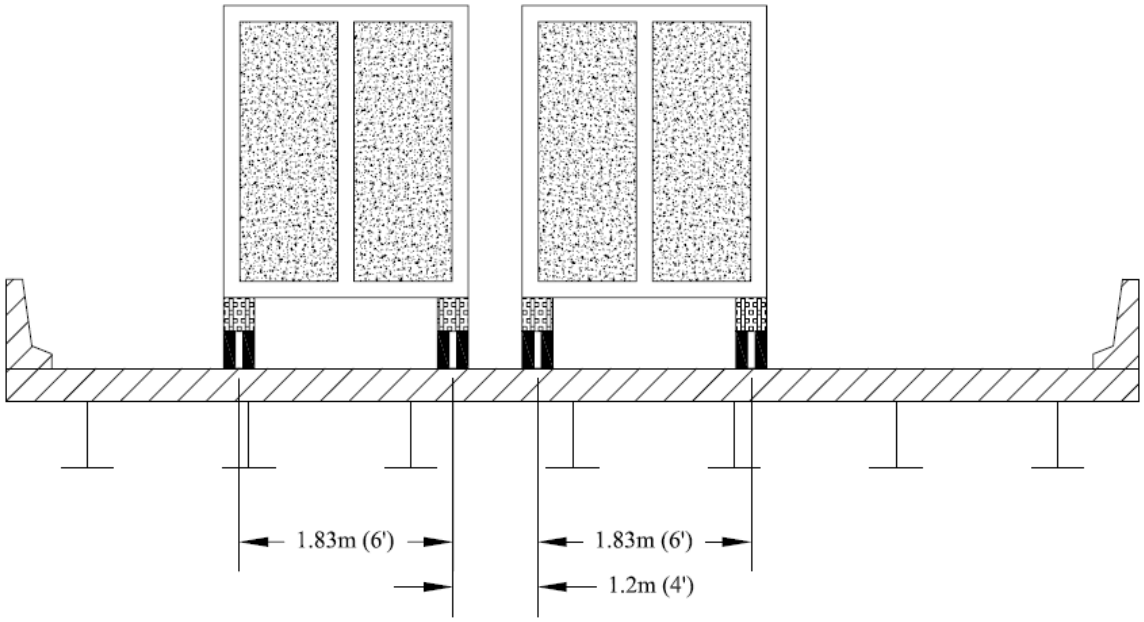

Figure **5-3**. Minimum Side-by-Side HS20 Truck Spacing

The approach used two side-by-side AASHTO HS-20 trucks and incrementally increased the axle load until the first member in the bridge failed. Failure was defined as

yielding in tension or yielding, buckling or interaction of the two in compression. HS-20 trucks were used because of their widespread use in the bridge engineering community as a design load. Also, side-by-side vehicles were used because they were considered to be the governing loading condition on the basis of bridge loading models assembled during the calibration of the AASHTO LRFD Bridge Code (Ghosn and Moses 1998). Figure 5-4 shows a schematic of side-by-side HS-20 trucks. The increase in axle load was an increment of an HS-20 truck. For example, three HS-20 trucks is defined as representing two stacks of three HS-20 trucks side-by-side (six trucks total). This was accomplished in SAP2000 by tripling the axle loads for an individual HS-20 truck. The number of HS-20 trucks that caused the first member to fail determines the amount of redundancy or capacity inherent in that structure (Ghosn and Moses 1998).

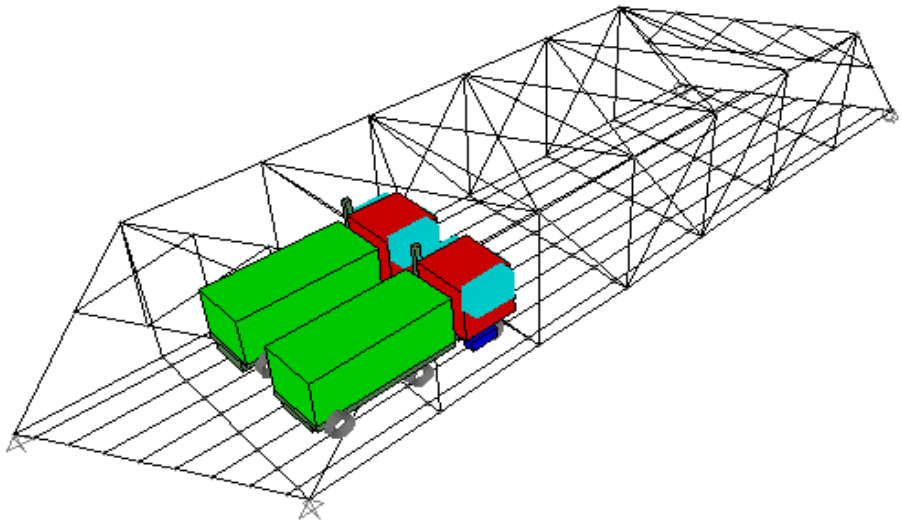

Figure **5-4**. Schematic of Side-by-Side HS-20 Trucks

The side-by-side HS-20 trucks traversed the length of the bridge in both directions. Figure 5-4 shows the forward direction, termed west-east direction, of the side-by-side HS-20 trucks. Figure 5-5 shows the other direction, termed east-west. This was necessary because the bridge was not symmetric and the forces in the members were different depending on the direction of the HS-20 tucks. The trucks were positioned so that the highest load was distributed to the north truss and then to the south truss. The lanes were 3.05 m (10 ft) wide and the truck axle spacing was 1.83 m (6 ft). The center of the lane was positioned to give the maximum effect to both trusses. Figure 5-6 shows

the centerline of each pair of side-by-side trucks; Lane 1 corresponding to causing maximum effect in the north truss and Lane 2 causing maximum effect to the south truss. This was accomplished by using the minimum curb distance of 0.61 m (2 ft), the width of the axles shown in Figure 5-2, and the minimum required transverse spacing between HS-20 trucks shown in Figure 5-3.

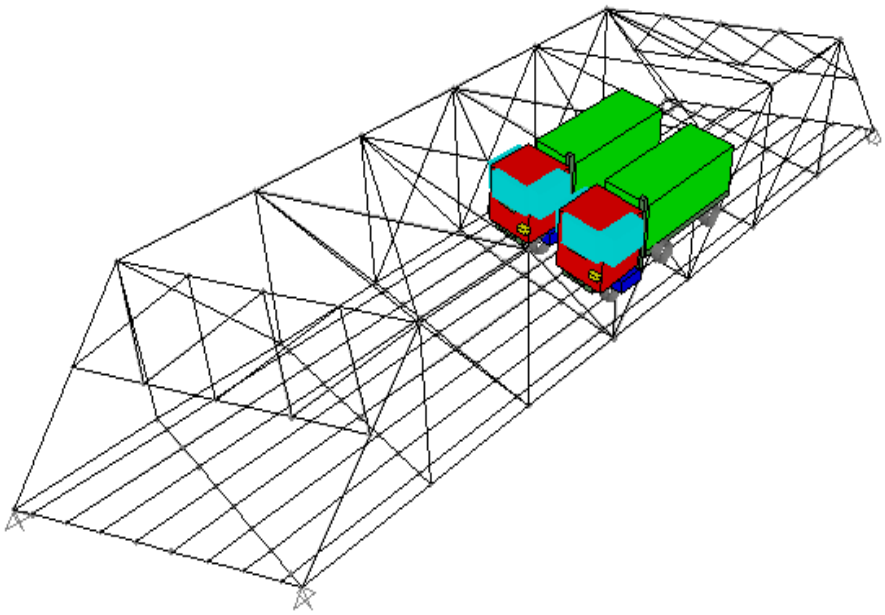

Figure **5-5**. HS-20 Trucks Traversing East to West

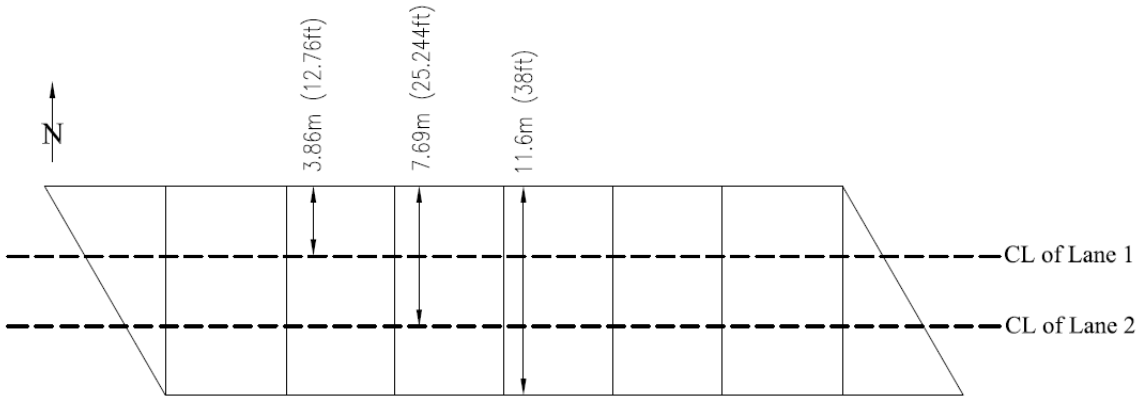

Figure **5-6**. Lane Designations

5.2.2 Critical Member Identification

Using the prescribed loading scheme, a multi-step static analysis was completed in SAP2000 to determine the critical members of the Beech Creek Veterans Memorial Bridge. The multi-step static analysis used a specific time-step size and total number of time steps along with the speed of the moving vehicle to determine the location of the loads and the response of the bridge at each time step. There are several assumptions when using the step-by-step analysis including; (1) the longitudinal position of each vehicle in its lane at the current time is determined from its starting position, speed and direction; (2) the vehicle is centered transversely in the lane; and (3) axle loads are applied to the bridge deck and then distributed to the joints.

The critical member was determined by running multiple HS-20 trucks across the bridge to determine which member yielded first in either tension or compression. The first members to fail were the counters in the center of the truss due to buckling. Counters are additional diagonals placed into central panels of a truss bridge that are

designed to carry tension only. The counters help distribute the tension load in other diagonal members to the verticals in the truss bridge. The true purpose of a counter is to distribute tensile forces to surrounding members. Depending on the direction and location of the HS-20 truck, either center diagonal could be in compression. Therefore, in the model, a compression limit of zero was applied to the center diagonals, the counters, of each truss. If the member was in compression, the analysis would redistribute the load to surrounding members.

Once the center diagonals had a compression limit defined in the model, the analysis was run to determine additional critical members in the truss. For this analysis, a member that yields, buckles, or a combination of both was considered incapable of carrying any load. This follows the approach proposed by Ghosn and Moses (1998) who considered a member being incapable of carrying any additional load after it yields. For tension members, the cross sectional area and the yield stress was used to determine their capacity. For compression members, the critical buckling load was determined based on Euler buckling load along with the moment of inertia, the unbraced length of the member, the modulus of elasticity, and the pinned-pinned boundary conditions. The critical buckling load was then compared to the compression yielding force for each of the members to determine which controlled. These boundary conditions were assumed from the modeling procedure and the connections were pinned connections. After the compression and tension limits were determined, a combination of the axial and bending effects were determined to see if any of the frame members (top and bottom chord of the truss) had a combined stress greater than the yield stress.

Since the capacity of the tension member does not depend on the unbraced length, the capacity of each element was determined first using the cross sectional area and a yield stress of 20.68 kN/cm^2 (30 ksi). Table 5-1 details the capacity of each of the tension elements in the north truss. Figures 5-7 and 5-8 show the north and south truss member identifications that will be used for the remainder of the chapter. The end posts have two elements because a node was needed to connect the lateral bracing at the top ends of the bridge. The lateral bracing is shown in Figure 5-6. The established capacity was compared to the results from the analytical model to determine how many multiple HS-20 trucks caused a member to yield or buckle.

Element ID	Location	Area cm^2 (in^2)	Yield Stress MPa (ksi)	Capacity kN (kips)
EL1	1001, 1002, 1009, 1010	257.93 (39.98)	182.9 (30)	5337.3 (1199.4)
EL2	1003, 1008	234.64 (36.37)		4855.4 (1091.1)
EL3	1004, 1005, 1006	281.13 (43.575)		5817.3 (1307.25)
EL4	1023-1025, 1027-1029	245.64 (38.075)		5083.0 (1142.25)
EL5	1026	280.48 (43.475)		5803.9 (1304.25)
EL6	1011, 1014, 1019, 1022	98.58 (15.28)		2039.9 (458.4)
EL7	1013, 1015, 1018, 1020	121.29 (18.8)		2509.8 (564)
EL8	1012, 1021	121.61 (18.85)		2516.5 (565.5)
EL9	1016, 1017	52.45 (8.13)		1085.4 (243.9)

Table **5-1**. Tensile Capacity of Members

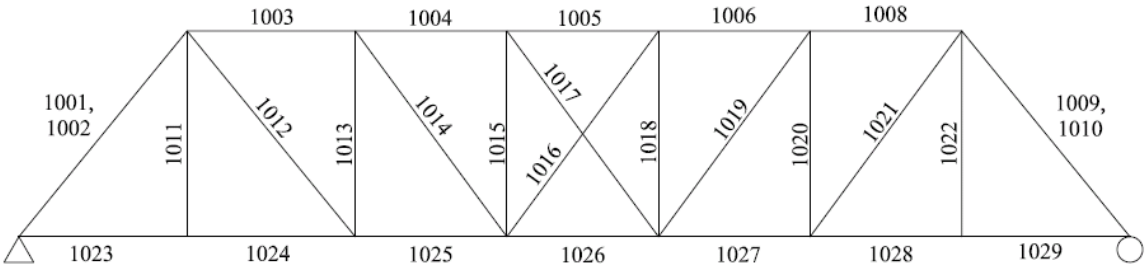

Figure **5-7**. North Truss Member Identification

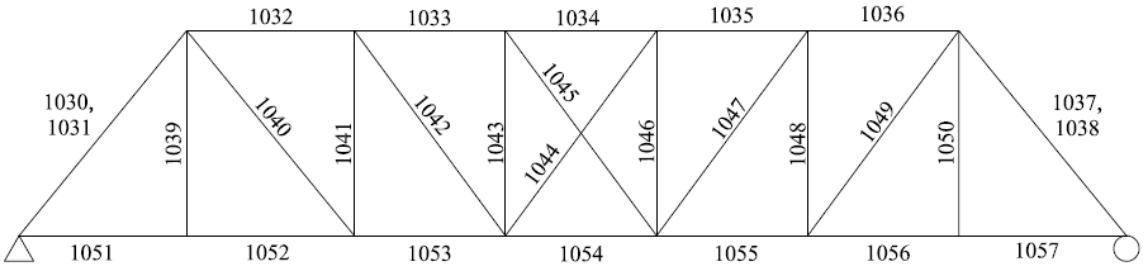

Figure **5-8**. South Truss Member Identification

From the linear elastic analysis of the Beech Creek Veterans Memorial Bridge results for stacked side-by-side HS-20 trucks were compiled. The compiled results were the maximum tensile and compressive forces when the trucks traversed the structure in both directions. The critical number of side-by-side HS-20 trucks was determined to be eight. Eight side-by-side HS-20 trucks caused two members in each truss, other than the counters, to go above their tensile capacity. It was unknown which member failed first under a loading of eight HS-20 trucks. Since this was unknown, each member was investigated to determine the load redistribution and failure pattern. Also, the critical location of the HS-20 trucks varied for each member and all four members would never fail at the same time since the trucks were at different locations along the length of the bridge. An individual analysis of each member was then completed to determine exactly where the HS-20 truck was located when that member reached its maximum axial force. Also, individual analyses were performed on each critical member to establish failure patterns to compare with the deteriorated model to determine if deterioration played a role in the global behavior of the bridge.

Tables 5-2 through 5-4 show the maximum tensile or compressive stresses in each member of the north truss calculated using axial force information from Tables B5-1 through B5-6 in Appendix B, which tabulate maximum axial forces in each members in the north and south truss caused by self weight and multiple HS-20 trucks. Negative values represent compression while positive values represent tension. The total stress in each member was determined using the stress from the member's self weight and the loading of multiple HS-20 trucks. The stresses in the members under a loading of eight HS-20 trucks showed that two members yielded in tension in the north truss. Members 1012 and 1021 had a stress of 221.9 MPa (32.2 ksi) and 222.5 MPa (32.3 ksi), respectively and can be seen in Tables 5-3 and 5-4 as the shaded values. Data for the south truss is shown in Tables B5.7 through B5.9 in Appendix B. Two members in the south truss, members 1040 and 1049, yielded under the eight trucks. Table 5-5 summarizes the critical axial force and stress in each of the critical members from the loading of eight stacked HS-20 trucks for the north and south truss.

Member ID	1 Truck MPa (ksi)	2 Truck MPa (ksi)	3 Truck MPa (ksi)	4 Truck MPa (ksi)	5 Truck MPa (ksi)	6 Truck MPa (ksi)	7 Truck MPa (ksi)	8 Truck MPa (ksi)
1001	-30.8 (-4.46)	-46.2 (-6.71)	-61.7 (-8.96)	-77.2 (-11.20)	-92.7 (-13.45)	-108.2 (-15.70)	-123.6 (-17.94)	-139.1 (-20.19)
1002	-29.5 (-4.29)	-44.5 (-6.46)	-59.5 (-8.64)	-74.5 (-10.81)	-89.5 (-12.99)	-104.5 (-15.17)	-119.5 (-17.34)	-134.5 (-19.52)
1003	-34.6 (-5.02)	-52.6 (-7.64)	-70.6 (-10.25)	-88.6 (-12.86)	-106.6 (-15.48)	-124.6 (-18.09)	-142.6 (-20.70)	-160.6 (-23.31)
1004	-33.1 (-4.80)	-50.1 (-7.27)	-67.1 (-9.74)	-84.1 (-12.21)	-101.1 (-14.68)	-118.2 (-17.15)	-135.2 (-19.62)	-152.2 (-22.09)
1005	-32.6 (-4.73)	-49.1 (-7.13)	-65.6 (-9.53)	-82.2 (-11.92)	-98.7 (-14.32)	-115.2 (-16.72)	-131.7 (-19.11)	-148.2 (-21.51)
1006	-33.3 (-4.84)	-50.3 (-7.31)	-67.3 (-9.77)	-84.3 (-12.24)	-10104 (-14.71)	-118.4 (-17.18)	-135.4 (-19.65)	-152.4 (-22.12)
1008	-33.6 (-4.88)	-50.7 (-7.35)	-67.7 (-9.82)	-84.7 (-12.29)	-101.7 (-14.77)	-118.8 (-17.24)	-135.8 (-19.71)	-152.8 (-22.18)
1009	-30.0 (-4.35)	-45.3 (-6.57)	-60.6 (-8.80)	-76.0 (-11.02)	-91.3 (-13.25)	-106.6 (-15.48)	-122.0 (-17.70)	-137.3 (-19.93)
1010	-32.2 (-4.67)	-48.2 (-6.99)	-64.2 (-9.31)	-80.2 (-11.64)	-96.2 (-13.96)	-112.2 (-16.28)	-128.2 (-18.60)	-144.2 (-20.93)

Table **5-2**. Total Stress in North Truss Members Due to Self Weight and HS-20 Trucks

Member ID	1 Truck MPa (ksi)	2 Truck MPa (ksi)	3 Truck MPa (ksi)	4 Truck MPa (ksi)	5 Truck MPa (ksi)	6 Truck MPa (ksi)	7 Truck MPa (ksi)	8 Truck MPa (ksi)
1011	27.7 (4.02)	49.8 (7.23)	71.9 (10.44)	94.1 (13.65)	116.2 (16.86)	138.3 (20.07)	160.4 (23.29)	182.6 (26.50)
1012	44.6 (6.47)	69.9 (10.15)	95.2 (13.82)	120.6 (17.50)	145.9 (21.18)	171.3 (24.86)	196.6 (28.54)	221.9 (32.21)
1013	-24.5 (-3.56)	-39.1 (-5.67)	-53.6 (-7.78)	-68.1 (-9.89)	-82.7 (-12.00)	-97.2 (-14.11)	-111.7 (-16.22)	-126.3 (-18.33)
1014	33.6 (4.88)	56.3 (8.16)	78.9 (11.45)	101.5 (14.73)	124.2 (18.02)	146.8 (21.31)	169.4 (24.59)	192.1 (27.88)
1015	3.6 (0.53)	9.5 (1.38)	15.4 (2.24)	21.3 (3.09)	27.2 (3.95)	33.1 (4.80)	39.0 (5.66)	44.9 (6.51)
1016	14.4 (2.08)	30.7 (4.46)	47.1 (6.84)	63.5 (9.22)	79.9 (11.60)	96.3 (13.97)	112.7 (16.35)	129.0 (18.73)
1017	12.1 (1.76)	26.9 (3.91)	41.7 (6.06)	56.5 (8.21)	71.3 (10.35)	86.1 (12.50)	101.0 (14.65)	115.8 (16.80)
1018	-8.1 (-1.18)	-13.7 (-1.98)	-19.2 (-2.78)	-24.7 (-3.59)	-30.2 (-4.39)	-35.7 (-5.19)	-41.3 (-5.99)	-46.8 (-6.79)
1019	35.8 (5.20)	60.0 (8.71)	84.2 (12.22)	108.4 (15.73)	132.6 (19.24)	156.7 (22.75)	180.9 (26.26)	205.1 (29.77)
1020	-26.1 (-3.79)	-41.5 (-6.02)	-56.9 (-8.26)	-72.3 (-10.49)	-87.7 (-12.72)	-103.1 (-14.96)	-118.5 (-17.19)	-133.9 (-19.43)

Table **5-3**. Total Stress in North Truss Members Due to Self Weight and HS-20 Trucks

Member ID	1 Truck MPa (ksi)	2 Truck MPa (ksi)	3 Truck MPa (ksi)	4 Truck MPa (ksi)	5 Truck MPa (ksi)	6 Truck MPa (ksi)	7 Truck MPa (ksi)	8 Truck MPa (ksi)
1021	44.9 (6.51)	70.2 (10.19)	95.6 (13.87)	121.0 (17.56)	146.3 (21.24)	171.7 (24.92)	197.1 (28.60)	222.4 (32.28)
1022	28.0 (4.06)	51.6 (7.50)	75.3 (10.93)	99.0 (14.36)	122.6 (17.79)	146.3 (21.23)	169.9 (24.66)	193.6 (28.09)
1023	17.4 (2.53)	26.4 (3.82)	35.3 (5.12)	44.2 (6.41)	53.1 (7.70)	62.0 (9.00)	70.9 (10.29)	79.8 (11.58)
1024	14.7 (2.14)	22.4 (3.26)	30.1 (4.37)	37.8 (5.49)	45.5 (6.61)	53.2 (7.73)	60.9 (8.84)	68.6 (9.96)
1025	24.6 (3.57)	37.7 (5.47)	50.8 (7.37)	63.8 (9.26)	76.9 (11.16)	90.0 (13.06)	103.0 (14.95)	116.1 (16.85)
1026	25.1 (3.64)	37.9 (5.50)	50.7 (7.36)	63.5 (9.22)	76.3 (11.08)	89.1 (12.94)	101.9 (14.80)	114.8 (16.660
1027	23.5 (3.41)	35.8 (5.20)	48.2 (6.99)	60.5 (8.78)	72.8 (10.57)	85.1 (12.35)	97.4 (14.14)	109.8 (15.93)
1028	13.9 (2.02)	21.3 (3.09)	28.7 (4.16)	36.1 (5.24)	43.5 (6.31)	50.9 (7.39)	58.3 (8.46)	65.7 (9.54)
1029	15.7 (2.27)	24.0 (3.48)	32.3 (4.69)	40.7 (5.90)	49.0 (7.11)	57.3 (8.32)	65.7 (9.53)	74.0 (10.74)

Table **5-4**. Total Stress in North Truss Members Due to Self Weight and HS-20 Trucks

Member	Axial Force kN (kips)	Stress MPa (ksi)
1012	2702 (607.2)	222 (32.2)
1021	2708.3 (608.6)	222.7 (32.3)
1040	2647.3 (594.9)	217.9 (31.6)
1049	2691.4 (604.8)	221.3 (32.1)

Table **5-5**. Critical Axial Tensile Force and Stress for North and South Truss Members

After the critical tensile members were determined, critical compression members were checked to ensure none of the members buckled under the eight HS-20 trucks. Table 5-6 shows the moment of inertia and unbraced length for each of the compression members as well as the critical buckling load. A comparison between the yield load in compression and the critical buckling load determined that for every member except for Member 7, the yield load controlled in compression. The compression members were the end posts, the top chord, and the verticals. The critical load was determined using the Euler buckling equation (Equation 5.1).

$$P_{CR} = \frac{\pi^2 EI}{L^2} \tag{5.1}$$

where E is the modulus of elasticity, I is the least moment of inertia for the member's cross sectional area, and L is the unbraced length of the member (Hibbeler 2004).

Element ID	Location	Moment of Inertia cm^4 (in^4)	Length m (ft)	Buckling Load kN (kips)	Yield Load kN (kips)
EL1	1001, 1002, 1009, 1010	77652.1 (1865.6)	10.53 (34.55)	13823.5 (3106.4)	5337.3 (1199.4)
EL2	1003	72757.3 (1748)	6.67 (21.875)	32310.3 (7260.7)	4855.4 (1091.1)
EL3	1004	82351.4 (1978.5)	6.01 (19.719)	45005.1 (10113.5)	5817.3 (1307.25)
EL3	1005	82351.4 (1978.5)	6.01 (19.719)	45005.1 (10113.5)	5817.3 (1307.25)
EL3	1006	82351.4 (1978.5)	6.01 (19.719)	45005.1 (10113.5)	5817.3 (1307.25)
EL2	1008	72757.3 (1748)	6.01 (19.719)	39761.9 (8935.3)	4855.4 (1091.1)
EL7	1011, 1013, 1015, 1018, 1020, 1022	7267.4 (174.6)	8.15 (26.75)	2158.2 (485.0)	2509.8 (564)

Table **5-6**. Critical Buckling Load for Compression Members

Using axial forces from Tables B5-1 through B5-6, the maximum compressive forces were compared to the critical buckling load. The maximum compressive force was 4288.9 kN (963.8 kips) in upper chord, Member 1006. Member 1006 has a critical buckling load of 3773.2 kN (847.9 kips). The maximum compressive force in the vertical members was 1495.6 kN (336.1 kips) and the critical buckling load was 2158.2 kN (485.0 kips). Outside of the counters, loads in all of the compression members in the Beech Creek Veterans Memorial Bridge were under the critical elastic buckling loads determined in Table 5-2.

The top and bottom chords of the truss needed to be checked for combined axial and bending forces. The top chord was in compression and acted as a beam column while the bottom chord combined tension and bending. This check was needed because these members were modeled as frame elements as discussed in Chapter 4 Section 3,

capable of carrying axial and bending forces. Table 5-7 shows the combined axial and bending stresses for the top and bottom chord of the North Truss. The axial and bending forces were compiled from running the eight side-by-side HS-20 trucks. The maximum axial and bending moment (about the x-axis) were compiled from the SAP2000 output. The determined stresses were compared to the yield stress of 182.9 MPa (30 ksi) to determine if any members of the top and bottom chord were above yield under combined compression and bending. From the analysis, none of the members had stresses greater than the yield stress under combined loads.

Member	Element	Area cm^2 (in^2)	S_x cm^3 (in^3)	P kN (kip)	M kN-m (kip-in)	P/A MPa (ksi)	M/Sx MPa (ksi)	P/A + M/Sx MPa (ksi)
1001	EL1	257.4 (39.9)	3666.4 (223.7)	-3185.8 (-715.9)	61.4 (543.4)	-109.4 (-17.9)	14.8 (2.43)	124.2 (20.4)
1002	EL1	257.4 (39.9)	3666.4 (223.7)	-2187.2 (-491.5)	180.8 (1600.4)	-75.1 (-12.3)	43.6 (7.15)	118.7 (19.5)
1003	EL2	234.8 (36.4)	3333.7 (203.4)	-1652.6 (-371.4)	266.7 (2359.8)	-62.2 (-10.2)	70.7 (11.60)	132.9 (21.8)
1004	EL3	281.2 (43.6)	4090.9 (249.6)	-3814.6 (-857.2)	23.9 (211.7)	-119.9 (-19.7)	5.2 (0.85)	125.0 (20.5)
1005	EL3	281.2 (43.6)	4090.9 (249.6)	-3718.8 (-835.7)	-6.7 (-59.2)	-116.9 (-19.2)	-1.4 (-0.24)	118.3 (19.4)
1006	EL3	281.2 (43.6)	4090.9 (249.6)	-3829.7 (-860.6)	-15.3 (-135.2)	-120.3 (-19.7)	-3.3 (-0.54)	123.7 (20.3)
1008	EL2	234.8 (36.4)	3333.7 (203.4)	-3199.0 (-718.9)	20.7 (183.5)	-120.4 (-19.7)	5.5 (0.90)	125.9 (20.7)
1009	EL1	257.4 (39.9)	3666.4 (223.7)	-3167.9 (-711.9)	47.0 (415.5)	-108.8 (-17.8)	11.3 (1.86)	120.1 (19.7)
1010	EL1	257.4 (39.9)	3666.4 (223.7)	-3305.8 (-742.9)	-26.9 (-237.8)	-113.5 (-18.6)	-6.5 (-1.06)	120.0 (19.7)
1023	EL4	245.7 (38.1)	5913.5 (360.8)	1775.4 (399.0)	215.0 (1902.9)	63.8 (10.5)	32.2 (5.27)	96.0 (15.7)
1024	EL4	245.7 (38.1)	5913.5 (360.8)	1514.4 (340.3)	82.7 (732.2)	54.5 (8.9)	12.4 (2.03)	66.8 (11.0)
1025	EL4	245.7 (38.1)	5913.5 (360.8)	2570.2 (577.6)	69.6 (615.8)	92.4 (15.2)	10.4 (1.71)	102.8 (16.9)
1026	EL5	280.6 (43.5)	6711.7 (409.5)	2703.6 (607.6)	54.9 (486.2)	85.2 (14.0)	7.2 (1.19)	92.4 (15.2)
1027	EL4	245.7 (38.1)	5913.5 (360.8)	2424.1 (544.7)	75.8 (670.9)	87.2 (14.3)	11.3 (1.86)	98.5 (16.2)
1028	EL4	245.7 (38.1)	5913.5 (360.8)	1456.0 (327.2)	83.9 (742.2)	52.4 (8.6)	12.5 (2.06)	64.9 (10.6)
1029	EL4	245.7 (38.1)	5913.5 (360.8)	1639.4 (368.4)	226.4 (2004.0)	59.0 (9.7)	33.9 (5.55)	92.8 (15.2)

Table **5-7**. Combined Axial and Bending Stresses for Top and Bottom Chord, North Truss

Four members were determined to be critical in the Beech Creek Veterans Memorial Bridge from the pristine elastic analysis: 1012, 1021, 1040 and 1049 (see

Figures 5-6 and Figure 5-7 for member's IDs). The maximum stress in each of the members occurred at different times while the eight side-by-side stacked truck traversed the bridge. The next step in the analysis was to determine where the eight side-by-side HS-20 trucks were located when the axial force in the member was a maximum so that loads from the trucks can be distributed to the floorsystem to perform the critical member removal and load redistribution analyses.

5.2.3 Critical Load Location

The critical location of the multiple HS-20 trucks was needed to determine where the truck was when each member had its maximum axial force so that the truck load could be positioned correctly for future plastic analyses. The critical location was determined by running a multi-step static analysis and analyzing each time step. The duration of the loading was 200 seconds and the load traversed the bridge in 10 seconds intervals. The speed of the truck was 30.5 cm/sec (1 ft/sec). With those settings, the analysis produced results every 3.05 m (10 ft) along the length of the bridge.

Each of the four critical members determined previously had critical locations for the truck stacks traversing the structure in both directions. Both directions were investigated because of the skew of the bridge and the different axle configuration. The first direction investigated was the truck traversing west to east across the bridge as shown in Figure 5-4. Then the truck traversing east to west was investigated as shown in Figure 5-6. Figure 5-9 through Figure 5-16 show the axial forces in each critical member for single side-by-side HS-20 trucks through eight stacked side-by-side HS-20 trucks.

The horizontal axis represents the time steps and the vertical axis is the axial force in the member due to the different HS-20 trucks. Also shown on each plot is the yield capacity for each member of 2516.5 kN (565.5 kips).

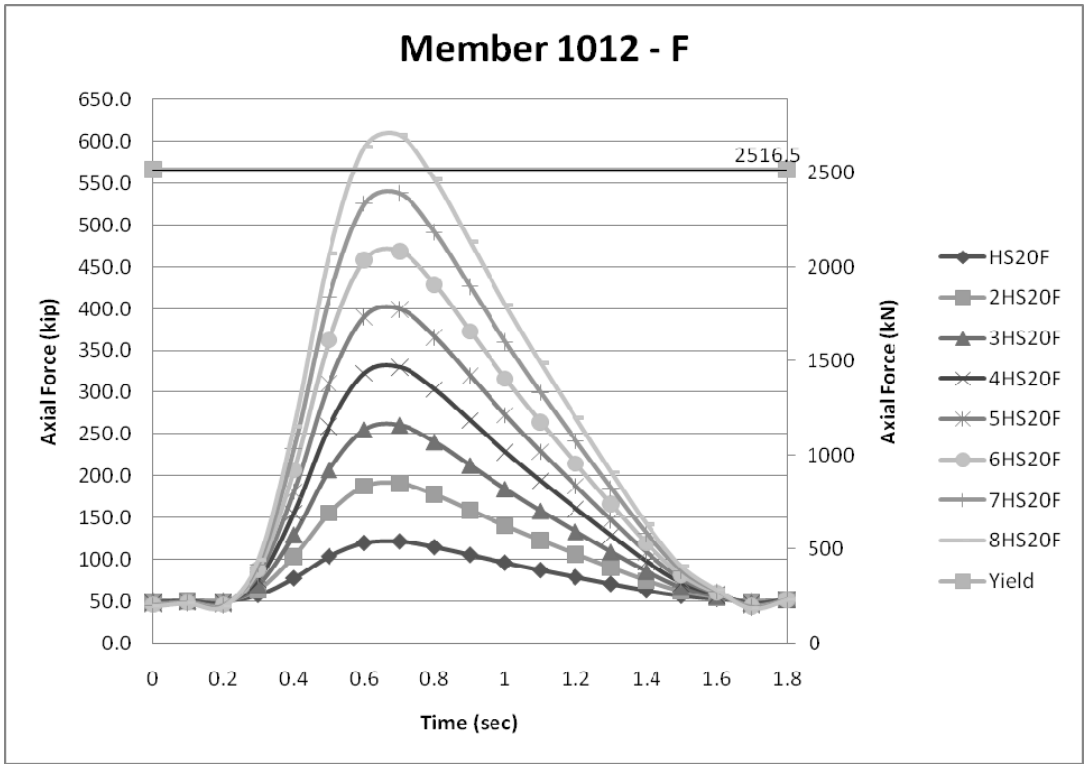

Figure **5-9**. Axial Force in Member 1012 Due to Incrementing West to East HS-20

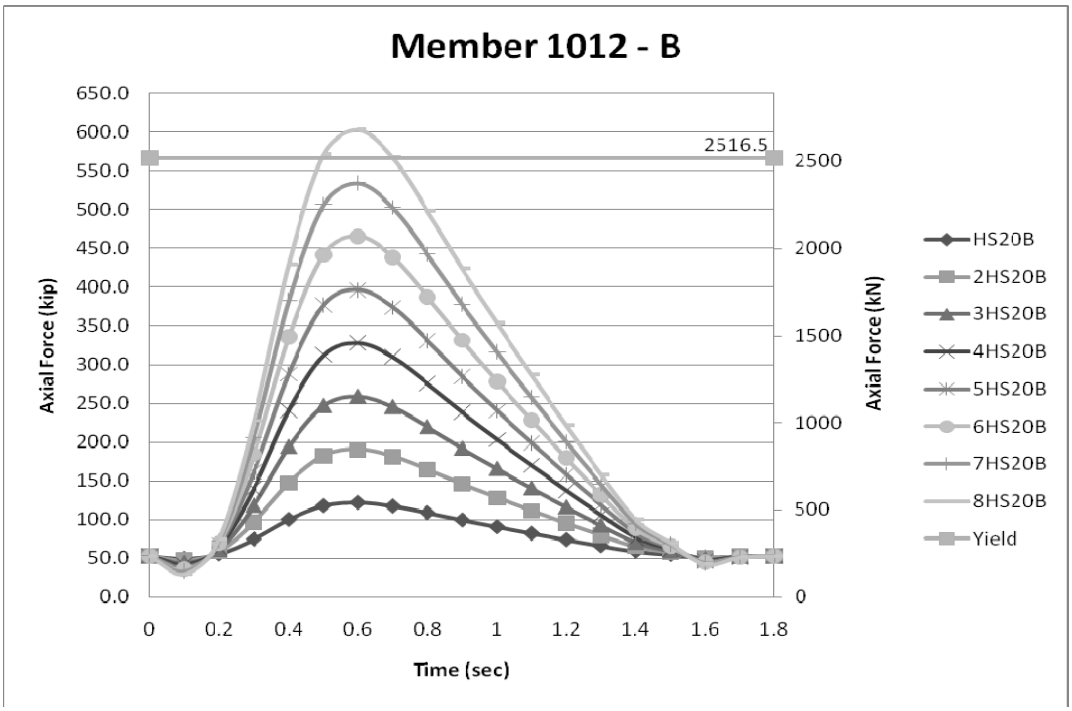

Figure **5-10**. Axial Force in Member 1012 Due to Incrementing East to West HS-20

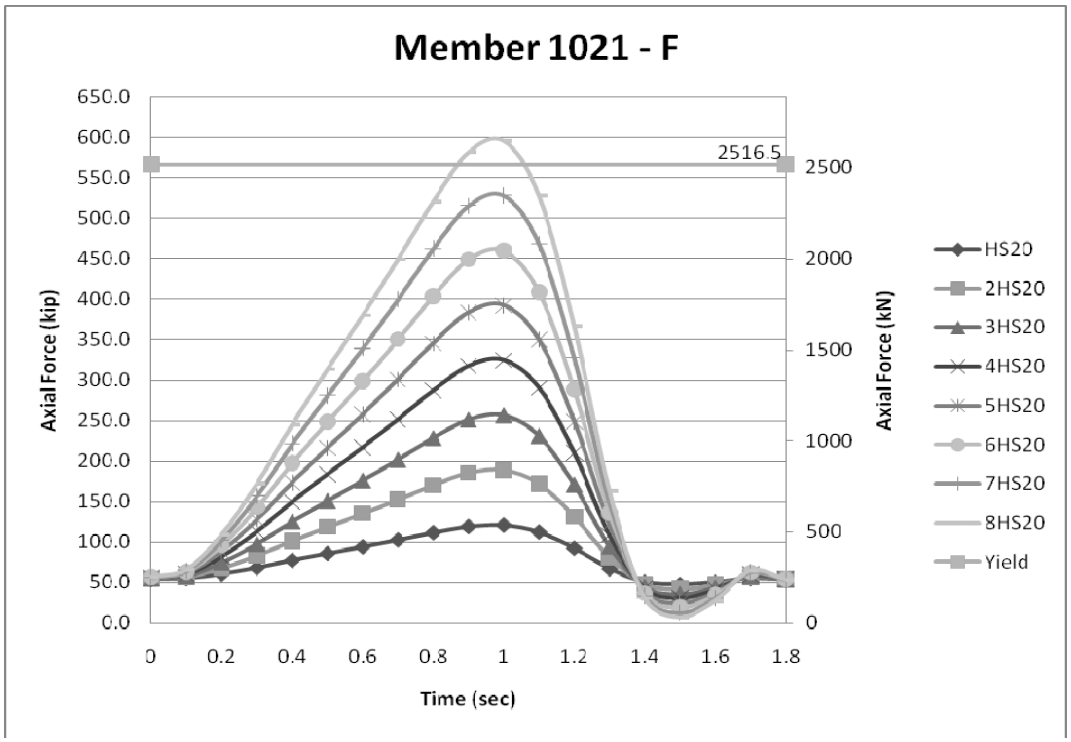

Figure **5-11**. Axial Force in Member 1021 Due to Incrementing West to East HS-20

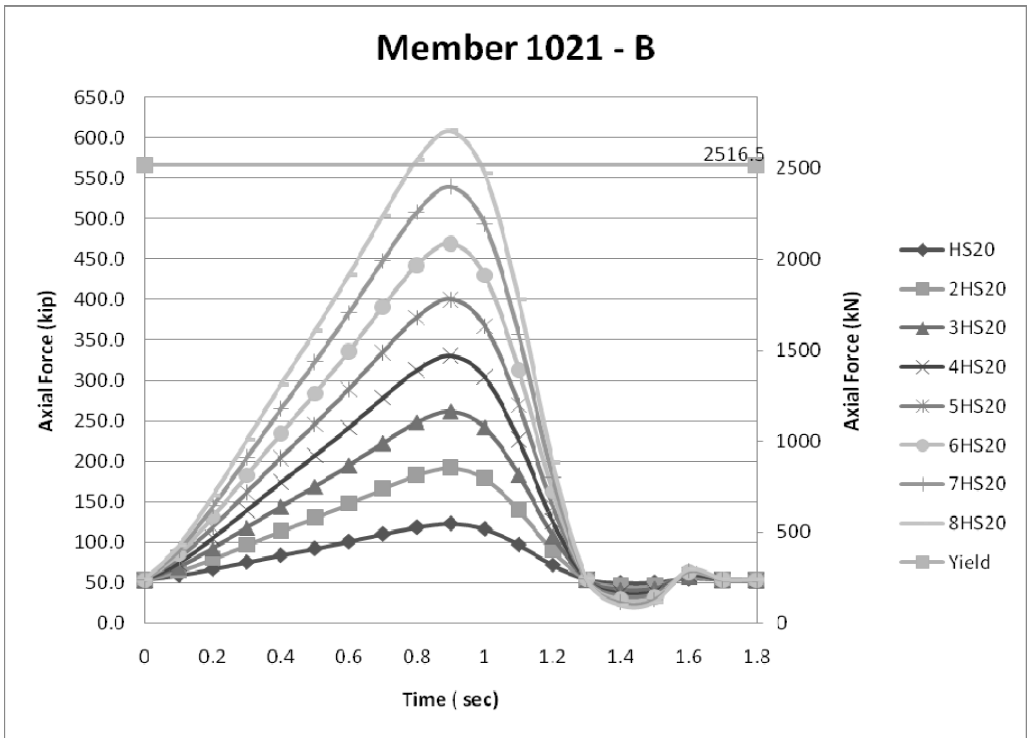

Figure **5-12**. Axial Force in Member 1021 Due to Incrementing East to West HS-20

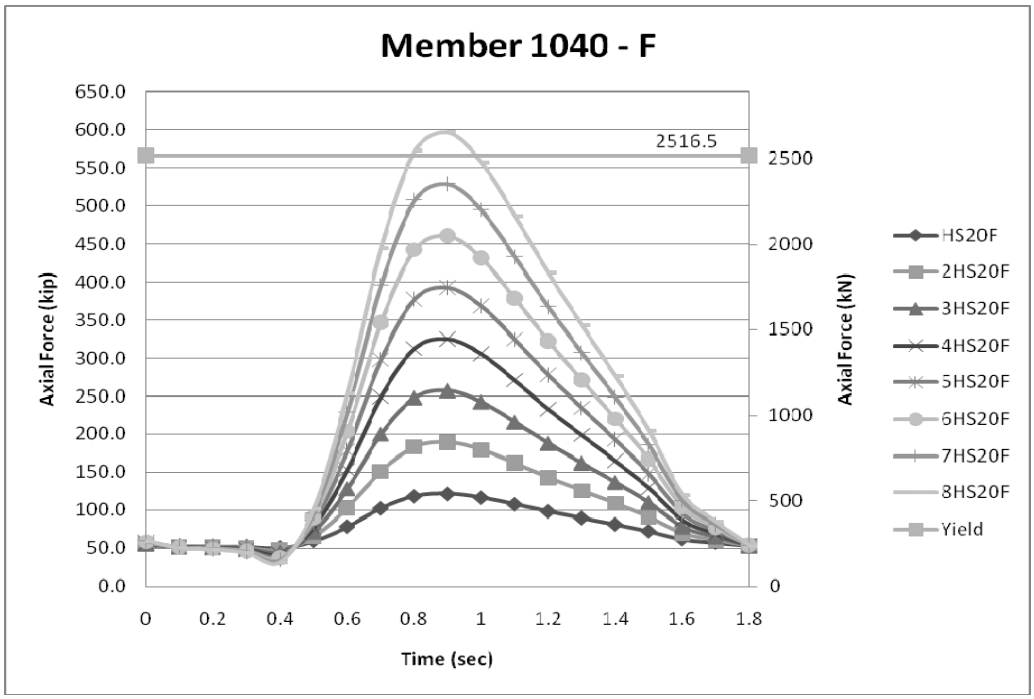

Figure **5-13**. Axial Force in Member 1040 Due to Incrementing West to East HS-20

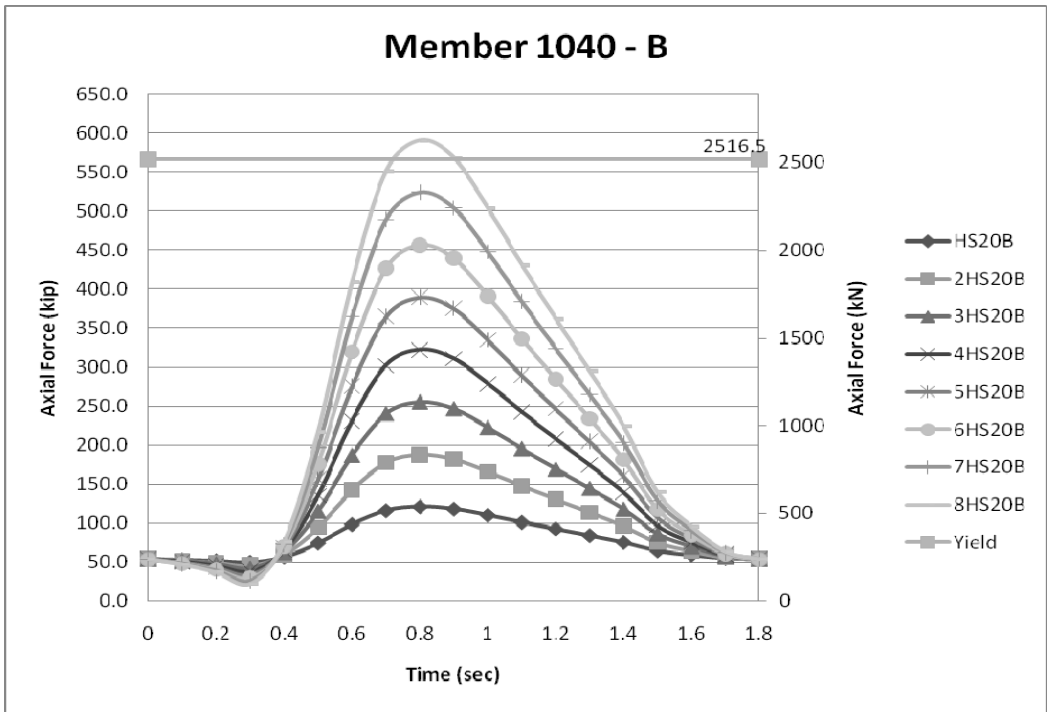

Figure **5-14**. Axial Force in Member 1040 Due to Incrementing East to West HS-20

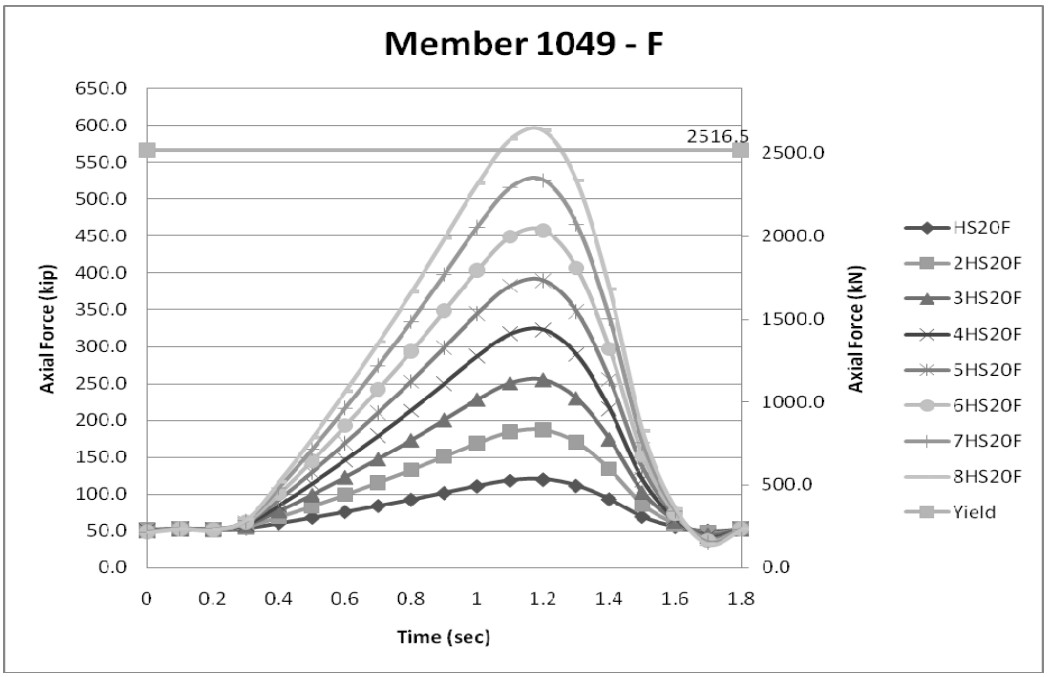

Figure **5-15**. Axial Force in Member 1049 Due to Incrementing West to East HS-20

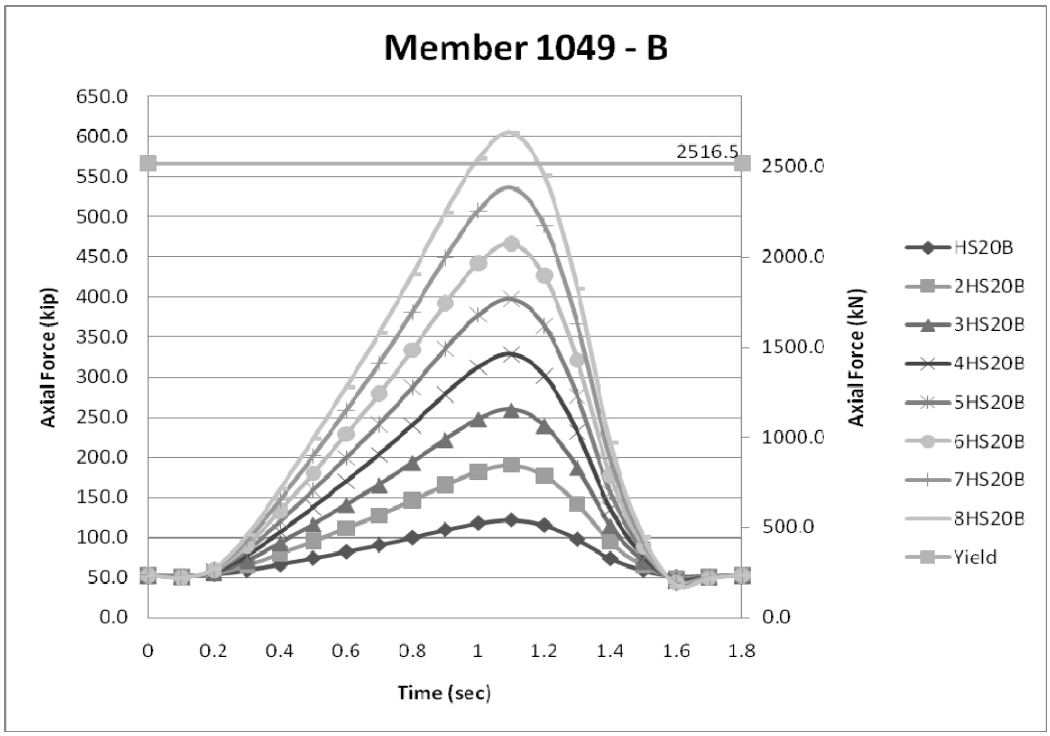

Figure **5-16**. Axial Force in Member 1049 Due to Incrementing East to West HS-20

Figures 5-9 and 5-10 show that, for Member 1012 with the truck traversing forward, the critical load occurred at time 0.7 seconds. Therefore, the critical location for Member 1012 with the truck traversing west to east was 21.35 m (70 ft) from the west abutment. The lead axle is located at the critical location and the remaining axles are spaced accordingly behind the lead axle. The critical location for the truck traversing east to west for Member 1012 was 18.29 m (60 ft) from the west abutment. These two locations indicate where the eight HS-20 trucks were located when the axial forces in Member 1012 were maximum. The truck traversing forward was the critical case because it caused the highest axial force of 2702 kN (607.2 kips) in the member.

Figures 5-11 and 5-12 indicate that the critical location for Member 1021, in the north truss, was determined to be 30.48 m (100 ft) from the west abutment for the truck traversing west to east. For trucks travelling in the other direction the critical location was determined to be 27.43 m (90 ft) from the west abutment. Eight stacked side-by-side trucks traversing east to west and located 27.43 m (90 ft) from the west abutment caused the highest axial force of 2707.8 kN (608.5 kips) in member 1021.

Figures 5-13 and 5-14 show that, for Member 1040 with the truck traversing west to east, the critical load occurred at 0.9 seconds, or 27.43 m (90 ft) from the west abutment. The critical location for the truck traversing the opposite direction was 24.38 m (80 ft) from the west abutment. The worst case was the trucks traversing west to east with an axial force of 2655.8 kN (596.8 kips).

Figures 5-15 and 5-16 indicate that the critical location for Member 1049, in the north truss, was determined to be 36.58 m (120 ft) from the west abutment for the truck traversing west to east. For the opposite travel direction the critical location was determined to be 33.53 m (110 ft) from the west abutment. Eight stacked side-by-side trucks traversing east to west caused the highest axial force of 2691.4 kN (604.8 kips) in member 1049.

Table 5-8 summarizes the eight critical truck stack locations for the four critical members. The shaded values are the most critical load locations. At these critical load locations, the loads from the eight HS-20 trucks were distributed both transversely and longitudinally to the surrounding joints using the lever rule. This was completed for the critical member removal analysis because the multi-step analysis procedure in SAP2000 could not distribute trucks loads to the superstructure and then redistribute them to the

superstructure when members failed. Loads had to be placed directly onto the structure model so that the multi-step analysis could be completed.

Critical Member	Truck Direction	Critical Location m (ft)
Member 1012	8HS-20 F	21.34 (70)
	8HS-20 B	18.29 (60)
Member 1021	8HS-20 F	30.48 (100)
	8HS-20 B	27.43 (90)
Member 1040	8HS-20 F	27.43 (90)
	8HS-20 B	24.38 (80)
Member 1049	8HS-20 F	36.58 (120)
	8HS-20 B	33.53 (110)

Table **5-8**. Critical Location, Distance From West Abutment

Figure 5-17 shows a typical floorsystem in the Beech Creek Veterans Memorial Bridge and the wheel load distribution completed for transferring the loads to the surrounding joints. The wheel loads were first transversely distributed to the stringers assuming the deck was simply supported. After the load was transferred to the stringers, the point loads were longitudinally distributed to the floorbeams assuming the stringers were simply supported and the floorbeams carried these loads to the truss lower chord. This process was completed for each critical load location. Once the loads were distributed to the joints, a critical member removal analysis was completed to determine the member failure sequence and load redistribution.

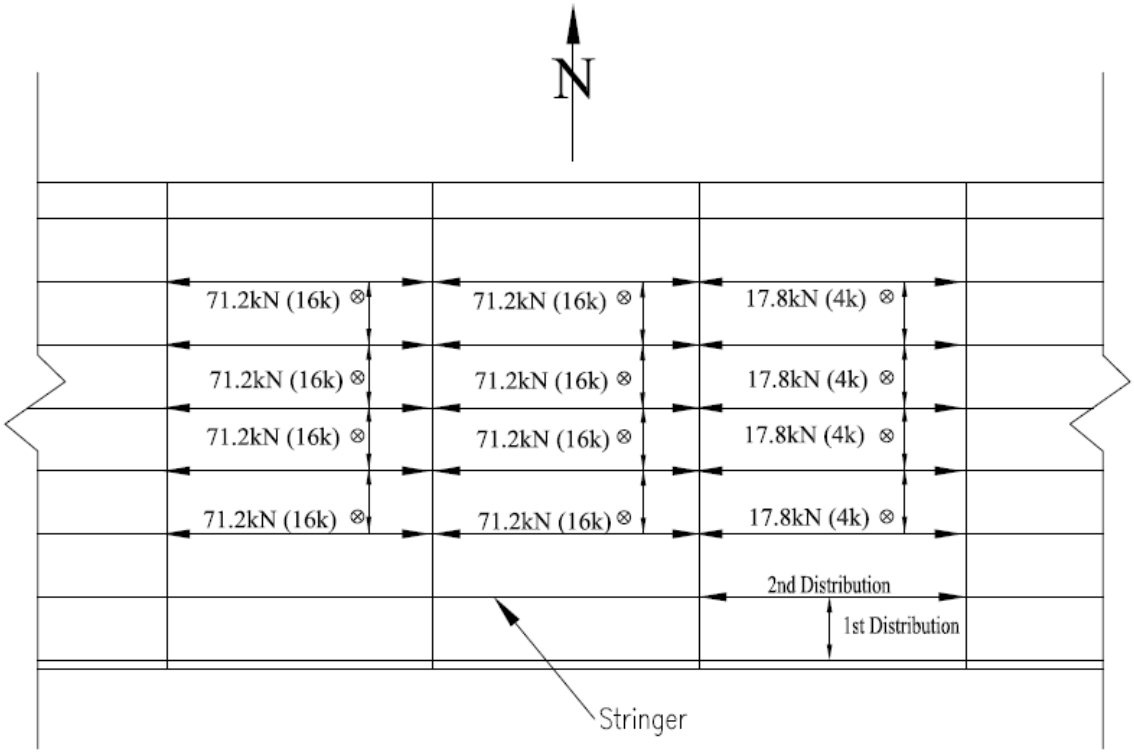

Figure **5-17**. Typical Wheel Load Distribution to Joints for HS-20 Truck

5.2.4 Critical Member Removal and Load Redistribution Analysis

A critical member removal and load redistribution analysis was completed to understand the load path when a member failed under a specific load using SAP2000. Since a member was incapable of carrying any load after it fails, the member was considered removed from the model and the load was redistributed to the rest of the structure. The effects of the load redistribution were analyzed. Also, removal analysis determined the global failure sequence of the bridge for each of the critical members determined in the previous section. Individual analyses were completed to establish failure patterns for each of the critical members to compare with the deteriorated model.

The analyses also were completed to determine if one member could be identified as the most critical member in the bridge.

To achieve critical member removal, axial force hinges were used. SAP2000 has two types of hinges; deformation controlled and force controlled. Deformation controlled hinges use either a defined force-displacement model or stress-strain curve to establish the yield value and the deformations following yield. Force controlled hinges have several hinge properties including; axial force, shear, torsion, moment, or interacting shear and moment capacities. For this analysis, axial force controlled hinges were used because the members that were shown to be critical from the initial analysis were tension diagonals in the truss bridge and they do not incorporate bending effects. Axial force controlled hinges causes the hinge to lose all carrying capacity once the maximum axial force was attained. Once the maximum axial force is met in the hinge, the hinge unloads causing a redistribution of the force to other members remaining in the truss. Force controlled hinges were used in the analysis because the maximum tensile and compressive force for members in the truss were known. The yield force was specified as the maximum tensile force and the Euler buckling load or the yield compression force was specified as the maximum compressive force because the member was considered incapable of carrying any load once it failed. The combined axial and bending effects were checked at each member removal step to ensure that none of the top or bottom chord members were critical.

The critical member removal analysis began with placing force controlled hinges in the center diagonals. The center diagonals were designed as counters and only able to carry tensile forces. Depending on the location of the critical load, one of the center

diagonals was in tension and the other was in compression. After hinges were placed in the center diagonals, a force controlled hinge was placed in the critical member determined from the previous section. The location and length of the force controlled hinge was not critical because the critical members only carried axial forces and when one part of the member had failed, the entire member had failed. An analysis, with the eight HS-20 trucks at the critical load location, was completed to cause the critical member to fail. The analysis started with a load of zero at the critical load location on the structure and was ramped to the eight stacked HS-20 trucks. Once the hinge was activated, the load the member was carrying was redistributed to surrounding members. The surrounding members were then checked to determine if any of the members had a load greater than the yield or buckling critical load. The combined axial and bending stresses were checked in the top and bottom chord. If a member yielded, buckled or a combination of both, an axial force controlled hinge was placed in that member. Another analysis was completed and local redistribution occurred as the second hinge was activated. Table 5-1 and Table 5-6 give the maximum tensile and compressive forces used in defining the force controlled hinges. These values for the critical members in the Beech Creek Veterans Memorial Bridge were based on the yield strength, area of the member, the unbraced length of the member, and the moment of inertia. This process continued until the global failure limit of the structure, as defined below, was reached.

One failure limit was defined for this analysis. The failure limit was termination of the analysis in SAP2000, more than likely caused by excessive instability that was indicative of collapse of the structure. SAP2000 limits the negative slope of a hinge to be no stiffer than 10% of the elastic stiffness of the frame element containing the hinge.

SAP2000 tried to maintain the unloading curve close to the loading curve and in the case that it could not, the analysis stops, which was indicative of a global instability of the bridge. Therefore, after several members fail in the structure, the removal of one more member caused the member to unload too quickly and SAP2000 terminated the analysis.

Using the critical member removal and load redistribution analysis, Member 1012 was the first critical member analyzed. Force controlled hinges were placed in Members 1016 and 1017, the counters, and in Member 1012. The load was ramped from zero to eight side-by-side stack trucks. All of the remaining tensile and compressive forces in the members in the trusses were checked using Tables 5-1 and 5-2 to determine if any of the members yielded or buckled. Member 1016 had a tensile force greater than the limit; therefore a force controlled hinge was placed in that member. Another analysis was completed to determine the load redistribution once Member 1016 failed. After the hinge was activated, the truss was examined again and Member 1011 had a tensile force greater than the tensile limit for that member. A force controlled hinge was placed in Member 1011 with hinge properties defined in Tables 5-1 and 5-2. An elastic analysis was completed again to determine the local redistribution once Member 1011 failed. The load had redistributed causing Member 1019 to reach its critical tensile load. A hinge was placed in Member 1019 and the analysis was completed again. The removal of Member 1019 caused SAP2000 to terminate the analysis. Figure 5-18 shows the members in which hinges formed during analysis. The number in parenthesis shows the order in which the members yielded or buckled as well as whether the member was in tension or compression. Figure 5-19 shows the deflected shape of the North Truss after all of the members except the final member, Member 1019, has failed. After the final member

failed, it was impossible to retrieve a deflected shape because the bridge was assumed to have collapsed. Since it appears that there are large bending effects in the top and bottom chord they needed to be checked for combined axial and bending effects to ensure that the members were under the yield stress.

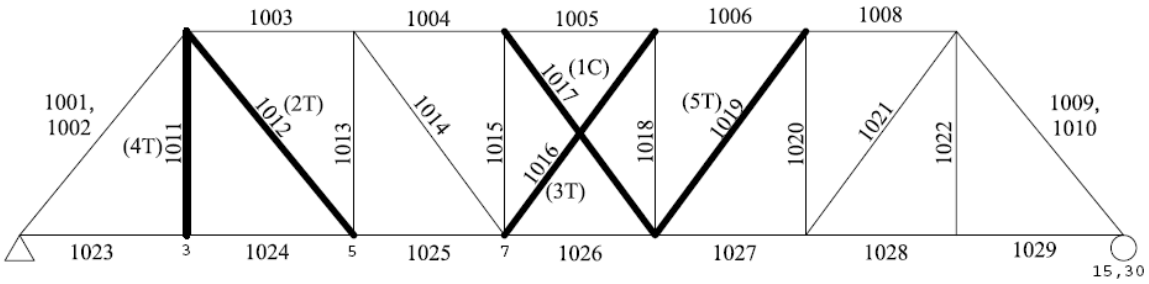

Figure **5-18**. Failed Members in North Truss, Critical Member 1012

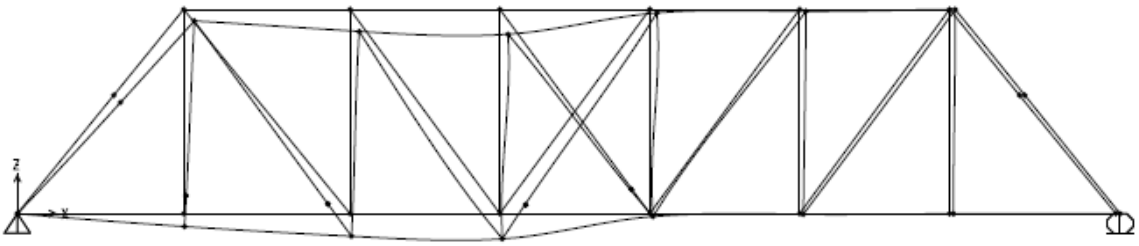

Figure **5-19**. Deflected Shape, Critical Member 1012

Table 5-9 summarizes the combined axial and bending affects due to the removed members. The forces in the members were determined after Member 1011 was removed from the truss and the forces were redistributed prior to the collapse of the bridge. None of the members were determined to have combined stresses greater than the yield stress, although stresses in certain member approached the yield stress.

Member	Element	Area cm^2 (in^2)	Sx cm^3 (in^3)	P kN (kip)	M kN-m (kip-in)	P/A MPa (ksi)	M/Sx MPa (ksi)	P/A + M/Sx MPa (ksi)
1001	EL1	257.4 (39.9)	3666.4 (223.7)	-3348.4 (-752.4)	-182.4 (-1614.2)	-115.0 (-18.9)	-44.0 (-7.22)	159.0 (26.1)
1002	EL1	257.4 (39.9)	3666.4 (223.7)	-4187.2 (-940.9)	93.7 (828.8)	-143.8 (-23.6)	22.6 (3.70)	166.4 (27.3)
1003	EL2	234.8 (36.4)	3333.7 (203.4)	-4306.4 (-967.7)	-60.4 (-534.2)	-162.1 (-26.6)	-16.0 (-2.63)	178.1 (29.2)
1004	EL3	281.2 (43.6)	4090.9 (249.6)	-3620.8 (-813.7)	-51.8 (-458.3)	-113.8 (-18.7)	-11.2 (-1.84)	125.0 (20.5)
1005	EL3	281.2 (43.6)	4090.9 (249.6)	-3563.3 (-800.7)	-8.2 (-72.6)	-112.0 (-18.4)	-1.8 (-0.29)	113.7 (18.7)
1006	EL3	281.2 (43.6)	4090.9 (249.6)	-3341.9 (-751.0)	-18.2 (-161.2)	-105.0 (-17.2)	-3.9 (-0.65)	109.0 (17.9)
1008	EL2	234.8 (36.4)	3333.7 (203.4)	-2109.3 (-474.0)	39.4 (348.9)	-79.4 (-13.0)	10.5 (1.72)	89.9 (14.7)
1009	EL1	257.4 (39.9)	3666.4 (223.7)	-1793.2 (-403.0)	-70.0 (-619.2)	-61.6 (-10.1)	-16.9 (-2.77)	78.5 (12.9)
1010	EL1	257.4 (39.9)	3666.4 (223.7)	-1888.1 (-424.3)	-21.1 (-186.4)	-64.8 (-10.6)	-5.1 (-0.83)	69.9 (11.5)
1023	EL4	245.7 (38.1)	5913.5 (360.8)	2411.4 (541.9)	208.0 (1840.6)	86.7 (14.2)	31.1 (5.10)	117.8 (19.3)
1024	EL4	245.7 (38.1)	5913.5 (360.8)	2037.6 (457.9)	234.0 (2070.7)	73.3 (12.0)	35.0 (5.74)	108.3 (17.8)
1025	EL4	245.7 (38.1)	5913.5 (360.8)	3304.5 (742.6)	86.5 (765.4)	118.8 (19.5)	12.9 (2.12)	131.8 (21.6)
1026	EL5	280.6 (43.5)	6711.7 (409.5)	2552.5 (573.6)	79.7 (705.7)	80.4 (13.2)	10.5 (1.72)	90.9 (14.9)
1027	EL4	245.7 (38.1)	5913.5 (360.8)	1466.2 (329.5)	98.7 (873.6)	52.7 (8.6)	14.8 (2.42)	67.5 (11.1)
1028	EL4	245.7 (38.1)	5913.5 (360.8)	775.4 (174.2)	71.9 (636.4)	27.9 (4.6)	10.8 (1.76)	38.6 (6.3)
1029	EL4	245.7 (38.1)	5913.5 (360.8)	944.5 (212.3)	-87.6 (-775.0)	34.0 (5.6)	-13.1 (-2.15)	47.1 (7.7)

Table **5-9**. Combined Axial and Bending Stress for Top and Bottom Chord, Critical Member

Member 1021 was analyzed in the same manner as Member 1012. Force controlled hinges were placed in the two counters and then the critical member, member 1021. After the load had been redistributed to the remaining structure one member was above the critical tensile force, Member 1019. A force controlled hinge was placed in the member, using hinge properties shown in Tables 5-1 and 5-6, and the analysis was completed again. Member 1017 failed during the analysis and the load in the member was redistributed to surrounding members. After a hinge was put in the member and the analysis was completed again, Member 1022 was the next critical member. During this analysis, the program terminated. Figure 5-20 displays the critical members and shows the four diagonals that failed under the eight HS-20 trucks. Figure 5-21 shows the deflected shape of the North Truss after all of the members except the final member, Member 1022, has failed. After the final member failed, it was impossible to retrieve a deflected shape because the bridge was assumed to have collapsed. Since it appears that there are large bending effects in the top and bottom chord they needed to be checked for combined axial and bending effects to ensure that the members were under the yield stress.

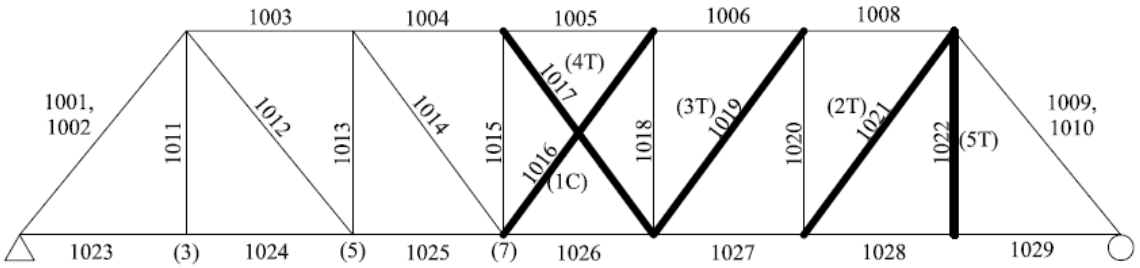

Figure **5-20**. Failed Members, Critical Member 1021, North Truss

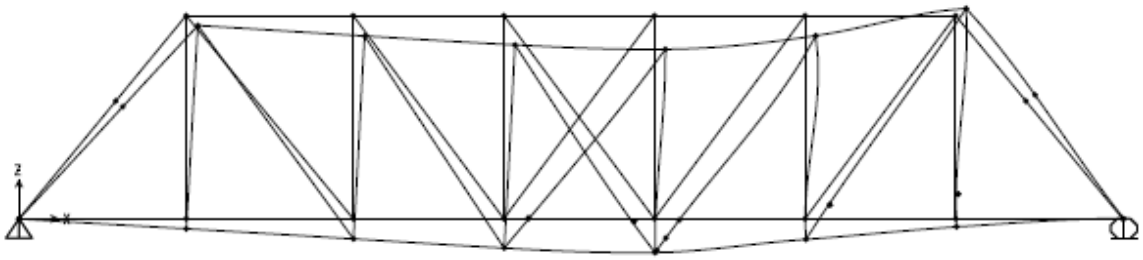

Figure **5-21**. Deflected Shape, Critical Member 1021

Table 5-10 summarizes the combined axial and bending affects due to the removed members. The forces in the members were determined after Member 1017 was removed from the truss and the forces were redistributed prior to the collapse of the bridge. None of the members were determined to have combined stresses greater than the yield stress, although stresses in certain member approached the yield stress.

Member	Element	Area cm^2 (in^2)	Sx cm^3 (in^3)	P kN (kip)	M kN-m (kip-in)	P/A MPa (ksi)	M/Sx MPa (ksi)	P/A + M/Sx MPa (ksi)
1001	EL1	257.4 (39.9)	3666.4 (223.7)	-2815.4 (-632.7)	205.6 (1819.7)	-96.7 (-15.9)	49.6 (8.1)	146.3 (24.0)
1002	EL1	257.4 (39.9)	3666.4 (223.7)	-2459.4 (-552.7)	-183.2 (-1621.5)	-84.5 (-13.9)	-44.2 (-7.2)	128.6 (21.1)
1003	EL2	234.8 (36.4)	3333.7 (203.4)	-2386.3 (-536.3)	341.3 (3020.2)	-89.8 (-14.7)	90.5 (14.8)	180.4 (29.6)
1004	EL3	281.2 (43.6)	4090.9 (249.6)	-3768.1 (-846.8)	-266.3 (-2356.7)	-118.4 (-19.4)	-57.6 (-9.4)	176.0 (28.9)
1005	EL3	281.2 (43.6)	4090.9 (249.6)	-4125.3 (-927.0)	-56.4 (-499.3)	-129.6 (-21.3)	-12.2 (-2.0)	141.8 (23.3)
1006	EL3	281.2 (43.6)	4090.9 (249.6)	-4141.7 (-930.7)	-239.4 (-2118.9)	-130.2 (-21.3)	-51.8 (-8.5)	181.9 (29.8)
1008	EL2	234.8 (36.4)	3333.7 (203.4)	-3211.6 (-721.7)	-163.0 (-1442.8)	-120.9 (-19.8)	-43.2 (-7.1)	164.1 (26.9)
1009	EL1	257.4 (39.9)	3666.4 (223.7)	-2732.6 (-614.1)	284.3 (2515.6)	-93.8 (-15.4)	68.6 (11.2)	162.4 (26.6)
1010	EL1	257.4 (39.9)	3666.4 (223.7)	-2876.0 (-646.3)	-308.7 (-2731.6)	-98.8 (-16.2)	-74.5 (-12.2)	173.2 (28.4)
1023	EL4	245.7 (38.1)	5913.5 (360.8)	1186.3 (266.6)	-802.7 (-7103.9)	42.7 (7.0)	-120.0 (-19.7)	162.7 (26.7)
1024	EL4	245.7 (38.1)	5913.5 (360.8)	911.5 (204.8)	868.2 (7682.7)	32.8 (5.4)	129.8 (21.3)	162.6 (26.7)
1025	EL4	245.7 (38.1)	5913.5 (360.8)	1941.4 (436.3)	717.6 (6350.5)	69.8 (11.5)	107.3 (17.6)	177.1 (29.1)
1026	EL5	280.6 (43.5)	6711.7 (409.5)	2888.4 (649.1)	227.5 (2013.3)	91.0 (14.9)	30.0 (4.9)	120.9 (19.8)
1027	EL4	245.7 (38.1)	5913.5 (360.8)	2370.1 (532.6)	-615. (-5444.3)	85.2 (14.0)	-92.0 (-15.1)	177.2 (29.1)
1028	EL4	245.7 (38.1)	5913.5 (360.8)	1159.1 (260.5)	732.9 (6485.9)	41.7 (6.8)	109.6 (18.0)	151.3 (24.8)
1029	EL4	245.7 (38.1)	5913.5 (360.8)	1406.8 (316.1)	-746.1 (-6603.1)	50.6 (8.3)	-111.6 (-18.3)	162.2 (26.6)

Table **5-10**. Combined Axial and Bending Stress for Top and Bottom Chord, Critical Member

Member 1040 of the south truss was then analyzed. Force controlled hinges were placed in the counters of both trusses to prevent the members from carrying any compression forces. A force controlled hinge was also placed in Member 1040 since under the prescribed loading it yielded. After the analysis was completed and the load was redistributed to the other members in the truss, Member 1044 had a tensile force greater than the critical load for that member. A hinge was placed in the member and the analysis was completed again to determine where the load would redistribute once Member 1044 failed. When Member 1044 redistributed the load it was carrying, Member 1039 had an increase in tensile force causing it to go above the critical tensile load. A hinge was placed in Member 1039 and the analysis was completed again. After Member 1039 formed a hinge and failed; Member 1047 had a tensile force greater than the critical tensile force. When hinges were put in for those members, the analysis was terminated in SAP2000. Figure 5-22 shows the critical members and the order in which the hinges formed. The member failure sequence was the same as Member 1021, with the counter buckling first followed by the first diagonal in the west end of the bridge failing in tension. The other center diagonal failed in tension next followed by the first vertical in the west end of the bridge failing in tension. The last member to fail in tension was the diagonal in the fifth panel of the bridge from the west end. Figure 5-23 shows the deflected shape of the South Truss after all of the members except the final member, Member 1047, has failed. After the final member failed, it was impossible to retrieve a deflected shape because the bridge was assumed to have collapsed. Since it appears that there are large bending effects in the top and bottom chord they needed to be checked for

combined axial and bending effects to ensure that the members were under the yield stress.

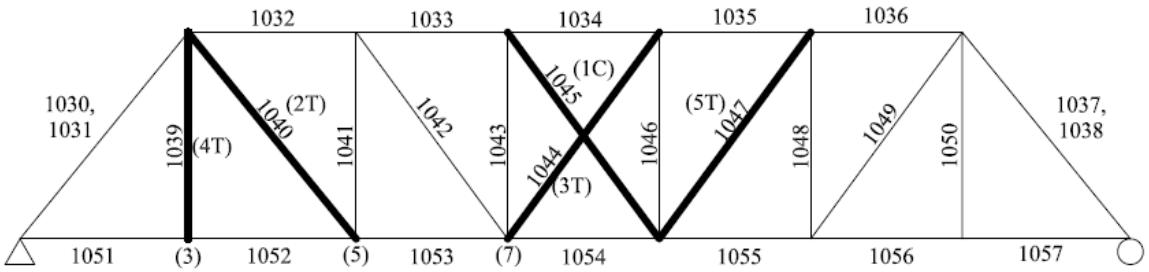

Figure **5-22**. Failed Member, Critical Member 1040, South Truss

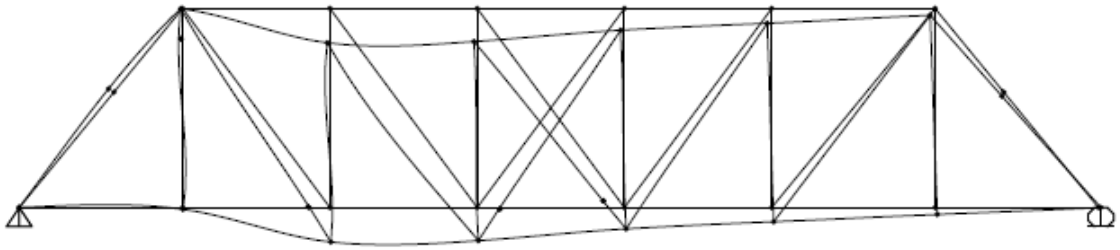

Figure **5-23**. Deflected Shape, Critical Member 1040

Table 5-11 summarizes the combined axial and bending affects due to the removed members. The forces in the members were determined after Member 1039 was removed from the truss and the forces were redistributed prior to the collapse of the bridge. None of the members were determined to have combined stresses greater than the yield stress, although stresses in certain member approached the yield stress.

Member	Element	Area cm^2 (in^2)	Sx cm^3 (in^3)	P kN (kip)	M kN-m (kip-in)	P/A MPa (ksi)	M/Sx MPa (ksi)	P/A + M/Sx MPa (ksi)
1030	EL1	257.4 (39.9)	3666.4 (223.7)	-4058.3 (-912.0)	129.3 (1144.5)	-139.4 (-22.9)	31.2 (5.1)	170.6 (28.0)
1031	EL1	257.4 (39.9)	3666.4 (223.7)	-4029.4 (-905.5)	181.7 (1608.2)	-138.4 (-22.7)	43.8 (7.2)	182.2 (29.9)
1032	EL2	234.8 (36.4)	3333.7 (203.4)	-2732.5 (-614.1)	139.9 (1237.9)	-102.9 (-16.9)	37.1 (6.1)	140.0 (23.0)
1033	EL3	281.2 (43.6)	4090.9 (249.6)	-3723.7 (-836.8)	-39.9 (-353.2)	-117.0 (-19.2)	-8.6 (-1.4)	125.6 (20.6)
1034	EL3	281.2 (43.6)	4090.9 (249.6)	-3679.6 (-826.9)	11.3 (100.3)	-115.6 (-19.0)	2.4 (0.4)	118.1 (19.4)
1035	EL3	281.2 (43.6)	4090.9 (249.6)	-3114.1 (-699.8)	34.1 (301.5)	-97.9 (-16.1)	7.4 (1.2)	105.2 (17.3)
1036	EL2	234.8 (36.4)	3333.7 (203.4)	-2132.2 (-479.1)	-98.4 (-870.4)	-80.3 (-13.2)	-26.1 (-4.3)	106.3 (17.4)
1037	EL1	257.4 (39.9)	3666.4 (223.7)	-1718.9 (-386.3)	79.8 (706.2)	-59.0 (-9.7)	19.2 (3.2)	78.3 (12.8)
1038	EL1	257.4 (39.9)	3666.4 (223.7)	-1840.8 (-413.7)	137.7 (1218.1)	-63.2 (-10.4)	33.2 (5.4)	96.4 (15.8)
1051	EL4	245.7 (38.1)	5913.5 (360.8)	2155.7 (484.4)	-420.9 (-3724.5)	77.5 (12.7)	-62.9 (-10.3)	140.5 (23.0)
1052	EL4	245.7 (38.1)	5913.5 (360.8)	1936.8 (435.2)	152.5 (1349.9)	69.6 (11.4)	22.8 (3.7)	92.5 (15.2)
1053	EL4	245.7 (38.1)	5913.5 (360.8)	1967.6 (442.2)	60.9 (538.8)	70.8 (11.6)	9.1 (1.5)	79.9 (13.10
1054	EL5	280.6 (43.5)	6711.7 (409.5)	2252.2 (506.1)	140.5 (1243.0)	70.9 (11.6)	18.5 (3.0)	89.4 (14.7)
1055	EL4	245.7 (38.1)	5913.5 (360.8)	1452.8 (326.5)	194.3 (1719.1)	52.2 (8.6)	29.1 (4.8)	81.3 (13.3)
1056	EL4	245.7 (38.1)	5913.5 (360.8)	818.8 (184.0)	-342.6 (-3032.0)	29.4 (4.8)	-51.2 (-8.4)	80.7 (13.2)
1057	EL4	245.7 (38.1)	5913.5 (360.8)	1047.7 (235.4)	-79.2 (-700.8)	37.7 (6.2)	-11.8 (-1.9)	49.5 (8.1)

Table **5-11**. Combined Axial and Bending Stress for Top and Bottom Chord, Critical Member

The last critical member analyzed was Member 1049. Force controlled hinges were placed in the two counters and then the critical member, Member 1049. After Member 1049 failed the load was redistributed to the rest of the structure. Member 1047 had a tensile force greater than the allowable and a hinge was placed in the member. The analysis was completed again and the load redistribution was analyzed. Member 1045 was the next member to fail. After the load redistribution, Member 1050 was a critical member with axial forces greater than the limit. At that point, the analysis terminated. Figure 5-24 shows the failed members and the sequence in which they failed in the analysis. Figure 5-25 shows the deflected shape of the South Truss after all of the members except the final member, Member 1050, has failed. After the final member failed, it was impossible to retrieve a deflected shape because the bridge was assumed to have collapsed. Since it appears that there are large bending effects in the top and bottom chord they needed to be checked for combined axial and bending effects to ensure that the members were under the yield stress.

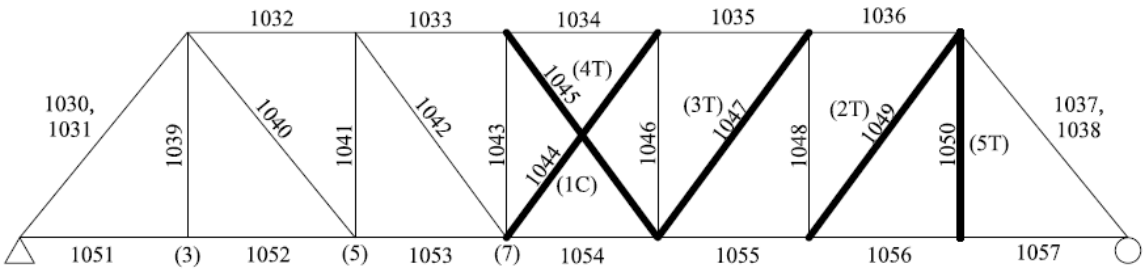

Figure **5-24**. Failed Members, Critical Member 1049, South Truss

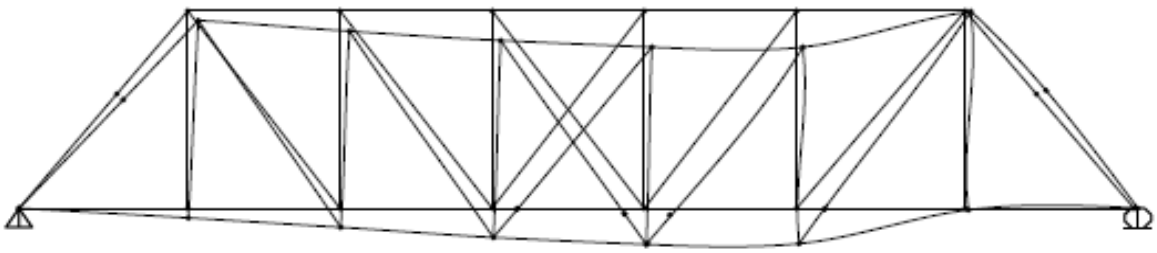

Figure **5-25**. Deflected Shape, Critical Member 1049

Table 5-12 summarizes the combined axial and bending affects due to the removed members. The forces in the members were determined after Member 1045 was removed from the truss and the forces were redistributed prior to the collapse of the bridge. None of the members were determined to have combined stresses greater than the yield stress, although stresses in certain member approached the yield stress.

Member	Element	Area cm^2 (in^2)	Sx cm^3 (in^3)	P kN (kip)	M kN-m (kip-in)	P/A MPa (ksi)	M/Sx MPa (ksi)	P/A + M/Sx MPa (ksi)
1030	EL1	257.4 (39.9)	3666.4 (223.7)	-2340.9 (-526.1)	205.7 (1820.0)	-80.4 (-13.2)	49.6 (8.1)	130.0 (21.3)
1031	EL1	257.4 (39.9)	3666.4 (223.7)	-2275.4 (-511.3)	-122.4 (-1082.9)	-78.1 (-12.8)	-29.5 (-4.8)	107.7 (17.7)
1032	EL2	234.8 (36.4)	3333.7 (203.4)	-2514.1 (-565.0)	-46.0 (-406.8)	-94.6 (-15.5)	-12.2 (-2.0)	106.8 (17.5)
1033	EL3	281.2 (43.6)	4090.9 (249.6)	-3622.8 (-814.1)	18.2 (160.7)	-113.8 (-18.7)	3.9 (0.6)	117.8 (19.3)
1034	EL3	281.2 (43.6)	4090.9 (249.6)	-3971.2 (-892.4)	5.6 (49.5)	-124.8 (-20.5)	1.2 (0.2)	126.0 (20.7)
1035	EL3	281.2 (43.6)	4090.9 (249.6)	-4018.1 (-902.9)	28.5 (251.8)	-126.3 (-20.7)	6.2 (1.0)	132.4 (21.7)
1036	EL2	234.8 (36.4)	3333.7 (203.4)	-2741.4 (-616.0)	-59.8 (-528.9)	-103.2 (-16.9)	-15.9 (-2.6)	119.0 (19.5)
1037	EL1	257.4 (39.9)	3666.4 (223.7)	-2995.7 (-673.2)	-119.1 (-1054.3)	-102.9 (-16.9)	-28.7 (-4.7)	131.6 (21.6)
1038	EL1	257.4 (39.9)	3666.4 (223.7)	-3093.9 (-695.3)	-53.9 (-477.3)	-106.2 (-17.4)	-13.0 (-2.1)	119.2 (19.6)
1051	EL4	245.7 (38.1)	5913.5 (360.8)	1122.0 (252.1)	-358.7 (-3174.7)	40.3 (6.6)	-53.6 (-8.8)	94.0 (15.4)
1052	EL4	245.7 (38.1)	5913.5 (360.8)	822.2 (184.8)	232.3 (2056.0)	29.6 (4.8)	34.7 (5.7)	64.3 (10.5)
1053	EL4	245.7 (38.1)	5913.5 (360.8)	1707.7 (383.8)	199.1 (1762.0)	61.4 (10.1)	29.8 (4.9)	91.2 (15.0)
1054	EL5	280.6 (43.5)	6711.7 (409.5)	2710.5 (609.1)	105.3 (932.2)	85.4 (14.0)	13.9 (2.3)	99.3 (16.3)
1055	EL4	245.7 (38.1)	5913.5 (360.8)	1939.8 (435.9)	-196.8 -(1741.7)	69.8 (11.4)	-29.4 (-4.8)	99.2 (16.3)
1056	EL4	245.7 (38.1)	5913.5 (360.8)	1882.6 (423.1)	279.9 (2476.7)	67.7 (11.1)	41.9 (6.9)	109.6 (18.0)
1057	EL4	245.7 (38.1)	5913.5 (360.8)	1727.2 (388.1)	218.8 (1936.7)	62.1 (10.2)	32.7 (5.4)	94.8 (15.6)

Table **5-12**. Combined Axial and Bending Stress for Top and Bottom Chord, Critical Member

From the critical member removal and load redistribution analysis, the failure pattern for each critical member and location for the pristine bridge model was determined. Several trends were observed from the analysis. First, the position of the eight stacked side-by-side HS-20 trucks was more critical when it was positioned in two panels of the floor versus three. This was critical because more load was distributed to a smaller area of the floor system. Secondly, HS-20 trucks traversing west to east on the bridge caused Members 1021 and 1049 in the north and south truss, respectively, to have critical axial forces. In the same manner, trucks traversing east to west on the bridge caused Members 1012 and 1040 in the north and south truss, respectively, to have critical axial forces. Therefore, depending on the direction of the truck, either west to east or east to west the location of the critical member changed. A truck travelling west to east caused diagonal members in the east end of the bridge to be critical. In the same manner, a truck travelling east to west caused diagonal members in the west end of the bridge to be critical. This could be attributed to the skew of the bridge and the distribution of the loads.

From Figures 5-18 through 5-25 failure patterns were established. Two failure patterns were defined for the analysis, a local response and a global response. The local failure pattern defined the order of the failed critical members. The global failure pattern looked at all of the members that failed to determine if certain members were more critical than others. Members 1012 and 1040 had the same member failure sequence. The failure started with the center diagonal buckling and then the first diagonal in the west end of the bridge failed. After the load was redistributed, the second diagonal in the center panel failed causing the first vertical in the west end of the bridge to fail. The last

member to fail was the diagonal in the fifth panel of the bridge causing the bridge to collapse. Members 1021 and 1049 had the same member failure sequence as well. The center diagonal buckled first and then the first diagonal in the east end of the bridge failed. The failure of diagonal members continued towards the center of the bridge. After the second diagonal in the center of the bridge failed, the first vertical in the east end of the bridge failed causing the bridge to collapse. For each failure pattern five members were removed before the structure collapsed. Of the five members that failed, two members were consistent in each member failure pattern. The compression counter was the first to fail in every analysis. This was to be expected because the buckling capacity of the counter was minimal. The tension member in the center diagonals also always failed during the critical member removal analysis. The failure of the tension member always occurred after the failure of the first critical member that was not a counter. In the case of Members 1012 and 1040, the center diagonal tension member failed immediately after the critical member failed. For Members 1021 and 1049, the center diagonal tension member was the fourth member to fail in the sequence. The tension counter in the center panel could then be considered the most critical member once the analysis was started since it failed in all of the failure patterns. The failure patterns for the pristine bridge will later be compared to the deteriorated bridge model to determine if deterioration played a role in the global failure response and load redistribution of the truss bridge.

5.3 Deteriorated Model

A deteriorated model of the Beech Creek Veterans Memorial Bridge was completed using the condition evaluation outlined in Chapter 3. The condition evaluation detailed the amount of section loss present in the floor system and trusses. For this analysis, only truss members that contained section loss and deterioration near the "splash zone" were changed. The "splash zone" is an area more susceptible to deterioration because it is a region where deicing salts are able to penetrate the structural steel.

The deteriorated model involved changing cross sectional properties for the truss members that had section loss based on the condition evaluation detailed in Chapter 3. Each member was considered prismatic and therefore the entire member was changed even though the section loss occurred in the "splash zone". Table 5-13 through Table 5-16 show sections of each north truss member and detail section loss (darkened sections), and corresponding loss of area.

Member		Loss	
End Post	1001, 1002 EL 1		1/16" of web depth - $A_L = 6.06cm^2$ ($0.94in^2$)
	1009, 1010 EL 1		1/16" of outside channel - $A_L = 9.6cm^2$ ($1.49in^2$)

Table **5-13**. Section Loss, North Truss End Posts, Beech Creek Veterans Memorial Bridge

Member		Loss	
Verticals	1011 EL6		3/32" of perimeter - A_L = 12.4cm^2 (1.92in^2)
	1013 EL7	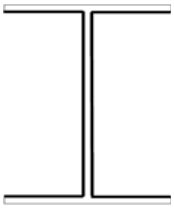	1/32" on inside perimeter - A_L = 9.1cm^2 (1.41in^2)
	1015 EL7		1/32" of 6" of web - A_L = 1.2cm^2 (0.19in^2)
	1018 EL7	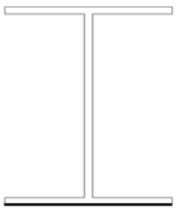	1/32" of bottom flange - A_L = 1.6 cm^2 (0.25in^2)
	1020 EL7	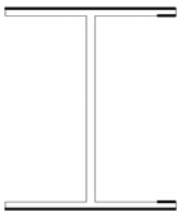	1/16" of flanges and 2" of underside of flanges - A_L = 11.3cm^2 (1.75in^2)
	1022 EL6	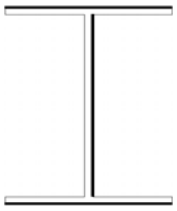	1/32" on outer flanges and web - A_L = 6.1cm^2 (0.95in^2)

Table **5-14**. Section Loss, North Truss Verticals, Beech Creek Veterans Memorial Bridge

Member		Loss	
Bottom Chord	1023 EL4	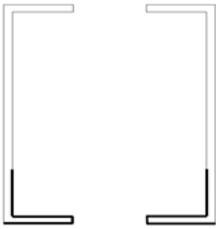	1/16" loss around bottom of channel - A_L = 8.4cm2 (1.31in^2)
	1024 EL4	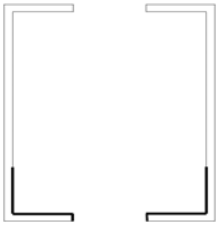	1/16" of sections of flange and web - A_L = 10.4cm2 (1.62in^2)
	1025 EL4	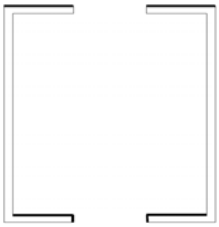	3/32" loss on top and bottom flange - A_L = 9.0cm2 (1.40in^2)
	1026 EL5	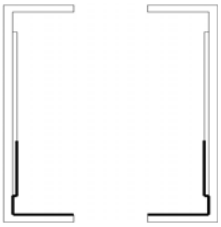	1/16" of sections of flange and web - A_L = 6.8cm2 (1.06in^2)
	1027 EL4	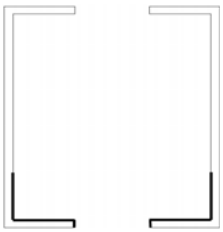	1/32" loss on inside of flange and web - A_L = 3.0cm2 (0.47in^2)

Table **5-15**. Section Loss, North Truss Bottom Chord, Beech Creek Veterans Memorial Bridge

Member		Loss	
Diagonals	1012 EL8	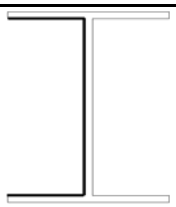	1/16" of inside flange and web - A_L = 9.1cm^2 (1.41in^2)
	1014 EL6		1/8" of sections of flange and web - A_L = 11.2 cm^2 (1.74in^2)
	1016 EL9	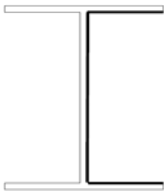	1/32" of flanges and web - A_L = 3.5 cm^2 (0.54in^2)
	1017 EL9	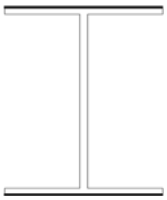	1/8" loss of full width of flanges - A_L = 10.5 cm^2 (1.63in^2)
	1019 EL6	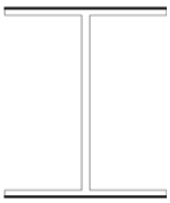	1/8" pitting of bottom flange - A_L = 16.1 cm^2 (2.50in^2)
	1021 EL8	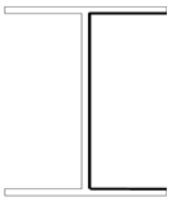	1/64" over web and inside flange - A_L = 1.1 cm^2 (0.17in^2)

Table **5-16**. Section Loss, North Truss Diagonals, Beech Creek Veterans Memorial Bridge

The south truss cross sectional properties were not changed because there was no considerable amount of deterioration reported from the condition evaluation. The south

truss did not have any section loss because it did not have a sidewalk attached that allowed water and deicing salts to collect. Since it did not have a sidewalk, water and deicing salts were able to drain properly causing no deterioration or section loss. Once the cross sectional properties were changed to mimic the condition prior to the rehabilitation in 1994, a static analysis was completed following the procedure discuss for the pristine structure. Critical member removal and load redistribution analyses were then completed to determine the final failure sequence and the load redistribution for the deteriorated structure.

5.3.1 Loading

The loading scheme used in the deteriorated truss model of the Beech Creek Veterans Memorial Bridge was the same used for the pristine truss model. Multiple stacked side-by-side HS-20 trucks traversed the length of the bridge until a member failed. Refer to Section 5.2.1 for information on the loading schematic that was used.

5.3.2 Critical Member Identification

A multi-step static analysis was completed in SAP2000 to determine the critical members of the Beech Creek Veterans Memorial Bridge using the same procedure as that detailed for the pristine model in Section 5.2.2. Tension members were checked to see if any of the members yielded under the prescribed loading and compression members were checked to see if any of the members buckled following Ghosn and Moses (1998)

Combined axial and bending effects were also checked at each member removal step to determine if any top and bottom chord members were critical.

New tensile capacities were calculated based on the reduced cross sectional areas. The yield stress remained 206.8 MPa (30ksi). Table 5-17 details the capacity of each of the reduced cross sections and describes the location of the member by its ID and the location.

Element ID	Location	Area cm^2 (in^2)	Yield Stress kN/cm^2 (ksi)	Capacity kN (kips)
EL2	1003, 1004, 1006. 1008	234.64 (36.37)	206.8 (30)	4855.4 (1091.1)
EL3	1005	281.13 (43.575)		5817.3 (1307.25)
EL4	1028, 1029	160.97 (24.95)		3330.8 (748.5)
L0-L1-1	1023	152.06 (23.57)		3146.6 (707.1)
L1-L2-1	1024	147.94 (22.93)		3061.2 (687.9)
L1-U1-1	1011	87.87 (13.62)		1818.3 (408.6)
L2-L3	1025	148.97 (23.09)		3082.5 (692.7)
L2-U1	1012	112.58 (17.45)		2329.6 (523.5)
L2-U2	1013	112.06 (17.37)		2318.9 (521.1)
L3-L4	1026	236.97 (36.73)		4903.5 (1101.9)
L3-U2	1014	87.42 (13.55)		1808.9 (406.5)
L3-U4	1016	49.03 (7.6)		1014.6 (228.0)
L4-L5	1027	155.68 (24.13)		3221.4 (723.9)
L4-U3	1017	42.39 (6.57)		877.1 (197.1)
L4-U5	1019	83.03 (12.87)		1718.1 (386.1)
L5-U5	1020	110.39 (17.11)		2284.2 (513.3)
L5-U6	1021	120.52 (18.68)		2493.8 (560.4)
L6-U6	1022	94.19 (14.6)		1949.1 (438.0)

Table **5-17**. Tensile Capacity of Deteriorated Members

From the analysis, the critical number of stacked side-by-side HS-20 trucks was determined to be seven trucks. The south truss did not have any members' yield which was attributed to no section loss present in the south truss.

Tables 5-18 through 5-20 show the maximum or minimum stresses in each member of the north truss. The stress was determined by using the member's reduced cross sectional area and the axial forces shown in Tables B5-10 through B5-12 in Appendix B. The stresses under self weight and seven stacked side-by-side HS-20 trucks showed that two members yielded in the north truss. Table 5-21 shows the axial force and stress in the critical members under seven stacked side-by-side HS-20 trucks.

Member ID	1 Truck MPa (ksi)	2 Truck MPa (ksi)	3 Truck MPa (ksi)	4 Truck MPa (ksi)	5 Truck MPa (ksi)	6 Truck MPa (ksi)	7 Truck MPa (ksi)
1001	-30.9 (-4.48)	-46.8 (-6.79)	-62.7 (-9.11)	-78.7 (-11.42)	-94.6 (-13.73)	-110.6 (-16.05)	-126.5 (-18.36)
1002	-29.9 (-4.34)	-45.4 (-6.59)	-61.0 (-8.85)	-76.6 (-11.11)	-92.1 (-13.37)	-107.7 (-15.63)	-123.3 (-17.89)
1003	-33.9 (-4.92)	-52.0 (-7.55)	-70.1 (-10.17)	-88.2 (-12.80)	-106.2 (-15.42)	-124.3 (-18.04)	-142.4 (-20.67)
1004	-32.5 (-4.71)	-49.6 (-7.19)	-66.6 (-9.67)	-83.7 (-12.15)	-100.8 (-14.63)	-117.9 (-17.11)	-135.0 (-19.59)
1005	-32.1 (-4.66)	-48.7 (-7.07)	-65.4 (-9.49)	-82.0 (-11.90)	-98.6 (-14.32)	-115.3 (-16.73)	-131.9 (-19.15)
1006	-32.7 (-4.75)	-49.8 (-7.22)	-66.8 (-9.69)	-83.8 (-12.17)	-100.9 (-14.64)	-117.9 (-17.11)	-135.0 (-19.59)
1008	-33.1 (-4.80)	-50.2 (-7.28)	-67.2 (-9.76)	-84.3 (-12.23)	-101.3 (-14.71)	-118.4 (-17.19)	-135.5 (-19.66)
1009	-31.3 (-4.54)	-47.2 (-6.85)	-63.2 (-9.17)	-79.1 (-11.48)	-95.1 (-13.80)	-111.0 (-16.11)	-127.0 (-18.43)
1010	-33.5 (-4.86)	-50.2 (-7.28)	-66.9 (-9.70)	-83.6 (-12.13)	-100.3 (-14.55)	-117.0 (-16.98)	-133.7 (-19.40)
1011	30.6 (4.44)	55.4 (8.04)	80.3 (11.65)	105.1 (15.25)	129.9 (18.86)	154.7 (22.46)	179.6 (26.06)

Table **5-18**. Stresses in Deteriorated North Truss for Self Weight and HS-20 Trucks

Member ID	1 Truck MPa (ksi)	2 Truck MPa (ksi)	3 Truck MPa (ksi)	4 Truck MPa (ksi)	5 Truck MPa (ksi)	6 Truck MPa (ksi)	7 Truck MPa (ksi)
1012	47.0 (6.82)	74.5 (10.81)	101.9 (14.79)	129.4 (18.78)	156.9 (22.77)	184.3 (26.75)	211.8 (30.74)
1013	-25.4 (-3.69)	-40.9 (-5.94)	-5604 (-8.18)	-71.8 (-10.42)	-87.3 (-12.67)	-102.8 (-14.91)	-118.2 (-17.16)
1014	37.7 (5.47)	63.2 (9.18)	88.8 (12.89)	111.4 (16.60)	140.0 (20.31)	165.5 (24.02)	191.1 (27.73)
1015	3.0 (0.44)	8.5 (1.24)	14.1 (2.04)	19.6 (2.84)	25.1 (3.64)	30.6 (4.44)	3601 (5.25)
1016	16.9 (2.46)	35.7 (5.18)	54.5 (7.91)	73.3 (10.64)	92.1 (13.37)	110.9 (16.09)	129.7 (18.82)
1017	14.9 (2.17)	32.4 (4.70)	49.9 (7.24)	67.3 (9.77)	84.8 (12.31)	102.3 (14.84)	119.7 (17.38)
1018	-8.8 (-1.28)	-14.8 (-2.15)	-20.9 (-3.03)	-26.9 (-3.91)	-32.9 (-4.78)	-39.0 (-5.66)	-45.0 (-6.53)
1019	41.5 (6.02)	70.0 (10.16)	98.5 (14.29)	127.0 (18.43)	155.5 (22.57)	184.0 (26.70)	212.5 (30.84)
1020	-27.7 (-4.02)	-44.6 (-6.48)	-61.5 (-8.93)	-78.4 (-11.38)	-95.3 (-13.83)	-112.1 (-16.28)	-129.0 (-18.73)

Table **5-19**. Stresses in Deteriorated North Truss for Self Weight and HS-20 Trucks

Member ID	1 Truck MPa (ksi)	2 Truck MPa (ksi)	3 Truck MPa (ksi)	4 Truck MPa (ksi)	5 Truck MPa (ksi)	6 Truck MPa (ksi)	7 Truck MPa (ksi)
1021	43.8 (6.36)	69.5 (10.09)	95.2 (13.82)	120.9 (17.55)	146.6 (21.28)	172.3 (25.01)	198.0 (28.74)
1022	30.9 (4.49)	55.9 (8.11)	80.9 (11.74)	105.9 (15.36)	130.8 (18.99)	155.8 (22.61)	180.8 (26.24)
1023	27.2 (3.95)	41.9 (6.08)	56.6 (8.22)	71.3 (10.35)	86.0 (12.48)	100.6 (14.61)	115.3 (16.74)
1024	22.1 (3.21)	34.3 (4.98)	46.6 (6.76)	58.8 (8.53)	71.0 (10.31)	83.2 (12.08)	95.4 (13.85)
1025	37.3 (5.42)	57.9 (8.40)	78.4 (11.38)	98.9 (14.36)	119.5 (17.34)	140.0 (20.32)	160.5 (23.30)
1026	28.2 (4.09)	43.0 (6.24)	57.8 (8.40)	72.7 (10.55)	87.5 (12.70)	102.4 (14.86)	117.2 (17.01)
1027	34.5 (5.01)	53.1 (7.71)	71.7 (10.41)	90.3 (13.10)	108.9 (15.80)	127.5 (18.50)	146.1 (21.20)
1028	20.6 (2.99)	31.3 (4.55)	42.0 (6.10)	52.7 (7.65)	63.4 (9.20)	74.1 (10.75)	84.7 (12.30)
1029	25.0 (3.63)	37.5 (5.44)	49.9 (7.24)	62.3 (9.04)	74.7 (10.85)	87.1 (12.65)	99.6 (14.45)

Table **5-20**. Stresses in Deteriorated North Truss for Self Weight and HS-20 Trucks

Member	Axial Force kN (kips)	Stress MPa (ksi)
1012	2387 (536.4)	211.7 (30.7)
1019	1766.2 (396.9)	212.3 (30.8)

Table **5-21**. Critical Axial Tensile Force and Stress for North Truss Members

Once the critical members were determined, the compression members were checked to ensure none of the members buckled under the seven HS-20 trucks. Table 5-22 shows the critical buckling load for the deteriorated compression members in the model. The element ID shows whether the member has section loss or not. Members identified as their exact location have section loss while members with generic element identifications (i.e. EL2 or EL3) have no section loss. The table also shows the yield load for each of the compression members. For every member except for the verticals the yield load controls. The critical load was determined using the Euler buckling equation (Eqn. 5.1) with reduced moment of inertias for the deteriorated members.

Element ID	Location	Moment of Inertia cm^4 (in^4)	Length m (ft)	Buckling Load kN (kips)	Yield Load kN (kips)
L0-U1	1001, 1002	76390.1 (1835.28)	10.53 (34.55)	13598.8 (3055.9)	5193.2 (1167.0)
L7-U6	1009, 1010	74983.3 (1801.48)	10.53 (34.55)	13348.4 (2999.6)	5139.8 (1155)
EL2	1003	72757.3 (1748)	6.67 (21.875)	32310.3 (7260.7)	4859.4 (1092)
EL3	1004	82351.4 (1978.5)	6.01 (19.719)	45005.1 (10113.5)	5820.6 (1308)
EL3	1005	82351.4 (1978.5)	6.01 (19.719)	45005.1 (10113.5)	5820.6 (1308)
EL3	1006	82351.4 (1978.5)	6.01 (19.719)	45005.1 (10113.5)	5820.6 (1308)
EL2	1008	72757.3 (1748)	6.01 (19.719)	39761.9 (8935.3)	4859.4 (1092)
L3-U3	1015	7266.6 (174.58)	8.15 (26.75)	2158.0 (484.9)	2525.8 (567.6)
L4-U4	1018	7074.7 (169.97)	8.15 (26.75)	2101.0 (472.1)	2536.5 (570)

Table **5-22**. Critical Buckling Load for Deteriorated Compression Members

The maximum compressive force was in the top chord and end posts of the bridge. The top chord did not have any section loss so the members would not buckle under the seven HS-20 trucks. The end posts had some deterioration but the critical buckling load was 13348.2 kN (2999.6 kips) and the maximum compression force was 2905.4 kN (652.9 kips). Other compression members, like the verticals, have a maximum compressive force of 1306.1 kN (293.5 kips) and the critical buckling load was 2101.0 kN (472.1 kip). When loaded with the seven stacked trucks, all of the compression members in the Beech Creek Veterans Memorial Bridge model were under the critical buckling loads determined in Table 5-22.

The top and bottom chords of the truss needed to be checked for combined axial and bending forces. The top chord was in compression and acted as a beam column while the bottom chord combined tension and bending. This check was needed because these members were modeled as frame elements as discussed in Chapter 4 Section 3, capable of carrying axial and bending forces. Table 5-23 shows the combined axial and bending stresses for the top and bottom chord of the North Truss. The axial and bending forces were compiled from running the seven side-by-side HS-20 trucks. The determined stresses were compared to the yield stress of 182.9 MPa (30 ksi) to determine if any members of the top and bottom chord were above yield under combined compression and bending. From the analysis, none of the members had stresses greater than the yield stress under combined loads.

Member	Element	Area cm^2 (in^2)	Sx cm^3 (in^3)	P kN (kip)	M kN-m (kip-in)	P/A MPa (ksi)	M/Sx MPa (ksi)	P/A + M/Sx MPa (ksi)
1001	L0-U1	250.9 (38.9)	3558.3 (217.1)	-2794.7 (-628.0)	51.9 (459.2)	-98.4 (-16.1)	12.9 (2.12)	111.3 (18.3)
1002	L0-U1	250.9 (38.9)	3558.3 (217.1)	-2740.2 (-615.8)	31.9 (282.1)	-96.5 (-15.8)	7.9 (1.30)	104.4 (17.1)
1003	EL2	234.8 (36.4)	3333.7 (203.4)	-2972.9 (-668.1)	-26.9 (-238.2)	-111.9 (-18.4)	-7.1 (-1.17)	119.0 (19.5)
1004	EL3	281.2 (43.6)	4090.9 (249.6)	-3366.0 (-756.4)	-11.3 (-100.1)	-105.8 (-17.3)	-2.4 (-0.40)	108.2 (17.8)
1005	EL3	281.2 (43.6)	4090.9 (249.6)	-3278.5 (-736.7)	-7.9 (-69.7)	-103.0 (-16.9)	-1.7 (-0.28)	104.7 (17.2)
1006	EL3	281.2 (43.6)	4090.9 (249.6)	-3357.6 (-754.5)	-7.4 (-65.3)	-105.5 (-17.3)	-1.6 (-0.26)	107.1 (17.6)
1008	EL2	234.8 (36.4)	3333.7 (203.4)	-2805.8 (-630.5)	-35.7 (-316.2)	-105.6 (-17.3)	-9.5 (-1.55)	115.1 (18.9)
1009	L7-U6	248.3 (38.5)	3522.2 (214.9)	-2774.7 (-623.5)	48.5 (429.3)	-98.7 (-16.2)	12.2 (2.00)	110.9 (18.2)
1010	L7-U6	248.3 (38.5)	3522.2 (214.9)	-2905.5 (-652.9)	-71.8 (-635.4)	-103.4 (-17.0)	-18.0 (-2.96)	121.4 (19.9)
1023	L1-L2	221.2 (34.3)	5321.8 (324.7)	1564.2 (351.5)	184.0 (1628.1)	62.5 (10.2)	30.6 (5.01)	93.1 (15.3)
1024	L2-L3	232.8 (36.1)	5600.5 (341.7)	1267.0 (284.7)	54.8 (485.0)	48.1 (7.9)	8.7 (1.42)	56.7 (9.3)
1025	L3-L4	236.7 (36.7)	5695.5 (347.5)	1998.2 (449.0)	60.6 (536.4)	74.6 (12.2)	9.4 (1.54)	84.0 (13.8)
1026	L4-L5	259.3 (40.2)	6202.0 (378.4)	2464.1 (553.7)	25.2 (223.1)	84.0 (13.8)	3.6 (0.59)	87.6 (14.4)
1027	EL4	245.7 (38.1)	5913.5 (360.8)	2027.9 (455.7)	39.8 (351.9)	72.9 (12.0)	5.9 (0.98)	78.9 (12.9)
1028	EL4	245.7 (38.1)	5913.5 (360.8)	1205.4 (270.9)	67.9 (601.0)	43.3 (7.1)	10.2 (1.67)	53.5 (8.8)
1029	EL4	245.7 (38.1)	5913.5 (360.8)	1401.2 (314.9)	135.1 (1195.8)	50.4 (8.3)	20.2 (3.31)	70.6 (11.6)

Table **5-23**. Combined Axial and Bending Stresses for Top and Bottom Chord, Deteriorated North Truss

Since two members, Members 1012 and 1019, were determined to have yielded under seven stacked side-by-side HS-20 trucks, the critical load location for each needed to be determined. An individual analysis of each member was then completed to determine exactly where the HS-20 trucks were located when each critical member reached its maximum axial force.

5.3.3 Critical Load Location

The critical location of the multiple HS-20 trucks was determined in the same manner as for the pristine model. The critical load location was needed to distribute wheel loads to the floor system allowing for the critical member removal analyses to be completed. The critical location was determined by running a multi-step static analysis and compiling results for each time step. The HS-20 truck was moved in increments of 3.05 m (10 ft) along the length of the bridge and at every increment the axial force in the critical members was recorded.

Each of the two critical members determined previously had a critical location for trucks traversing in both directions. Both directions were investigated because of the skew of the bridge. The directions of the truck were the same as the pristine model. Figures 5-26 through 5-29 show the axial forces in each critical member for a single HS-20 truck through seven stacked HS-20 truck loadings. The horizontal axis represents the time steps and the vertical axis is the axial force in the member due to the different HS-20 trucks. Also shown on each plot is the yield capacity for each member.

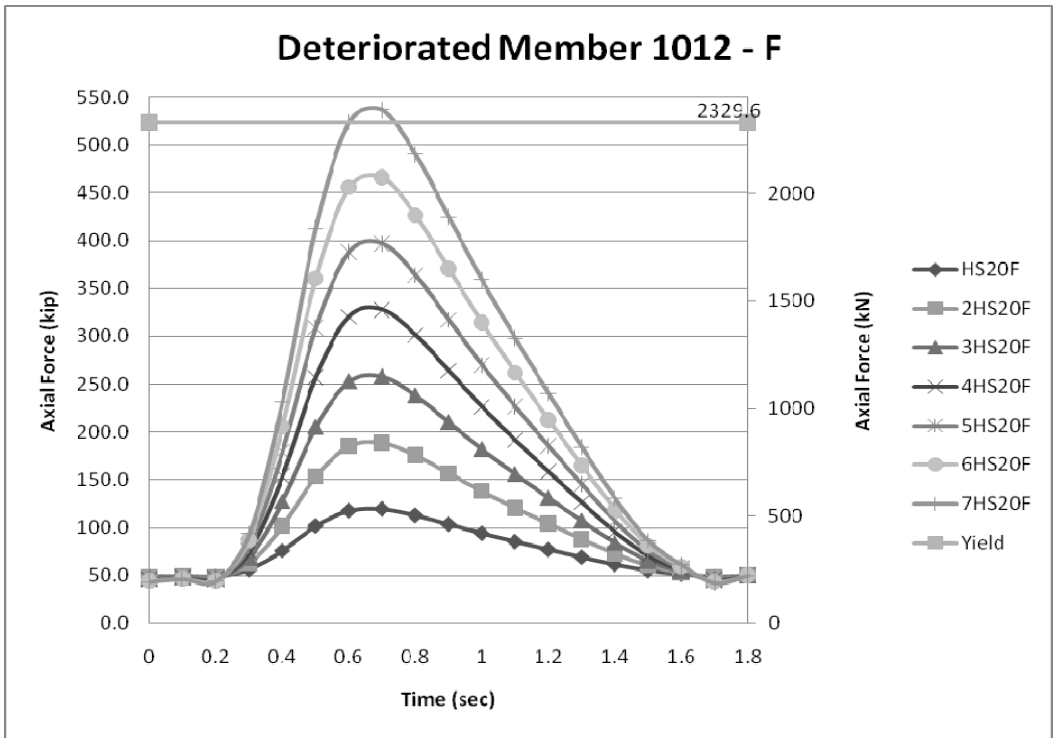

Figure **5-26**. Axial Force in Member 1012 Due to Incementing West to East HS-20 Truck

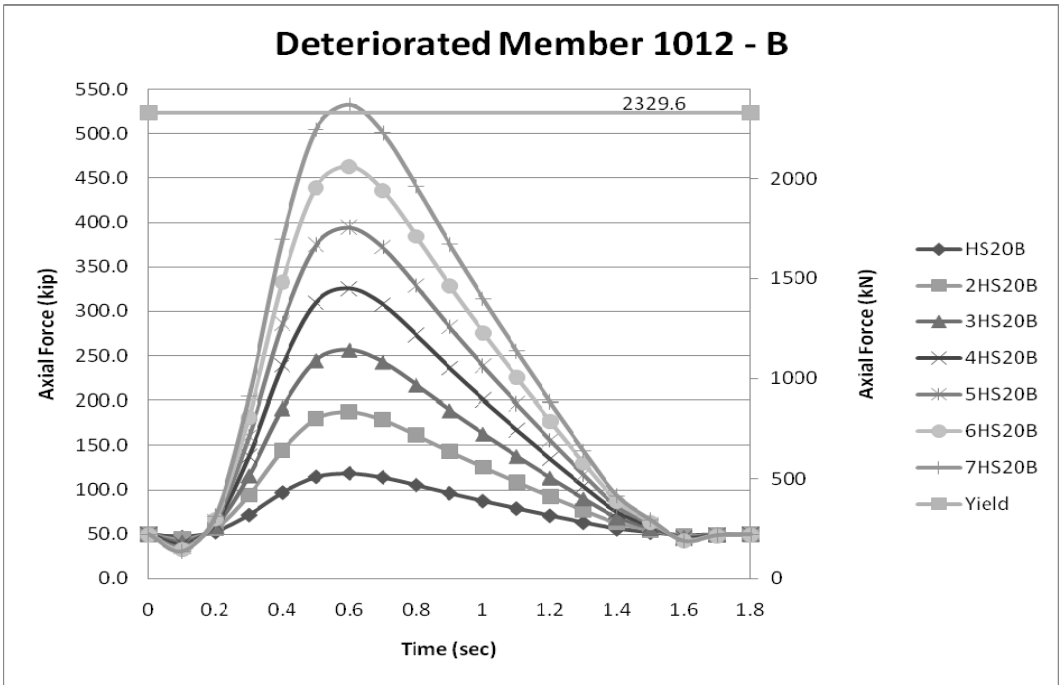

Figure **5-27**. Axial Force in Member 1012 Due to Incrementing East to West HS-20 Truck

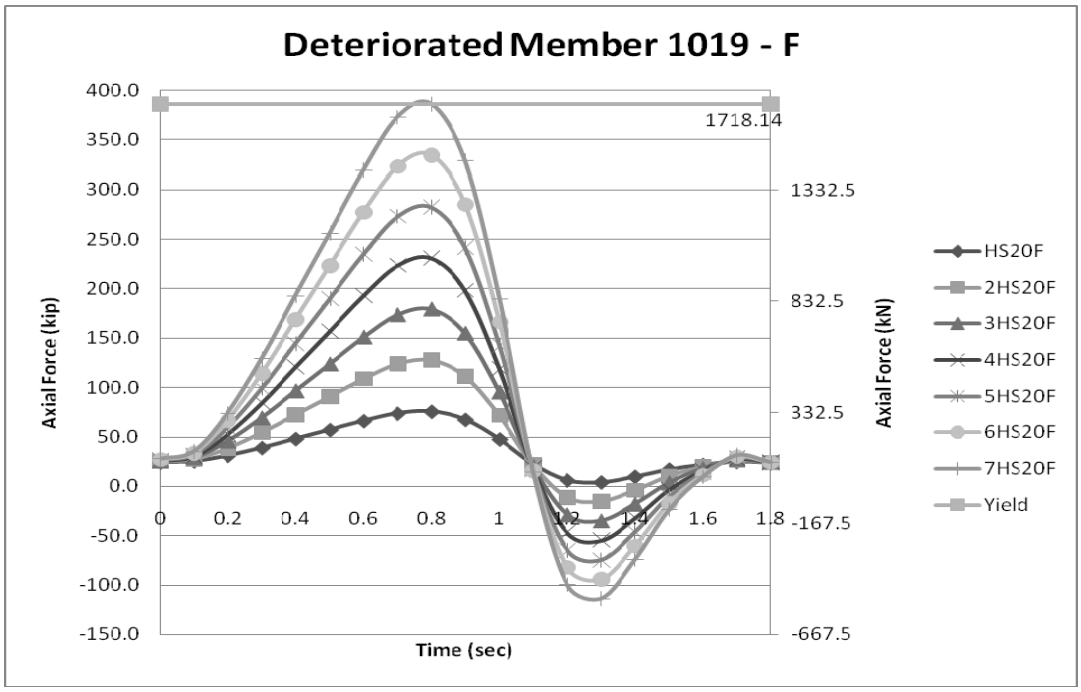

Figure **5-28**. Axial Force in Member 1019 Due to Incrementing West to East HS-20 Trucks

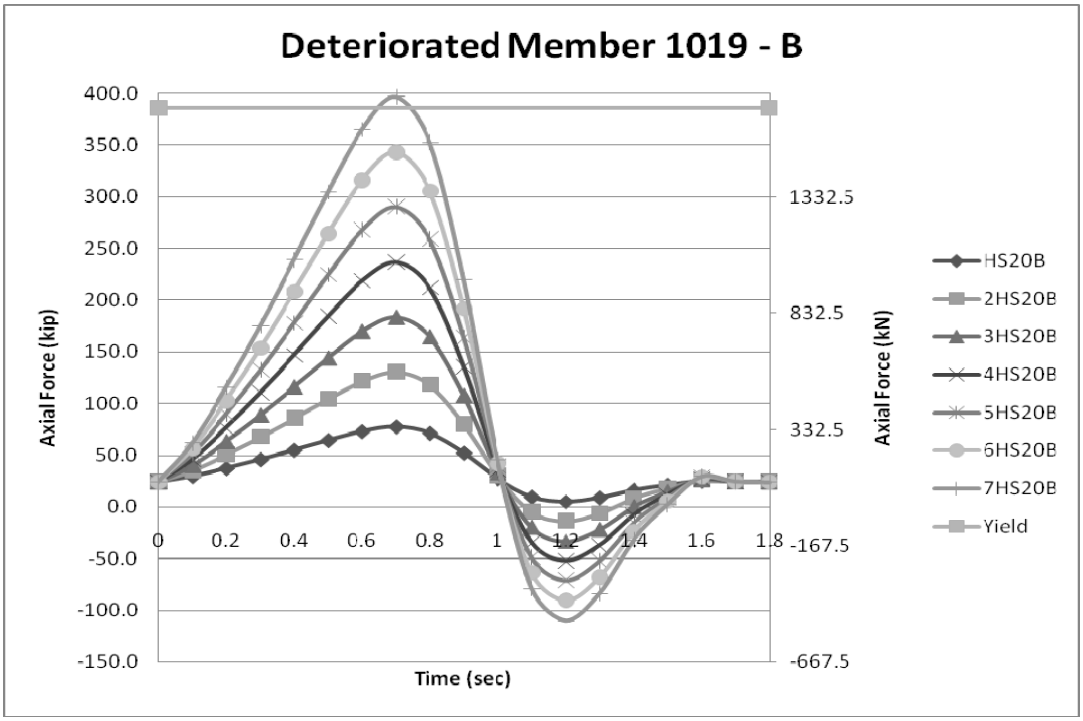

Figure **5-29**. Axial Force in Member 1019 Due to Incrementing East to West HS-20 Trucks

Figures 5-26 and 5-27 show the axial force for Member 1012, with the truck traversing west to east, and the critical load occurred at 0.7 seconds or 21.35 m (70 ft) from the west abutment. The lead axle was located at the critical location and the remaining axles are spaced accordingly behind the lead axle. The critical location for the truck traversing ease to west for Member 1012 was 18.29 m (60 ft) from the west abutment. The truck traversing west to east was the critical case because it caused the highest axial force of 2386.9 kN (536.39 kips) in the member.

Figures 5-28 and 5-29 indicated that the critical location for Member 1019 was determined to be 24.38 m (80 ft) from the west abutment for the truck travelling west to east. For the truck travelling in the east to west direction the critical location was determined to be 21.35 m (70 ft) from the west abutment. This member also had appreciable load reversal. The compressive capacity for the member was determined to be 602.1 kN (135.3 kips) and the maximum compressive force in the member under seven stacked side-by-side trucks was 507.3 kN (114 kips). Seven stacked side-by-side HS-20 trucks traversing east to west caused the highest axial force of 1766.2 kN (396.9 kips) in Member 1019.

The seven HS-20 truck loads for each critical location were distributed in the same manner discusses in Section 5.2.3 for the pristine bridge. Figure 5-17 details the typical wheel load distribution completed at each critical load location.

5.3.4 Critical Member Removal and Load Redistribution Analysis

The same critical member removal and load redistribution analysis was performed on the deteriorated model of the Beech Creek Veterans Memorial Bridge as the pristine model (see Section 5.2.4). For the deteriorated analysis, the hinge properties were modified to reflect the deterioration. Table 5-17 shows the tensile capacity and Table 5-22 shows the compression capacity of the deteriorated truss members. Combined axial and bending hinges were not used because the established critical members were truss members in the model and only carried axial forces. Individual analyses were completed to establish failure patterns for each of the critical members. The same failure limit from SAP2000 used for the pristine model was used for the deteriorated model.

Using the critical member removal and load redistribution analysis, Member 1012 was the first critical member analyzed. Force controlled hinges were placed in Members 1016 and 1017, the counters, and in Member 1012. The load was ramped from zero to seven side-by-side stacked trucks. All of the remaining tensile and compressive forces in the members in the trusses were checked using Tables 5-17 and 5-22 to determine if any of the members yielded or buckled. The combined axial and bending stresses were checked in the top and bottom chord as well. After the failure of Members 1017 (compression) and 1012 (tension), the load was redistributed and Member 1016 had a tensile force greater than the limit. A force controlled hinge was placed in the member and the analysis was completed again. After the load redistribution, Member 1019 had a tensile force greater than the critical limit. Again, a hinge was placed in the member and the analysis was completed. Member 1011 now had an axial force greater than the limit.

The failure of Member 1011 caused SAP2000 to terminate the analysis. Figure 5-30 shows the members and the sequence that members failed in the deteriorated truss member. None of the members in the south truss yielded or buckled during the analysis. Figure 5-31 shows the deflected shape of the North Truss after all of the members except the final member, Member 1011, has failed. After the final member failed, it was impossible to retrieve a deflected shape because the bridge was assumed to have collapsed. Since it appears that there are large bending effects in the top and bottom chord they needed to be checked for combined axial and bending effects to ensure that the members were under the yield stress.

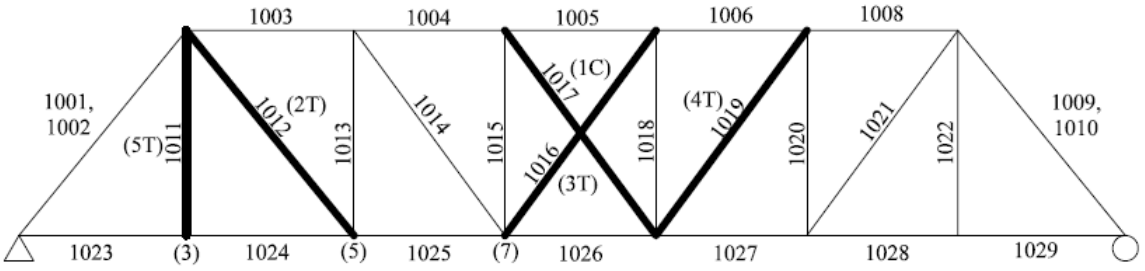

Figure **5-30**. Failed Members, Deteriorated Critical Member 1012

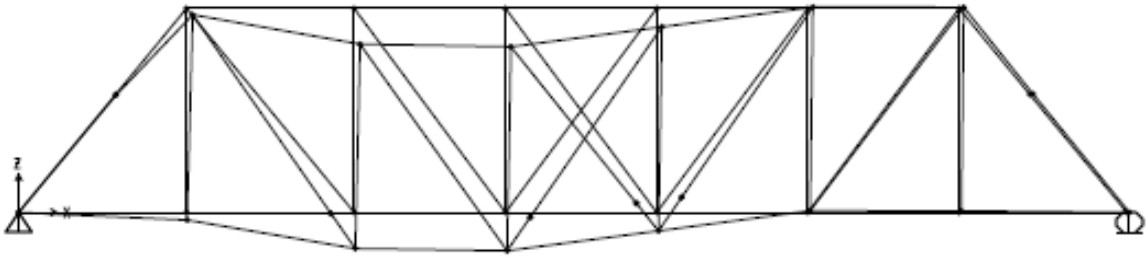

Figure **5-31**. Deflected Shape, Deteriorated Critical Member 1012

Table 5-24 summarizes the combined axial and bending affects due to the removed members. The forces in the members were determined after Member 1019 was removed from the truss and the forces were redistributed prior to the collapse of the bridge. None of the members were determined to have combined stresses greater than the yield stress, although stresses in certain members approached the yield stress.

Member	Element	Area cm^2 (in^2)	Sx cm^3 (in^3)	P kN (kip)	M kN-m (kip-in)	P/A MPa (ksi)	M/Sx MPa (ksi)	P/A + M/Sx MPa (ksi)
1001	L0-U1	250.9	3558.3	-4140.3	91.5	-145.8	22.7	168.6
		(38.9)	(217.1)	(-930.4)	(809.9)	(-23.9)	(3.73)	(27.6)
1002	L0-U1	250.9	3558.3	-4021.3	-160.8	-141.6	-40.0	181.6
		(38.9)	(217.1)	(-903.7)	(-1423.0)	(-23.2)	(-6.55)	(29.8)
1003	EL2	234.8	3333.7	-3201.7	-54.3	-120.5	-14.4	134.9
		(36.4)	(203.4)	(-719.5)	(-480.6)	(-19.8)	(-2.36)	(22.1)
1004	EL3	281.2	4090.9	-3042.7	26.0	-95.6	5.6	101.2
		(43.6)	(249.6)	(-683.7)	(230.4)	(-15.7)	(0.92)	(16.6)
1005	EL3	281.2	4090.9	-2890.0	-4.9	-90.8	-1.1	91.9
		(43.6)	(249.6)	(-649.4)	(-43.6)	(-14.9)	(-0.17)	(15.1)
1006	EL3	281.2	4090.9	-2619.4	-25.2	-82.3	-5.5	87.8
		(43.6)	(249.6)	(-588.6)	(-223.3)	(-13.5)	(-0.89)	(14.4)
1008	EL2	234.8	3333.7	-2504.9	58.3	-94.3	15.5	109.7
		(36.4)	(203.4)	(-562.9)	(515.8)	(-15.5)	(2.54)	(18.0)
1009	L7-U6	248.3	3522.2	-1618.4	-137.9	-57.6	-34.6	92.2
		(38.5)	(214.9)	(-363.7)	(-1220.3)	(-9.4)	(-5.68)	(15.1)
1010	L7-U6	248.3	3522.2	-1739.2	-22.5	-61.9	-5.7	67.6
		(38.5)	(214.9)	(-390.8)	(-199.4)	(-10.2)	(-0.93)	(11.1)
1023	L1-L2	221.2	5321.8	2811.8	-164.4	112.3	-27.3	139.6
		(34.3)	(324.7)	(631.9)	(-1454.6)	(18.4)	(-4.48)	(22.9)
1024	L2-L3	232.8	5600.5	2341.7	-253.3	88.9	-40.0	128.9
		(36.1)	(341.7)	(526.2)	(-2241.5)	(14.6)	(-6.56)	(21.1)
1025	L3-L4	236.7	5695.5	2181.5	121.1	81.4	18.8	100.2
		(36.7)	(347.5)	(490.2)	(1071.4)	(13.4)	(3.08)	(16.4)
1026	L4-L5	259.3	6202.0	1890.1	-111.1	64.4	-15.8	80.3
		(40.2)	(378.4)	(424.7)	(-983.4)	(10.6)	(-2.60)	(13.2)
1027	EL4	245.7	5913.5	1759.3	131.7	63.3	19.7	83.0
		(38.1)	(360.8)	(395.3)	(1165.9)	(10.4)	(3.23)	(13.6)
1028	EL4	245.7	5913.5	569.9	115.5	20.5	17.3	37.8
		(38.1)	(360.8)	(128.1)	(1021.7)	(3.4)	(2.83)	(6.2)
1029	EL4	245.7	5913.5	817.6	116.4	29.4	17.4	46.8
		(38.1)	(360.8)	(183.7)	(1030.2)	(4.8)	(2.86)	(7.7)

Table **5-24**. Combined Axial and Bending Stress for Top and Bottom Chord, Deteriorated Critical Member 1012

Member 1019 was analyzed in the same manner as Member 1012. Force controlled hinges were placed in the two counters and then the critical member, Member 1019. After the load had been redistributed to the remaining structure one member was above the critical tensile force, Member 1021. A force controlled hinge was placed in the member, using hinge properties shown in Tables 5-15 and 5-20, and the analysis was completed again. After Member 1021 failed, Member 1022 failed in tension. A hinge was placed in the member and the analysis was completed again. During that analysis, the program terminated. Figure 5-32 displays the critical members and shows the three diagonals and vertical post that failed under the seven HS-20 trucks. Figure 5-33 shows the deflected shape of the North Truss after all of the members except the final member, Member 1011, has failed. After the final member failed, it was impossible to retrieve a deflected shape because the bridge was assumed to have collapsed. Since it appears that there are large bending effects in the top and bottom chord they needed to be checked for combined axial and bending effects to ensure that the members were under the yield stress.

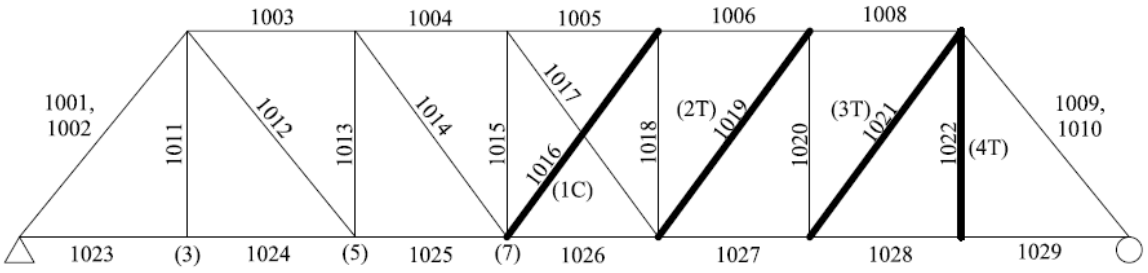

Figure **5-32**. Failed Members, Deteriorated Critical Member 1019

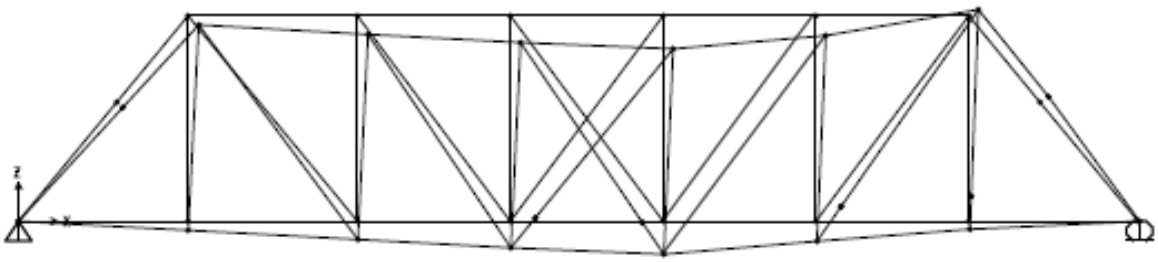

Figure **5-33**. Deflected Shape, Deteriorated Critical Member 1019

Table 5-25 summarizes the combined axial and bending affects due to the removed members. The forces in the members were determined after Member 1019 was removed from the truss and the forces were redistributed prior to the collapse of the bridge. None of the members were determined to have combined stresses greater than the yield stress, although stresses in certain members approached the yield stress.

Member	Element	Area cm^2 (in^2)	Sx cm^3 (in^3)	P kN (kip)	M kN-m (kip-in)	P/A MPa (ksi)	M/Sx MPa (ksi)	P/A + M/Sx MPa (ksi)
1001	L0-U1	250.9 (38.9)	3558.3 (217.1)	-2687.1 (-603.8)	-349.1 (-3089.3)	-94.6 (-15.5)	-86.8 (-14.23)	181.4 (29.8)
1002	L0-U1	250.9 (38.9)	3558.3 (217.1)	-2442.0 (-548.8)	281.9 (2495.1)	-86.0 (-14.1)	70.1 (11.49)	156.1 (25.6)
1003	EL2	234.8 (36.4)	3333.7 (203.4)	-3036.3 (-682.3)	-7.7 (-68.4)	-114.3 (-18.7)	-2.0 (-0.34)	116.3 (19.1)
1004	EL3	281.2 (43.6)	4090.9 (249.6)	-4231.6 (-950.9)	-5.2 (-46.3)	-133.0 (-21.8)	-1.1 (-0.19)	134.1 (22.0)
1005	EL3	281.2 (43.6)	4090.9 (249.6)	-4078.6 (-916.5)	5.6 (49.9)	-128.2 (-21.0)	1.2 (0.20)	129.4 (21.2)
1006	EL3	281.2 (43.6)	4090.9 (249.6)	-3507.9 (-788.3)	15.0 (132.7)	-110.2 (-18.1)	3.2 (0.53)	113.5 (18.6)
1008	EL2	234.8 (36.4)	3333.7 (203.4)	-3078.4 (-691.8)	-62.2 (-550.4)	-115.9 (-19.0)	-16.5 (-2.71)	132.4 (21.7)
1009	L7-U6	248.3 (38.5)	3522.2 (214.9)	-3177.0 (-713.9)	-187.1 (-1656.1)	-113.1 (-18.5)	-47.0 (-7.71)	160.0 (26.2)
1010	L7-U6	248.3 (38.5)	3522.2 (214.9)	-3212.7 (-722.0)	-200.7 (-1776.4)	-114.3 (-18.8)	-50.4 (-8.27)	164.7 (27.0)
1023	L1-L2	221.2 (34.3)	5321.8 (324.7)	1670.4 (375.4)	167.7 (1483.6)	66.7 (10.9)	27.9 (4.57)	94.6 (15.5)
1024	L2-L3	232.8 (36.1)	5600.5 (341.7)	1188.7 (267.1)	470.5 (4163.6)	45.1 (7.4)	74.3 (12.18)	119.4 (19.6)
1025	L3-L4	236.7 (36.7)	5695.5 (347.5)	1978.4 (444.6)	341.6 (3023.4)	73.9 (12.1)	53.0 (8.70)	126.9 (20.8)
1026	L4-L5	259.3 (40.2)	6202.0 (378.4)	2585.5 (581.0)	-246.9) (-2185.3)	88.1 (14.5)	-35.2 (-5.78)	123.3 (20.2)
1027	EL4	245.7 (38.1)	5913.5 (360.8)	2229.5 (501.0)	37.8 (334.8)	80.2 (13.1)	5.7 (0.93)	85.8 (14.1)
1028	EL4	245.7 (38.1)	5913.5 (360.8)	1992.3 (447.7)	99.1 (876.6)	71.6 (11.8)	14.8 (2.43)	86.5 (14.2)
1029	EL4	245.7 (38.1)	5913.5 (360.8)	2117.5 (475.8)	125.8 (1113.3)	76.1 (12.5)	18.8 (3.09)	95.0 (15.6)

Table **5-25**. Combined Axial and Bending Stress for Top and Bottom Chord, Deteriorated Critical Member 1019

From the critical member removal and load redistribution analysis, trends were observed for the deteriorated model. The trends observed were similar to the pristine model; including the truck direction determined what end of the bridge would have critical members, the position of the truck was critical to distribute the highest amount of load to the truss, and local and global failure patterns. Another trend similar to the pristine model was position of the truck. When the truck was position in two floor panels, the axial force in the critical members was the highest. These two trends were observed for both of the models.

From Figures 5-30 and 5-32 failure patterns were established for the deteriorated bridge model. Using the same definition from Section 5.2.4, the local and global failure patterns were observed. For Member 1012, the center compression diagonal failed first followed by Member 1012. The other center diagonal failed once the load was redistributed and then the diagonal in the fifth panel failed. The last member to fail before termination of the program was the first vertical at the west end of the bridge. Member 1019's failure sequence began with the center compression diagonal buckling followed by the diagonal in the fifth panel, Member 1019. The failure progressed to the next panel causing the diagonal to fail. The last member to fail was member last vertical post in the east end of the bridge. From both failure patterns, one member (Member 1019) besides the counters failed. This could be attributed to the amount of section loss present in the member. This member could then be considered the most critical member for the deteriorated bridge model since it failed in all of the failure patterns. The two failure patterns and trends for the deteriorated bridge were then compared to the failure

patterns and trends for the pristine bridge to determine if deterioration and aging played a role in the global response of the bridge.

5.4 Comparison of Pristine and Deteriorated Model

A comparison between the pristine and deteriorated Beech Creek Veterans Memorial Bridge model was completed comparing the critical load, critical location, and the final global failure patterns. The critical load was the number of stacked side-by-side HS-20 trucks that caused a member to yield. The critical location was the position of the HS-20 truck along the length of the bridge that caused a particular member the largest axial force. The final global failure pattern was the sequence of member failures that caused the program to terminate.

The pristine model had a critical load of eight HS-20 trucks while the deteriorated model had a critical load of seven HS-20 trucks. The amount of section loss determined from the condition evaluation played a major role in reduction of the critical load. The north truss of the bridge had excessive deterioration. From Tables 5-8 through 5-11, the center diagonals lost 20% of their cross sectional area while other diagonals had an average loss of 11% of their cross sectional area. Deterioration of the verticals averaged 6%.

After the critical load was determined for the pristine and deteriorated model, the critical location of the HS-20 trucks was determined. For the pristine bridge, with a load of eight side-by-side stacked HS-20 trucks, four critical locations were determined based on four members failing in the bridge. Members 1012, 1020, 1040, and 1049 yielded

under the prescribed loading. The deteriorated bridge had two critical locations located in the north truss. Member 1012 and 1019 were the members that failed under a loading of seven HS-20 trucks. Table 5-26 summarizes the critical locations due to either a forward or backward truck for each of the critical members.

Model	Member Identification	Vehicle Load	Critical Location m (ft)
Pristine Bridge	Member 1012	8HS-20B	18.29 (60)
	Member 1021	8HS-20F	30.48 (100)
	Member 1040	8HS-20F	27.43 (90)
	Member 1049	8HS-20B	33.53 (110)
Deteriorated Bridge	Member 1012	7HS-20B	18.29 (60)
	Member 1019	7HS-20F	21.34 (70)

Table **5-26**. Critical Locations, Pristine and Deteriorated Bridge

From the condition evaluation, Member 1012 had 6.7% section loss which resulted in 6.13 cm^2 (0.95 in^2) area lost. Member 1019 lost 16% of its cross sectional area. Even though other members had greater section loss, the reason for Member 1012 being critical for both analyses was a function of the section properties and the axial forces in the member. Other members that were in tension, like the bottom chord of the truss, had much greater cross sectional areas. Deterioration would not affect these members as much as members with smaller cross sectional areas. The other critical member in the north truss for the pristine model, Member 1021, did not control for the

deteriorated model because the amount of deterioration was almost negligible. Member 1019 was critical because such high amount of deterioration.

Some trends were observed for both the pristine and deteriorated model. First, the location of the truck to cause the maximum affect on a particular member was critical. For every critical location, the truck was positioned so that the wheel loads were within two floor panels to cause the maximum load distribution to the members. This truck position caused a more concentrated load to transfer to the members of the truss. This trend occurred for all of the critical members in the pristine and deteriorated bridge models. Another trend that was observed was the affect of the direction of the HS-20 trucks in relation to what member or members would be critical. A truck traversing west to east would cause members at the east end of the bridge to be critical whereas a truck traversing east to west would cause members at the west end of the bridge to be critical. This was observed for both the pristine and deteriorated model. Skew of the bridge and axle configuration may play a role in why this behavior occurred. The last trend that was observed was the most critical member in each analysis. In the pristine analysis, the tension counter diagonal failed for every critical load location. In the deteriorated model, Member 1019, which was not a counter, was determined to be the most critical member because it failed for both of the analyses. Member 1019 was the most critical because of the amount of section loss present. The member lost 16% of its cross sectional area. Deterioration played a role in transferring the most critical member from the center of the bridge to the diagonal in the fifth panel of the bridge.

The final member failure sequence initiated by Member 1012 for the pristine and deteriorated models was different. Figures 5-34 and 5-35 compare the pristine and

deteriorated member failure sequence. In the pristine model, Member 1017 buckled first under the load and then Member 1012 failed at a capacity of 2516.8 kN (565.5 kips). The load was then redistributed and Member 1016 failed. After redistribution again, Member 1011 failed and then caused Member 1019 to fail. The sequence of members failing was Members 1017, 1012, 1017, 1011, and finally 1019.

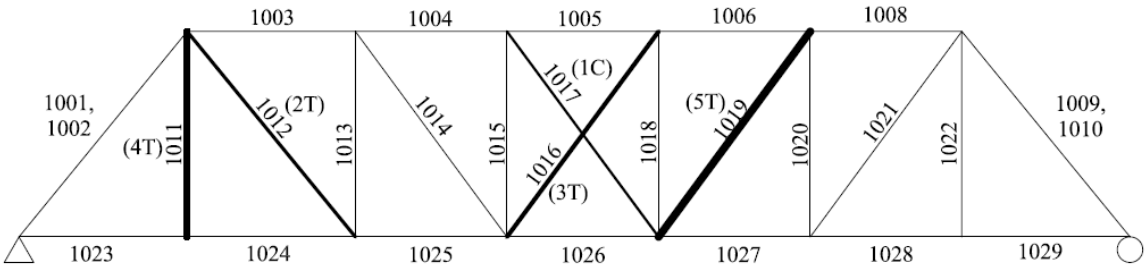

Figure **5-34**. Failure Members of the Pristine Model, Critical Member 1012

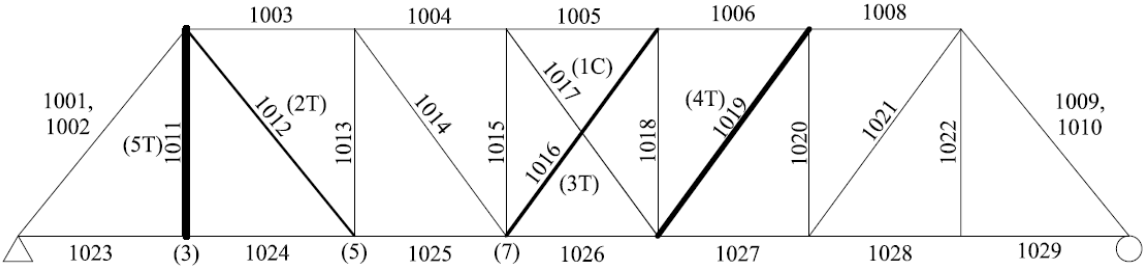

Figure **5-35**. Failure Members of the Deteriorated Model, Critical Member 1012

The deteriorated model had the same members fail but in a different sequence. Member 1017 buckled first and then Member 1012 failed at a capacity of 2329.6 kN (523.5 kips). Member 1016 failed followed by Member 1019. The last member to fail was Member 1011. The sequence of failure was Members 1017, 1012, 1016, 1019, and then 1011. The reduced section properties played a role in the sequence changing from

the pristine model failure pattern. Member 1019 had 16% section loss and Member 1011 only had 7.4% section loss. The difference in deterioration caused a member to yield before another because the reduction in area caused higher stresses at the same axial force.

The member failure sequence initiated by Member 1019 of the deteriorated bridge was compared to the member failure sequence initiated by Member 1021 of the pristine model to see if the global behavior of failure was similar even though the members were in different locations in the truss. The members could be compared because they were both diagonal members in the east end of the bridge. Figure 5-36 shows the failure sequence of Member 1021 of the pristine model and Figure 5-37 shows the failure sequence of Member 1019 of the deteriorated model. It was also observed that the direction of the sequence of members failing changed from the pristine model to the deteriorated model. In the pristine model, the failure was initiated on the outside of the bridge and progressed inward to the center diagonals. The deteriorated model had a failure that was initiated in the center of the bridge and progressed outward to the east end of the bridge. For both analyses, the outer vertical post was the last member to fail.

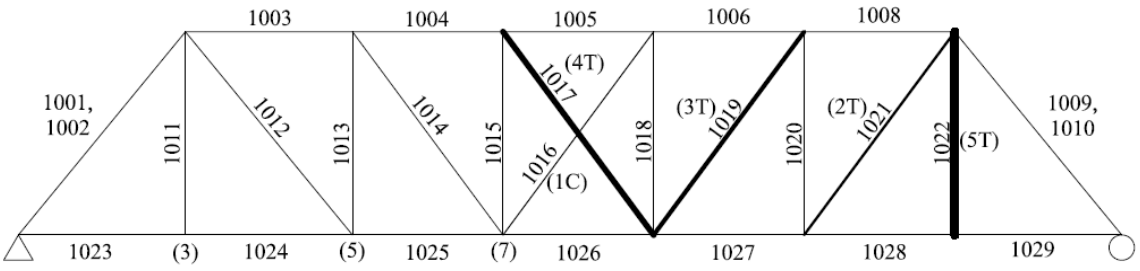

Figure **5-36**. Failure Members of the Pristine Model, Critical Member 1021

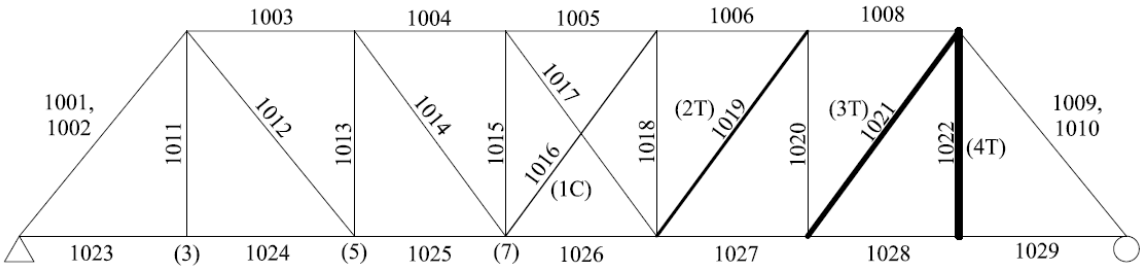

Figure **5-37**. Failure Members of the Deteriorated Model, Critical Member 1019

5.5 Conclusions

Section loss played a role in the critical load and final global failure pattern of the deteriorated truss bridge. The pristine bridge determined the expected behavior and failure sequence while the deteriorated model showed that the behavior changed when aging and deterioration were accounted for. Deterioration changed the overall capacity of the bridge and the collapse sequence of the bridge.

The level of deterioration and robustness of the bridge was apparent in the Beech Creek Veterans Memorial Bridge. Even though a member had 20% section loss, the capacity was only reduced by one side-by-side HS-20 truck. Since the redundancy of the structure was reduced due to the deterioration, the additional reserve strength of the in the bridge was reduced. The stacked HS-20 trucks represented the amount of redundancy inherent in the structure. The structure was able to carry well over its design load from a collapse perspective. The capacity may have decreased more if the south truss had experienced section loss and deterioration similar to the north truss. The deterioration

that was present in the north truss was due to the addition of a sidewalk which allowed water and deicing salts to collect on the structural members.

The amount of section loss present in the Beech Creek Veterans Memorial Bridge was not constant throughout the bridge. Some members had deterioration of 20% of their cross sectional area and others did not have any section loss. Even with that disparity, the redundancy of the bridge dropped from eight stacked side-by-side HS-20 trucks to seven. Although a member lost 20% of its cross sectional area, the redundancy only dropped by one side-by-side HS-20 truck showing that this bridge has a lot of resiliency. Owners should be aware of the risks associated with deterioration and section loss present in the bridge. They should also know that members with more section loss are more likely to become critical even though that was not the original design. For this bridge, diagonal members should be given special attention because in every failure pattern, it was a diagonal member which failed first after the counter.

This research looked at critical member removal of a deteriorated truss bridge to determine the effects of deterioration on the behavior of the bridge. Even though the Dysart Bridge in Cambria County collapsed after the removal of one critical member, the removal was due to vehicle collision. Vehicle collision or impact loading in conjunction with deterioration was not investigated in this research. The next chapter summarizes the research conducted and gives recommendations for designers when analyzing truss bridges and accounting for deterioration.

Chapter 6

Summary and Conclusions

6.1 Summary

The purpose of this study was to determine whether aging and deterioration play a role in the global behavior of truss bridges subjected to stacked side-by-side HS-20 trucks. The primary objective was to understand the behavior of a Pratt Truss when critical members were removed and to investigate load redistribution to the remaining members. The secondary objective was to observe the behavior of truss members in tension and compression and the susceptibility of the entire structure to collapse when the critical member was removed. The last objective of the study was to determine if aging and deterioration affected the load redistribution in the truss members and the global failure sequence of the truss.

The research conducted included three analytical models; one of the Rock Creek Bridge and two of the Beech Creek Veterans Memorial Bridge. The model of the Rock Creek Bridge was used to validate the modeling procedure of truss bridges proposed by Azizinamini et al. (1997). The models of the Beech Creek Veterans Memorial Bridge included a pristine model, which was based from the original plans and had no deterioration, and a deteriorated model, which contained deterioration and section loss from an earlier condition evaluation. A linear elastic analysis was completed to determine the critical member, critical load, and critical load location for the pristine and deteriorated model. A critical member removal and load redistribution analysis was then

completed on both models to determine the load redistribution when a critical member was removed and the failure pattern for each case. SAP2000 force controlled hinges were placed in the critical members and allowed for the member to redistribute the load it was carrying. A comparison was then made between the pristine and deteriorated truss models.

6.2 Conclusions

Several conclusions and trends were observed from the research. Table 6-1 summarizes the failure sequence for the pristine and deteriorated bridge. Refer to Figures 5-7 and 5-8 for member identification. For each analysis, the counter in compression buckled prior to any other member failing because it was unable to carrying any compressive force.

Model	Critical Member	Member Failure Sequence
Pristine Bridge	Member 1012	1017→1012→1016→1011→1019
	Member 1021	1016→1021→1019→1017→1022
	Member 1040	1045→1040→1044→1039→1047
	Member 1049	1044→1049→1047→1045→1050
Deteriorated Bridge	Member 1012	1017→1012→1016→1019→1011
	Member 1019	1016→1019→1021→1022

Table **6-1**. Member Failure Sequence, Pristine and Deteriorated Model[1]

Additional conclusions and recommendations from this research are as follows:

- Deterioration and aging had a direct affect on the capacity and load redistribution of the truss bridge. Deterioration lowered the capacity of the bridge from eight stacked HS-20 trucks to seven which meant that the overall capacity in the bridge was reduced slightly.

- Even though deterioration altered the capacity of the bridge, the deteriorated Beech Creek Veterans Memorial Bridge was able to carry seven stacked side-by-side HS-20 trucks before a member failed. This indicates that the bridge is able to carry seven times the amount of load than what the bridge was designed for. The ability to carry this amount of load showed that this structure was quite effective in redistributing loads and contained multiple load paths, even in its

[1] The truss counters, Members 1016, 1017, 1044, and 1045, always failed first in compression.

deteriorated state. Considering other cases of failure, the most common would be failure of the connections. The failure of the connection could be due to either deterioration or fatigue but generally leads to a brittle failure. The high level of redundancy for both the pristine and deteriorated model could be due to the fact that the connections were assumed to remain intact during member removal. Another type of failure, similar to that of the I-35W Bridge in Minneapolis, Minnesota is a design flaw that leads to members being under designed. The last type of failure that could occur is due to collision impact removing connections and members.

- Tension diagonals of the Beech Creek Veterans Memorial Bridge were determined to be the most critical members. In every critical member analysis, the tension diagonals failed. Also, when the load was redistributed once the critical member was removed from the truss, other tension diagonals then became critical and failed.

- Deterioration altered the member failure sequence. In the deteriorated analysis, some members having deterioration were determined to be critical before they were deemed critical in the pristine analysis.

- The position of the truck was critical to causing the maximum effect in the truss members. Trucks positioned within two floor panels were determined to be the most critical loading scheme because more wheel loads were distributed to the floor system supporting those panels.

- The direction of the truck played a role in which member was the most critical. For trucks traversing west to east, members in the east end of the truss were critical. For trucks traversing east to west, members in the west end of the truss were critical. The skew of the bridge and the axle configuration could have played a role in which members were critical depending on the direction of the stacked side-by-side HS-20 trucks.

- The most critical member for the pristine model was the tension counter in the center of the bridge. For the deteriorated model, Member 1019, a diagonal located in the fifth panel from the west end of the bridge, was the most critical member because it failed in all of the deteriorated analyses. The large amount of deterioration (16% of its cross sectional area) present in Member 1019 made it susceptible to failure sooner than other members.

- The member failure sequence initiating with Member 1012, for the pristine and deteriorated models, was different even though the critical load location was the same. This indicated that deterioration plays a role in the load redistribution and overall response of the bridge.

- The Beech Creek Veterans Memorial Bridge pristine and deteriorated model had significant capacity compared to present day bridge design standards. Conservatism was much higher when the Beech Creek Veterans Memorial Bridge was designed because there were greater unknowns in design. Also, the high capacity of the bridge could be related to the way the bridge was modeled.

Connections were assumed to be completely functional when a member was removed. If the connection was assumed to have failed, the failure of the bridge would have occurred at a much lower level and it would have been a brittle failure.

6.3 Future Research

The research completed for this project has provided information on the global behavior effects of deterioration and aging on Pratt Truss bridges by examining a single structure. This study was limited in the fact that only one Pratt Truss was investigated. Numerous Pratt Truss bridges should be investigated to categorize critical members, load redistribution, and failure patterns inherent to the specific geometry of the Pratt Truss.

A variety of truss bridges (Warren and Howe Trusses) should be analyzed to determine the effects from changing the geometry of the bridge, modeling connections, and determine if the skew of the bridge affects the behavior. Dynamic analyses of the bridge should be investigated as well to determine if the dynamic removal of the member changes the response and load redistribution of a structure. Impact loading in due to vehicle collision in conjunction with deterioration should be investigated because the Dysart Bridge collapsed from the removal of one critical member. Lastly, a method for determining how to account for deterioration in particular sections should be investigated to see if it changes the global response of the bridge.

Bibliography

AASHTO. (2003). "2003 Interim Revisions for the Manual for Condition Evaluation of Bridges." *American Association of State Highway and Transportation Officials*, Washington, DC.

AASHTO. (2004). "Manual for Condition Evaluation and Load and Resistance Factor Rating (LRFR) of Highway Bridges." *American Association of State Highway and Transportation Officials*, Washington, DC.

AASHTO. (2008). "AASHTO LRFD Bridge Design Specifications, 4th ed." *American Association of State Highway and Transportation Officials*, Washington, DC.

Aktan, A. E., Lee, K. L., Naghavi, R., and Hebbar, K. (1994). "Destructive Testing of Two 80-year-old Truss Bridges." *Transportation Research Record*, 1460, 62-72.

Azizinamini, A. (2002). "Full Scale Testing of Old Steel Truss Bridge." *Journal of Constructional Steel Research*, 58, 843-858.

Azizinamini, A., Mehrabi, A., Lotfi, H., and Mans, P. (1997). "Evaluation and Retrofitting of Historic Steel Truss Bridges." *NDOR Research Project Number STPB-STWD(13),* Federal Highway Administration, 472 pp.

Azizinamini, A., Mehrabi, A., Lotfi, H., Mans, P. (1997). "Evaluation and Retrofitting of Historic Steel Truss Bridges." *Final Report, STPB-STWD(13),* University of Nebraska-Lincoln, 479 pp.

Barker, R. M., and Puckett, J. A. (2007). "Introduction to Bridge Engineering." *Design of Highway Bridges An LRFD Approach*, John Wiley and Sons, New York, NY., 24-38.

Bhat, N. U. (1984). *Elements of Applied Stochastic Process* 2nd ed., John Wiley and Sons, Inc., N.Y.

Chen, P., and Powell, G. (1982). "Generalized Plastic Hinge Concenpts for 3D Beam-Column Elements." *Report Number UCB/EERC-82/20*, November, University of California at Berkeley, CA.

Dexter, R.J., Connor, R.J., and Mahmoud, H. (2005a). "NCHRP Synthesis 354: Inspection and Management of Bridges with Fracture-Critical Details." *Transportation Research Board, National Research Council*, Washington, DC, 76 pp.

Dexter, R.J., Connor, R.J., and Mahmoud, H. (2005b). "Review of Steel Bridges with Fracture-Critical Elements." *Transportation Research Record: Journal of the Transportation Research Board*, 1928, 75-82.

Dicker, D. F. (1971). "Point Pleasant Bridge Collapse Mechanism Analyzed." *Civil Engineering*, 41(7), 61-66.

Fisher, J. W. (1984). "Fatigue and Fracture of Structural Members at Details or Large Defects." *Fatigue and Fracture in Steel Bridges*, John Wiley & Sons, Inc., New York, NY., 20-33.

Ghosn, M., Moses, F. (1998). "NCHRP Report 406: Redundancy in Highway Bridge Superstructures." *Transportation Research Board, National Research Council,* Washington, DC, 50 pp.

Grata, J. (2007). "PennDOT Truck Escapes Bridge Collapse." *Pittsburgh Post-Gazette,* Pittsburgh, PA, <http://www.post-gazette.com/pg/07342/840217-147.stm> (July 25, 2008).

GSA. (2003). "Progressive Collapse Analysis and Design Guidelines for New Federal Office Buildings and Major Modernization Projects." *General Services Administration*, Washington, DC.

Historic American Engineering Record. (1976). "Trusses: a Study by the Historic American Engineering Record." *National Park Service*, Washington, DC.

Marjanishvili, S. (2004). "Progressive Analysis Procedure for Progressive Collapse." *Journal of Performance of Constructed Facilities,* 18(2), 79-85.

Mondkar, D., and Powell, G. (1975). "ANSRI, General Purpose Program for Analysis of Nonlinear Structural Response." *EERC, Report Number 75-37*, University of California at Berkeley, CA.

Nagavi, R. S., and Aktan, A. E. (2003). "Nonlinear Behavior of heavy Class Steel Truss Bridges." *Journal of Structural Engineering*, 129(8), 1113-1121.

Nair, R. S. (2003). "Progressive Collapse Basics." *Proc., Blast and Progressive Collapse Symposium*, AISC, New York, NY, 1-11.

National Institute of Standard and Technology (NIST). (2007). "Best Practices for Reducing the Potential for Progressive Collapse in Buildings (NISTR 7396)." 49-53.

Nonaka, T. (1977). "Approximation of Yield Condition for the Hysteric Behavior of a Bar Under Repeated Axial Loadings." *International Journal of Solids Structures,* 13, 637-643.

NTSB. (1968). "Collapse of US 35 Highway Bridge Point Pleasant, West Virginia." *National Transportation Safety Board*, Washington, DC., 5 pp.

NTSB. (1984). "Collapse of a Suspended Span of Route 95 Highway Bridge Over the Mianus River Greenwich, Connecticut." *National Transportation Safety Board*, Washington, DC., 4 pp.

NTSB. (2008). "Safety Recommendation." *National Transportation Safety Board*, Washington, DC., 5 pp.

Research and Innovative Technology Administration (RITA). (2008). "Condition of U.S. Highway Bridges by State: 2008." *U.S. Department of Transportation*, Washington, DC. <http://www.bts.gov/current_topics/2008_04_24_bridge_data/html/bridges_by_state.html>.

Rutz, F. R., and Rens, K. L. (2004). "Alternate Load Paths in Historic Truss Bridges: New Approaches for Preservation." *Proc., Structures 2004 – Building on the Past: Securing the Future,* Nashville, TN., 269-276.

SAP2000. (2000). "A Series of Computer Programs for the Finite Element Analysis of Structures." *Computers and Structures, Inc*., Berkeley, CA.

Scheffey, C. F. (1971). "Pt. Pleasant Bridge Collapse: Conclusions of the Federal Study." *Civil Engineering*, 41(7), 41-45.

Smith, J. W. (2006). "Structural Robustness Analysis and the Fast Fracture Analogy." *Structural Engineering International*, 16(2), 118-123.

Spyrakos, C. C., Raftoyiannis, I. G., and Ermopoulos, J. C. (2004). "Condition Assessment and Retrofit of a Historic Steel-Truss Railway Bridge." *Journal of Constructional Steel Research,* 60, 1213-1225.

Starossek, U. (2007). "Typology of Progressive Collapse." *Engineering Structures*, 29, 2302-2307.

Tennessee Department of Transportation. (2008). "History of Truss Bridges." *TDOT*, <http://www.tdot.state.tn.us/bridges/trussbridges.htm> (July 1, 2008).

Trautner, J. J., and Frangopol, D. M. (1990). "Computer Modeling and Reliability Evaluation of Steel Through Truss Bridges." *Structural Safety,* 7, 255-267.

United States Department of Defense (DoD). (2005). "Unified Facilities Criteria: Design of Buildings to Resist Progressive Collapse (UFC4-023-03)." 542 pp.

Appendix A

Figures

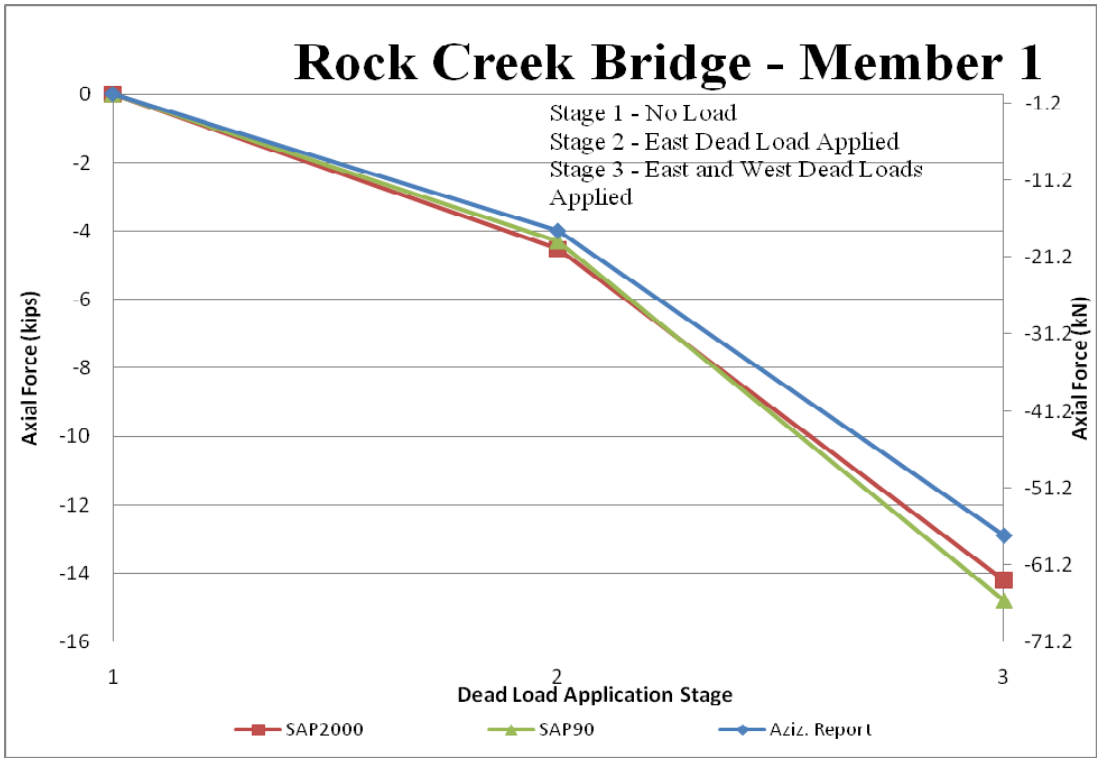

Figure **A4.1** – Axial Force in Member 1, Rock Creek Bridge

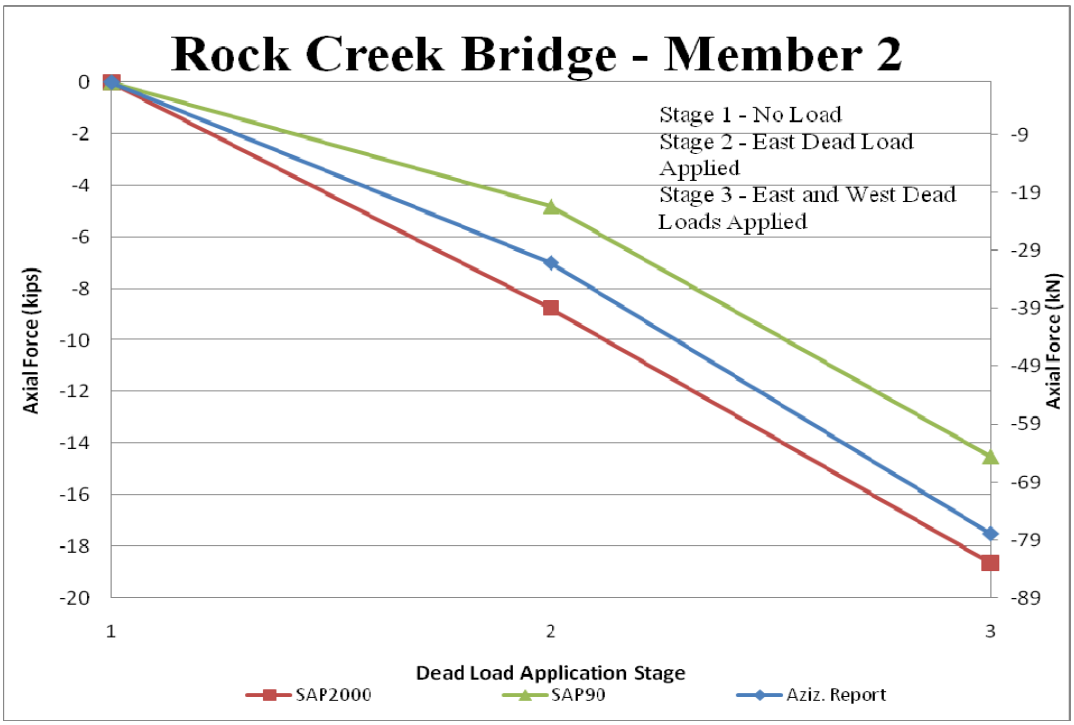

Figure **A4.2** – Axial Force in Member 2, Rock Creek Bridge

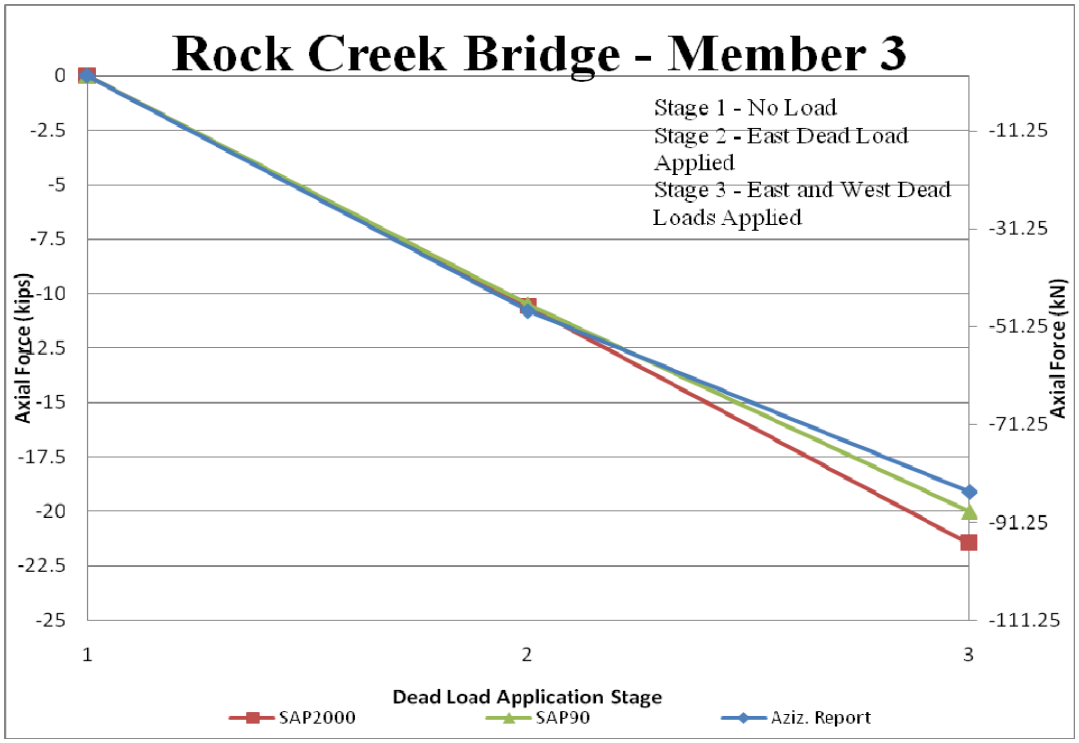

Figure **A4.3** – Axial Force in Member 3, Rock Creek Bridge

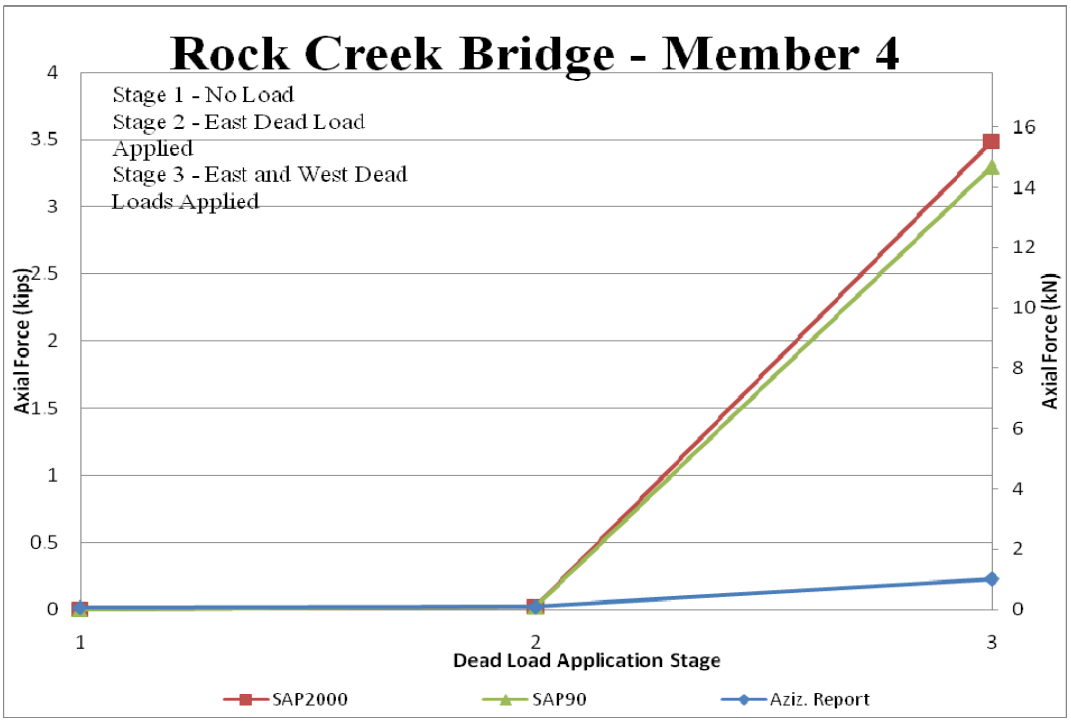

Figure **A4.4** –Axial Force in Member 4, Rock Creek Bridge

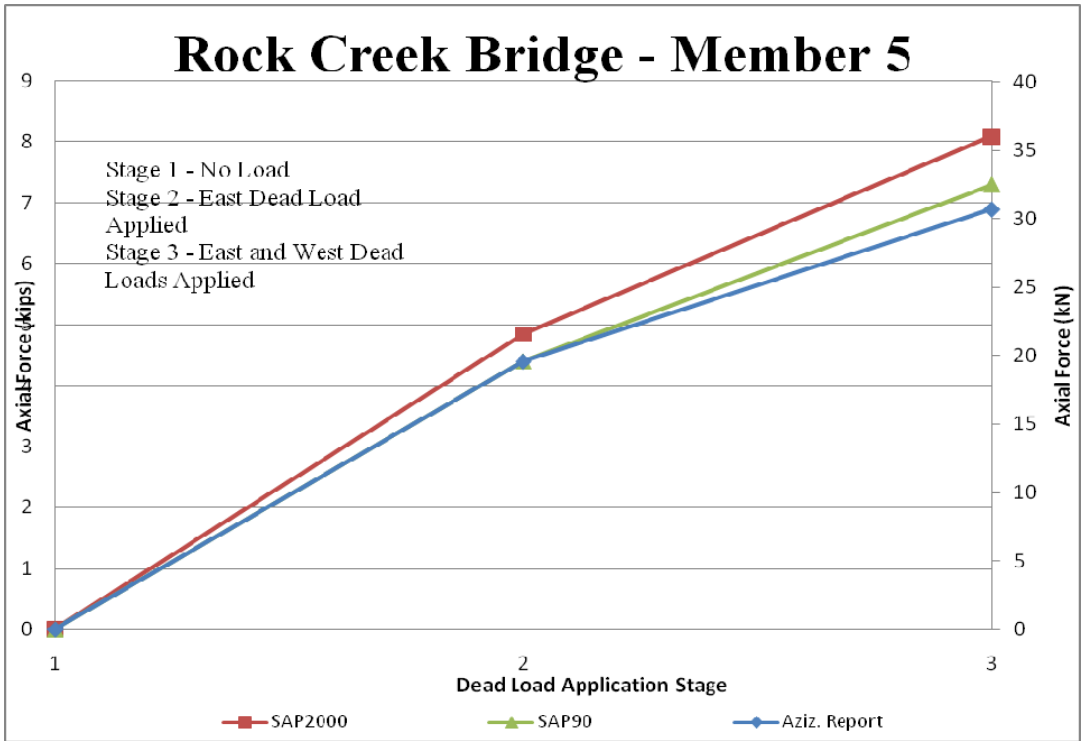

Figure **A4.5** –Axial Force in Member 5, Rock Creek Bridge

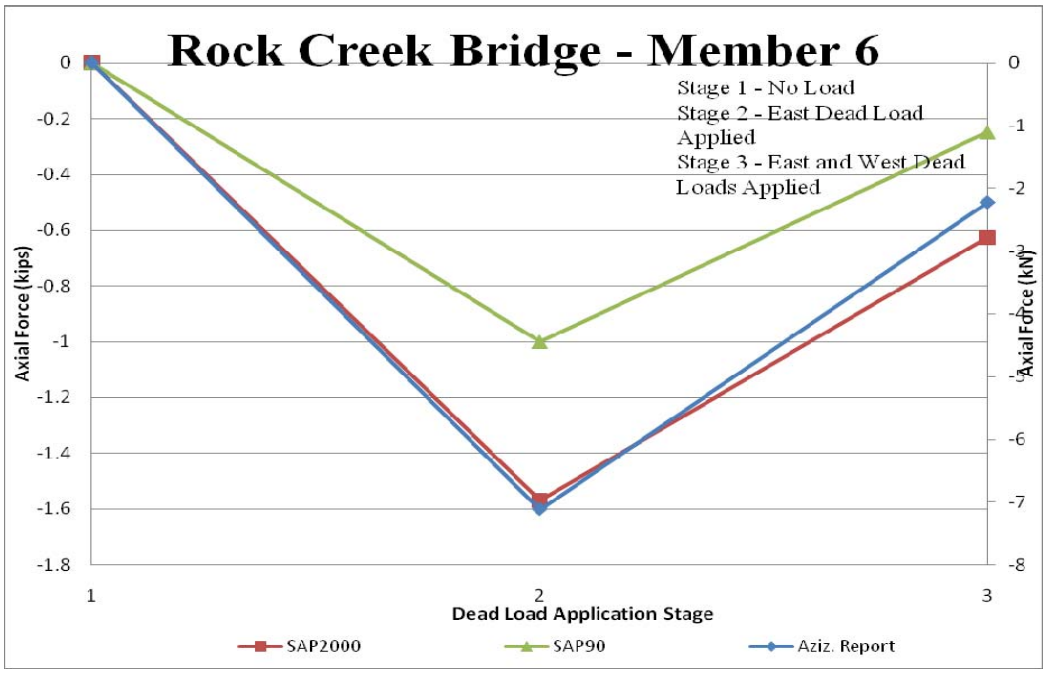

Figure **A4.6** – Axial Force in Member 6, Rock Creek Bridge

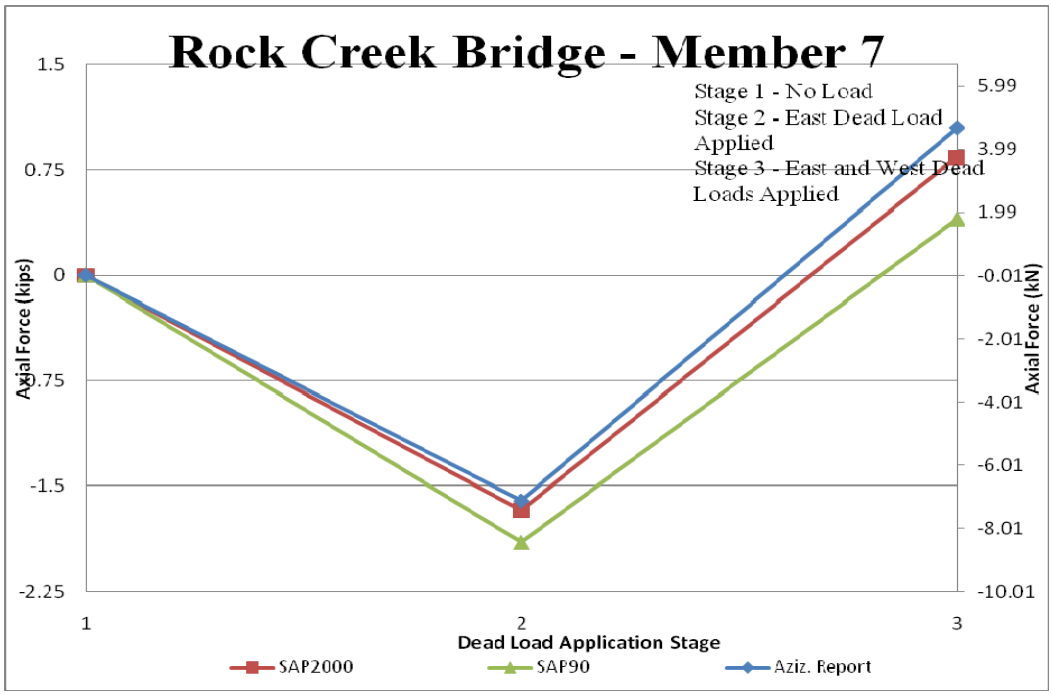

Figure **A4.7** –Axial Force in Member 7, Rock Creek Bridge

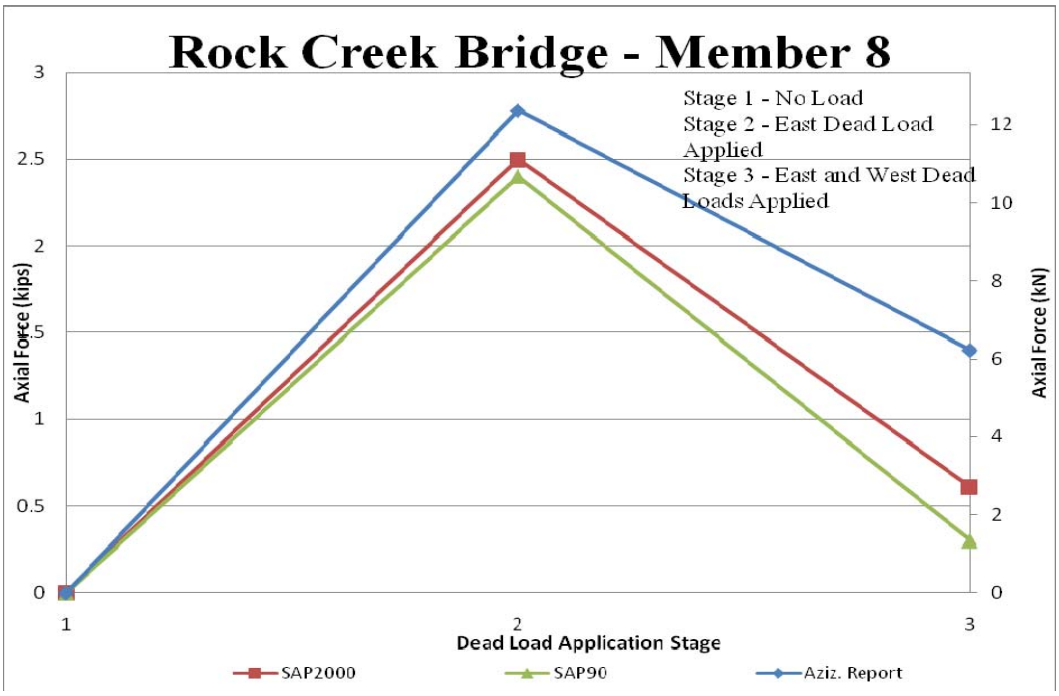

Figure **A4.8** – Axial Force in Member 8, Rock Creek Bridge

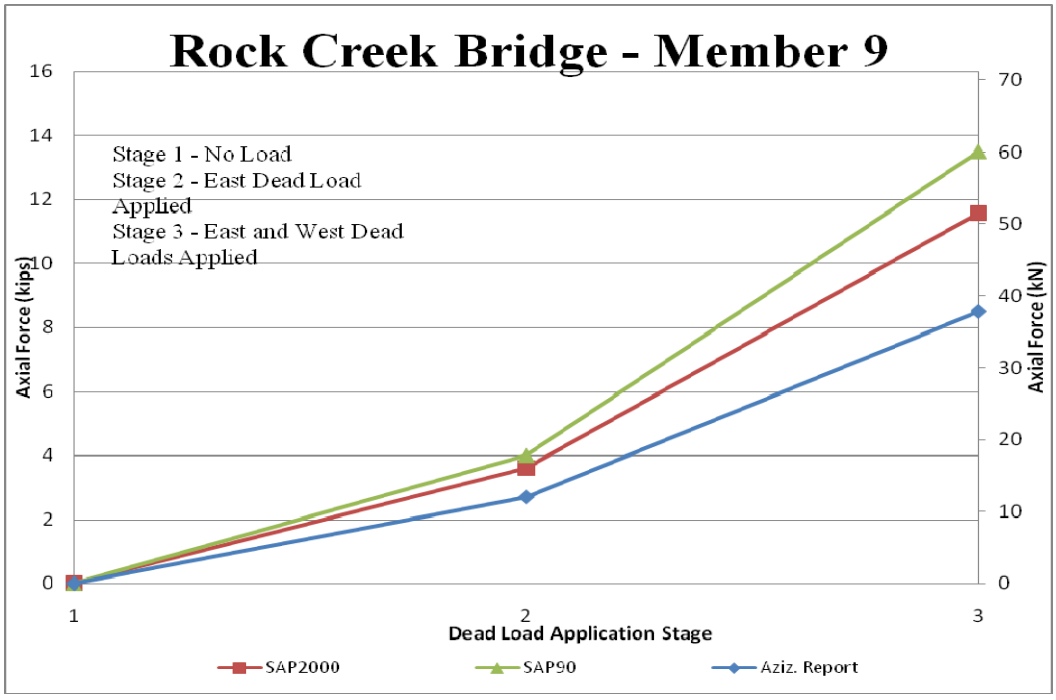

Figure **A4.9** –Axial Force in Member 9, Rock Creek Bridge

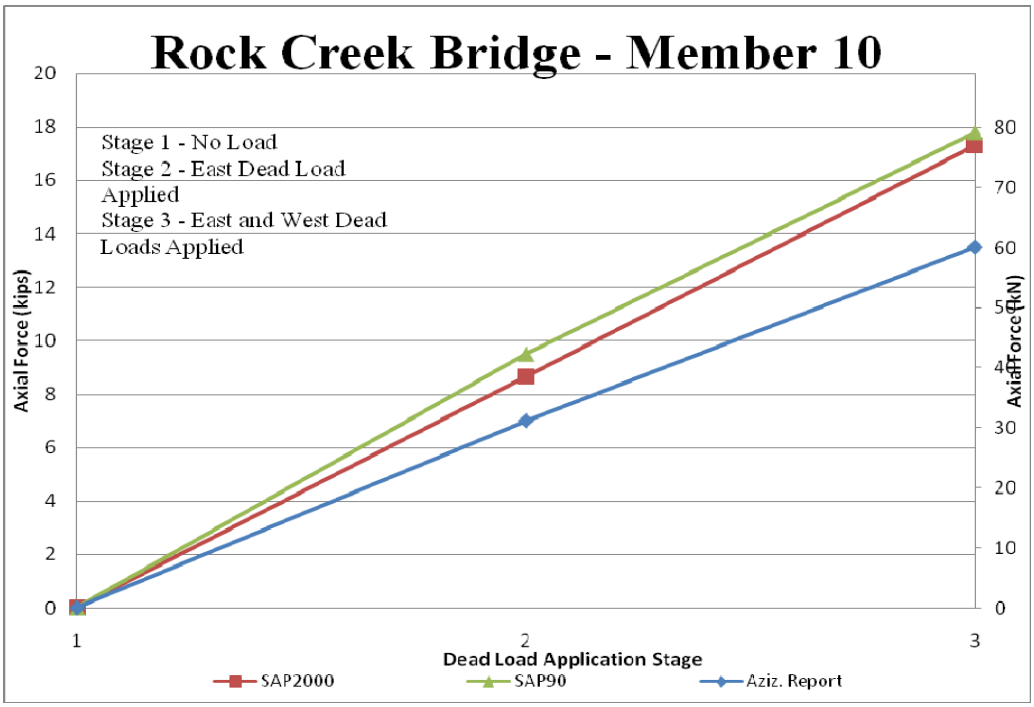

Figure **A4.10** –Axial Force in Member 10, Rock Creek Bridge

Appendix B

Tables

Member ID	Self Weight kN (kips)	1 Truck kN (kips)	2 Truck kN (kips)	3 Truck kN (kips)	4 Truck kN (kips)	5 Truck kN (kips)	6 Truck kN (kips)	7 Truck kN (kips)	8 Truck kN (kips)
1001	-394.52 -88.66	-399.70 -89.82	-799.41 -179.64	-1199.11 -269.46	-1598.81 -359.28	-1998.52 -449.11	-2398.22 -538.93	-2797.92 -628.75	-3197.63 -718.57
1002	-375.62 -84.41	-387.10 -86.99	-774.20 -173.98	-1161.30 -260.97	-1548.40 -347.96	-1935.51 -434.95	-2322.61 -521.93	-2709.71 -608.92	-3096.81 -695.91
1003	-390.28 -87.70	-422.87 -95.03	-845.75 -190.06	-1268.62 -285.08	-1691.50 -380.11	-2114.37 -475.14	-2537.25 -570.17	-2960.12 -665.20	-3383.00 -760.22
1004	-452.92 -101.78	-478.82 -107.60	-957.63 -215.20	-1436.45 -322.80	-1915.26 -430.40	-2394.08 -538.00	-2872.89 -645.59	-3351.71 -753.19	-3830.52 -860.79
1005	-452.96 -101.79	-464.85 -104.46	-929.69 -208.92	-1394.54 -313.38	-1859.39 -417.84	-2324.24 -522.30	-2789.08 -626.76	-3253.93 -731.22	-3718.78 -835.68
1006	-459.31 -103.22	-478.71 -107.58	-957.43 -215.15	-1436.14 -322.73	-1914.85 -430.30	-2393.57 -537.88	-2872.28 -645.46	-3350.99 -753.03	-3829.71 -860.61
1008	-390.39 -87.73	-399.87 -89.86	-799.75 -179.72	-1199.62 -269.58	-1599.49 -359.44	-1999.36 -449.30	-2399.24 -539.15	-2799.11 -629.01	-3198.98 -718.87
1009	-377.37 -84.80	-395.99 -88.99	-791.98 -177.97	-1187.98 -266.96	-1583.97 -355.95	-1979.96 -444.94	-2375.95 -533.92	-2771.95 -622.91	-3167.94 -711.90
1010	-417.22 -93.76	-413.22 -92.86	-826.44 -185.72	-1239.65 -278.57	-1652.87 -371.43	-2066.09 -464.29	-2479.31 -557.15	-2892.53 -650.01	-3305.74 -742.86

Table **B5-1**. Axial Force in North Truss Members for Self Weight and Truck Loading

Member ID	Self Weight kN (kips)	1 Truck kN (kips)	2 Truck kN (kips)	3 Truck kN (kips)	4 Truck kN (kips)	5 Truck kN (kips)	6 Truck kN (kips)	7 Truck kN (kips)	8 Truck kN (kips)
1011	54.84	218.50	437.00	655.50	874.00	1092.50	1311.00	1529.50	1748.00
	12.32	49.10	98.20	147.30	196.40	245.51	294.61	343.71	392.81
1012	234.09	308.50	617.00	925.50	1234.00	1542.50	1851.00	2159.50	2468.01
	52.61	69.33	138.65	207.98	277.30	346.63	415.96	485.28	554.61
1013	-121.56	-176.46	-352.91	-529.37	-705.82	-882.28	-1058.74	-1235.19	-1411.65
	-27.32	-39.65	-79.31	-118.96	-158.61	-198.27	-237.92	-277.57	-317.22
1014	108.38	223.39	446.77	670.16	893.54	1116.93	1340.31	1563.70	1787.08
	24.35	50.20	100.40	150.60	200.80	251.00	301.19	351.39	401.59
1015	-27.21	71.48	142.97	214.45	285.94	357.42	428.91	500.39	571.88
	-6.11	16.06	32.13	48.19	64.26	80.32	96.38	112.45	128.51
1016	-10.64	86.03	172.06	258.10	344.13	430.16	516.19	602.22	688.25
	-2.39	19.33	38.67	58.00	77.33	96.67	116.00	135.33	154.66
1017	-14.15	77.75	155.50	233.25	311.00	388.75	466.50	544.25	622.00
	-3.18	17.47	34.94	52.42	69.89	87.36	104.83	122.30	139.78
1018	-31.82	-67.03	-134.07	-201.10	-268.14	-335.17	-402.21	-469.24	-536.28
	-7.15	-15.06	-30.13	-45.19	-60.26	-75.32	-90.38	-105.45	-120.51
1019	115.09	238.62	477.24	715.87	954.49	1193.11	1431.73	1670.36	1908.98
	25.86	53.62	107.25	160.87	214.49	268.12	321.74	375.36	428.98

Table **B5-2**. Axial Force in North Truss Members for Self Weight and Truck Loading

Member ID	Self Weight kN (kips)	1 Truck kN (kips)	2 Truck kN (kips)	3 Truck kN (kips)	4 Truck kN (kips)	5 Truck kN (kips)	6 Truck kN (kips)	7 Truck kN (kips)	8 Truck kN (kips)
1020	-129.79	-186.95	-373.90	-560.85	-747.80	-934.74	-1121.69	-1308.64	-1495.59
	-29.17	-42.01	-84.02	-126.03	-168.04	-210.06	-252.07	-294.08	-336.09
1021	237.32	308.85	617.70	926.54	1235.39	1544.24	1853.09	2161.93	2470.78
	53.33	69.40	138.81	208.21	277.62	347.02	416.42	485.83	555.23
1022	42.82	233.43	466.86	700.29	933.72	1167.15	1400.58	1634.00	1867.43
	9.62	52.46	104.91	157.37	209.82	262.28	314.74	367.19	419.65
1023	209.92	219.06	438.13	657.19	876.26	1095.32	1314.39	1533.45	1752.52
	47.17	49.23	98.46	147.68	196.91	246.14	295.37	344.60	393.82
1024	173.15	189.30	378.60	567.90	757.19	946.49	1135.79	1325.09	1514.39
	38.91	42.54	85.08	127.62	170.16	212.70	255.23	297.77	340.31
1025	284.36	321.28	642.55	963.83	1285.11	1606.38	1927.66	2248.94	2570.21
	63.90	72.20	144.39	216.59	288.79	360.99	433.18	505.38	577.58
1026	344.18	359.70	719.40	1079.11	1438.81	1798.51	2158.21	2517.92	2877.62
	77.34	80.83	161.66	242.50	323.33	404.16	484.99	565.82	646.66
1027	275.16	303.01	606.02	909.03	1212.04	1515.05	1818.06	2121.07	2424.08
	61.83	68.09	136.18	204.28	272.37	340.46	408.55	476.64	544.74
1028	159.59	182.01	364.01	546.02	728.02	910.03	1092.03	1274.04	1456.04
	35.86	40.90	81.80	122.70	163.60	204.50	245.40	286.30	327.20
1029	180.45	204.93	409.85	614.78	819.71	1024.63	1229.56	1434.49	1639.42
	40.55	46.05	92.10	138.15	184.20	230.26	276.31	322.36	368.41

Table **B5-3**. Axial Force in North Truss Members for Self Weight and Truck Loading

Member ID	Self Weight kN (kips)	1 Truck kN (kips)	2 Truck kN (kips)	3 Truck kN (kips)	4 Truck kN (kips)	5 Truck kN (kips)	6 Truck kN (kips)	7 Truck kN (kips)	8 Truck kN (kips)
1030	-416.53 -93.60	-404.20 -90.83	-808.40 -181.66	-1212.61 -272.50	-1616.81 -363.33	-2021.01 -454.16	-2425.21 -544.99	-2829.42 -635.82	-3233.62 -726.66
1031	-387.74 -87.13	-399.04 -89.67	-798.07 -179.34	-1197.11 -269.01	-1596.14 -358.68	-1995.18 -448.36	-2394.22 -538.03	-2793.25 -627.70	-3192.29 -717.37
1032	-386.95 -86.96	-399.28 -89.73	-798.55 -179.45	-1197.83 -269.18	-1597.11 -358.90	-1996.38 -448.63	-2395.66 -538.35	-2794.93 -628.08	-3194.21 -717.80
1033	-452.99 -101.80	-474.73 -106.68	-949.46 -213.36	-1424.19 -320.04	-1898.92 -426.72	-2373.65 -533.41	-2848.38 -640.09	-3323.11 -746.77	-3797.84 -853.45
1034	-445.23 -100.05	-461.95 -103.81	-923.89 -207.62	-1385.84 -311.42	-1847.78 -415.23	-2309.73 -519.04	-2771.67 -622.85	-3233.62 -726.66	-3695.56 -830.46
1035	-444.39 -99.86	-476.56 -107.09	-953.12 -214.18	-1429.68 -321.28	-1906.24 -428.37	-2382.80 -535.46	-2859.36 -642.55	-3335.92 -749.64	-3812.48 -856.74
1036	-379.44 -85.27	-415.48 -93.37	-830.96 -186.73	-1246.44 -280.10	-1661.91 -373.46	-2077.39 -466.83	-2492.87 -560.20	-2908.35 -653.56	-3323.83 -746.93
1037	-357.86 -80.42	-384.61 -86.43	-769.22 -172.86	-1153.83 -259.29	-1538.44 -345.72	-1923.05 -432.15	-2307.65 -518.57	-2692.26 -605.00	-3076.87 -691.43
1038	-376.87 -84.69	-398.99 -89.66	-797.97 -179.32	-1196.96 -268.98	-1595.95 -358.64	-1994.94 -448.30	-2393.92 -537.96	-2792.91 -627.62	-3191.90 -717.28

Table **B5-4**. Axial Force in South Truss Members for Self Weight and Truck Loading

Member ID	Self Weight kN (kips)	1 Truck kN (kips)	2 Truck kN (kips)	3 Truck kN (kips)	4 Truck kN (kips)	5 Truck kN (kips)	6 Truck kN (kips)	7 Truck kN (kips)	8 Truck kN (kips)
1039	59.38 13.34	225.82 50.75	451.63 101.49	677.45 152.24	903.26 202.98	1129.08 253.73	1354.89 304.47	1580.71 355.22	1806.52 405.96
1040	230.22 51.74	302.16 67.90	604.31 135.80	906.47 203.70	1208.62 271.60	1510.78 339.50	1812.93 407.40	2115.09 475.30	2417.24 543.20
1041	-126.60 -28.45	-181.52 -40.79	-363.04 -81.58	-544.56 -122.37	-726.08 -163.16	-907.60 -203.96	-1089.12 -244.75	-1270.64 -285.54	-1452.16 -326.33
1042	110.60 24.85	231.67 52.06	463.34 104.12	695.01 156.18	926.69 208.24	1158.36 260.31	1390.03 312.37	1621.70 364.43	1853.37 416.49
1043	-29.97 -6.74	63.62 14.30	127.24 28.59	190.86 42.89	254.49 57.19	318.11 71.49	381.73 85.78	445.35 100.08	508.97 114.38
1044	-11.77 -2.64	76.48 17.19	152.96 34.37	229.43 51.56	305.91 68.74	382.39 85.93	458.87 103.12	535.34 120.30	611.82 137.49
1045	-12.68 -2.85	-81.03 -18.21	-162.06 -36.42	-243.09 -54.63	-324.12 -72.84	-405.15 -91.05	-486.18 -109.25	-567.21 -127.46	-648.24 -145.67
1046	-28.60 -6.43	68.00 15.28	135.99 30.56	203.99 45.84	271.98 61.12	339.98 76.40	407.98 91.68	475.97 106.96	543.97 122.24
1047	112.68 25.32	220.99 49.66	441.98 99.32	662.97 148.98	883.97 198.64	1104.96 248.31	1325.95 297.97	1546.94 347.63	1767.93 397.29
1048	-125.16 -28.13	-173.91 -39.08	-347.83 -78.16	-521.74 -117.25	-695.66 -156.33	-869.57 -195.41	-1043.49 -234.49	-1217.40 -273.57	-1391.32 -312.66

Table **B5-5**. Axial Force in South Truss Members for Self Weight and Truck Loading

Member ID	Self Weight kN (kips)	1 Truck kN (kips)	2 Truck kN (kips)	3 Truck kN (kips)	4 Truck kN (kips)	5 Truck kN (kips)	6 Truck kN (kips)	7 Truck kN (kips)	8 Truck kN (kips)
1049	233.13 52.39	307.26 69.05	614.52 138.09	921.78 207.14	1229.04 276.19	1536.30 345.24	1843.55 414.28	2150.81 483.33	2458.07 552.38
1050	40.09 9.01	207.22 46.57	414.44 93.13	621.66 139.70	828.87 186.26	1036.09 232.83	1243.31 279.40	1450.53 325.96	1657.75 372.53
1051	201.56 45.30	200.84 45.13	401.67 90.26	602.51 135.40	803.35 180.53	1004.19 225.66	1205.02 270.79	1405.86 315.92	1606.70 361.06
1052	167.46 37.63	178.49 40.11	356.98 80.22	535.47 120.33	713.96 160.44	892.45 200.55	1070.94 240.66	1249.43 280.77	1427.92 320.88
1053	275.91 62.00	301.06 67.66	602.13 135.31	903.19 202.97	1204.26 270.62	1505.32 338.28	1806.39 405.93	2107.45 473.59	2408.52 541.24
1054	339.76 76.35	356.46 80.10	712.92 160.21	1069.38 240.31	1425.83 320.41	1782.29 400.52	2138.75 480.62	2495.21 560.72	2851.67 640.82
1055	277.52 62.37	315.49 70.90	630.98 141.79	946.47 212.69	1261.97 283.59	1577.46 354.49	1892.95 425.38	2208.44 496.28	2523.93 567.18
1056	160.73 36.12	186.02 41.80	372.05 83.61	558.07 125.41	744.09 167.21	930.12 209.02	1116.14 250.82	1302.16 292.62	1488.19 334.42
1057	192.12 43.17	219.64 49.36	439.29 98.72	658.93 148.07	878.57 197.43	1098.22 246.79	1317.86 296.15	1537.50 345.51	1757.14 394.86

Table **B5-6**. Axial Force in South Truss Members for Self Weight and Truck Loading

Member ID	1 Truck MPa (ksi)	2 Truck MPa (ksi)	3 Truck MPa (ksi)	4 Truck MPa (ksi)	5 Truck MPa (ksi)	6 Truck MPa (ksi)	7 Truck MPa (ksi)	8 Truck MPa (ksi)
1030	-31.8 -4.61	-47.4 -6.89	-63.1 -9.16	-78.7 -11.43	-94.4 -13.70	-110.1 -15.97	-125.7 -18.24	-141.4 -20.52
1031	-30.5 -4.42	-45.9 -6.67	-61.4 -8.91	-76.8 -11.15	-92.3 -13.39	-107.7 -15.64	-123.2 -17.88	-138.6 -20.12
1032	-33.5 -4.86	-50.5 -7.32	-67.5 -9.79	-84.5 -12.26	-101.5 -14.73	-118.5 -17.19	-135.5 -19.66	-152.5 -22.13
1033	-33.0 -4.78	-49.8 -7.23	-66.7 -9.68	-83.6 -12.13	-100.4 -14.58	-117.3 -17.02	-134.2 -19.47	-151.0 -21.92
1034	-32.2 -4.68	-48.6 -7.06	-65.1 -9.44	-81.5 -11.82	-97.9 -14.21	-114.3 -16.59	-130.7 -18.97	-147.1 -21.35
1035	-32.7 -4.75	-49.7 -7.21	-66.6 -9.66	-83.5 -12.12	-100.4 -14.58	-117.4 -17.04	-134.3 -19.49	-151.2 -21.95
1036	-33.8 -4.91	-51.5 -7.48	-69.2 -10.05	-86.9 -12.61	-104.6 -15.18	-122.3 -17.75	-140.0 -20.31	-157.7 -22.88
1037	-28.8 -4.17	-43.6 -6.34	-58.5 -8.50	-73.4 -10.66	-88.3 -12.82	-103.2 -14.98	-118.1 -17.14	-133.0 -19.31
1038	-30.0 -4.36	-45.5 -6.60	-61.0 -8.85	-76.4 -11.09	-91.9 -13.33	-107.3 -15.57	-122.8 -17.82	-138.2 -20.06
1039	28.9 4.19	51.7 7.51	74.6 10.83	97.5 14.15	120.3 17.47	143.2 20.79	166.1 24.10	188.9 27.42

Table **B5-7**. Total Stress in South Truss Members Due to Self Weight and HS-20 Trucks

Member ID	1 Truck MPa (ksi)	2 Truck MPa (ksi)	3 Truck MPa (ksi)	4 Truck MPa (ksi)	5 Truck MPa (ksi)	6 Truck MPa (ksi)	7 Truck MPa (ksi)	8 Truck MPa (ksi)
1040	43.7 6.35	68.5 9.95	93.4 13.55	118.2 17.15	143.0 20.76	167.8 24.36	192.6 27.96	217.5 31.56
1041	-25.4 -3.68	-40.3 -5.85	-55.3 -8.02	-70.2 -10.19	-85.2 -12.36	-100.1 -14.53	-115.1 -16.70	-130.0 -18.87
1042	34.7 5.03	58.2 8.44	81.6 11.85	105.1 15.26	128.6 18.66	152.1 22.07	175.5 25.48	199.0 28.88
1043	2.8 0.40	8.0 1.16	13.3 1.92	18.5 2.68	23.7 3.44	29.0 4.20	34.2 4.97	39.4 5.73
1044	12.3 1.79	26.9 3.90	41.5 6.02	56.0 8.13	70.6 10.24	85.1 12.36	99.7 14.47	114.3 16.59
1045	-17.8 -2.59	-33.3 -4.83	-48.7 -7.07	-64.1 -9.31	-79.6 -11.55	-95.0 -13.79	-110.4 -16.03	-125.9 -18.27
1046	3.2 0.47	8.8 1.28	14.4 2.10	20.0 2.91	25.6 3.72	31.2 4.53	36.8 5.35	42.4 6.16
1047	33.8 4.91	56.2 8.16	78.6 11.41	101.0 14.66	123.4 17.91	145.8 21.16	168.2 24.41	190.6 27.66
1048	-24.6 -3.57	-39.0 -5.65	-53.3 -7.73	-67.6 -9.81	-81.9 -11.89	-96.2 -13.97	-110.6 -16.05	-124.9 -18.13

Table **B5-8**. Total Stress in South Truss Members Due to Self Weight and HS-20 Trucks

Member ID	1 Truck MPa (ksi)	2 Truck MPa (ksi)	3 Truck MPa (ksi)	4 Truck MPa (ksi)	5 Truck MPa (ksi)	6 Truck MPa (ksi)	7 Truck MPa (ksi)	8 Truck MPa (ksi)
1049	44.4	69.6	94.9	120.1	145.3	170.6	195.8	221.1
	6.44	10.11	13.77	17.43	21.09	24.76	28.42	32.08
1050	25.1	46.1	67.1	88.1	109.0	130.0	151.0	172.0
	3.64	6.68	9.73	12.78	15.83	18.87	21.92	24.97
1051	16.4	24.5	32.7	40.9	49.0	57.2	65.4	73.5
	2.37	3.56	4.75	5.93	7.12	8.30	9.49	10.67
1052	14.1	21.3	28.6	35.8	43.1	50.4	57.6	64.9
	2.04	3.10	4.15	5.20	6.26	7.31	8.36	9.42
1053	23.5	35.7	47.9	60.2	72.4	84.7	96.9	109.2
	3.41	5.18	6.96	8.74	10.51	12.29	14.07	15.84
1054	24.8	37.5	50.2	62.9	75.6	88.3	101.0	113.7
	3.60	5.44	7.28	9.13	10.97	12.81	14.66	16.50
1055	24.1	36.9	49.8	62.6	75.4	88.3	101.1	113.9
	3.50	5.36	7.22	9.09	10.95	12.81	14.67	16.53
1056	14.1	21.7	29.2	36.8	44.4	51.9	59.5	67.1
	2.05	3.14	4.24	5.34	6.44	7.54	8.63	9.73
1057	16.7	25.7	34.6	43.5	52.5	61.4	70.3	79.3
	2.43	3.73	5.02	6.32	7.62	8.91	10.21	11.50

Table **B5-9**. Total Stress in South Truss Members Due to Self Weight and HS-20 Trucks

Member ID	Self Weight kN (kips)	1 Truck kN (kips)	2 Truck kN (kips)	3 Truck kN (kips)	4 Truck kN (kips)	5 Truck kN (kips)	6 Truck kN (kips)	7 Truck kN (kips)
1001	-375.85	-400.63	-801.26	-1201.9	-1602.5	-2003.1	-2403.8	-2804.4
	-84.46	-90.03	-180.06	-270.09	-360.12	-450.15	-540.17	-630.20
1002	-359.56	-391.45	-782.91	-1174.4	-1565.8	-1957.3	-2348.7	-2740.2
	-80.80	-87.97	-175.93	-263.90	-351.87	-439.84	-527.80	-615.77
1003	-372.11	-424.71	-849.42	-1274.1	-1698.8	-2123.5	-2548.2	-2973
	-83.62	-95.44	-190.88	-286.32	-381.76	-477.20	-572.64	-668.08
1004	-432.95	-480.86	-961.73	-1442.6	-1923.5	-2404.3	-2885.2	-3366
	-97.29	-108.06	-216.12	-324.18	-432.24	-540.30	-648.35	-756.41
1005	-434.77	-468.35	-936.71	-1405.1	-1873.4	-2341.8	-2810.1	-3278.5
	-97.70	-105.25	-210.50	-315.74	-420.99	-526.24	-631.49	-736.74
1006	-441.11	-479.66	-959.31	-1439	-1918.6	-2398.3	-2877.9	-3357.6
	-99.13	-107.79	-215.58	-323.36	-431.15	-538.94	-646.73	-754.52
1008	-376.46	-400.82	-801.64	-1202.5	-1603.3	-2004.1	-2404.9	-2805.7
	-84.60	-90.07	-180.14	-270.22	-360.29	-450.36	-540.43	-630.50
1009	-380.52	-396.39	-792.78	-1189.2	-1585.6	-1981.9	-2378.3	-2774.7
	-85.51	-89.08	-178.15	-267.23	-356.30	-445.38	-534.46	-623.53
1010	-416.44	-415.07	-830.14	-1245.2	-1660.3	-2075.3	-2490.4	-2905.5
	-93.58	-93.27	-186.55	-279.82	-373.10	-466.37	-559.64	-652.92
1011	50.6677	218.428	436.857	655.285	873.713	1092.14	1310.57	1529
	11.39	49.09	98.17	147.26	196.34	245.43	294.51	343.60

Table **B5-10**. Axial Force in Deteriorated North Truss for Self Weight and HS-20 Trucks

Member ID	Self Weight kN (kips)	1 Truck kN (kips)	2 Truck kN (kips)	3 Truck kN (kips)	4 Truck kN (kips)	5 Truck kN (kips)	6 Truck kN (kips)	7 Truck kN (kips)
1012	219.919 49.42	309.587 69.57	619.173 139.14	928.76 208.71	1238.35 278.28	1547.93 347.85	1857.52 417.42	2167.11 486.99
1013	-114.11 -25.64	-177.1 -39.80	-354.19 -79.59	-531.29 -119.39	-708.39 -159.19	-885.48 -198.99	-1062.6 -238.78	-1239.7 -278.58
1014	105.999 23.82	223.764 50.28	447.528 100.57	671.291 150.85	895.055 201.14	1118.82 251.42	1342.58 301.70	1566.35 351.99
1015	-30.175 -6.78	66.3807 14.92	132.761 29.83	199.142 44.75	265.523 59.67	331.903 74.59	398.284 89.50	464.665 104.42
1016	-9.1448 -2.06	92.2396 20.73	184.479 41.46	276.719 62.18	368.958 82.91	461.198 103.64	553.438 124.37	645.677 145.10
1017	-10.698 -2.40	74.1014 16.65	148.203 33.30	222.304 49.96	296.406 66.61	370.507 83.26	444.608 99.91	518.71 116.56
1018	-32.894 -7.39	-71.863 -16.15	-143.73 -32.30	-215.59 -48.45	-287.45 -64.60	-359.32 -80.75	-431.18 -96.89	-503.04 -113.04
1019	107.748 24.21	236.927 53.24	473.854 106.48	710.781 159.73	947.708 212.97	1184.63 266.21	1421.56 319.45	1658.49 372.69
1020	-119.86 -26.93	-186.58 -41.93	-373.16 -83.86	-559.74 -125.78	-746.32 -167.71	-932.9 -209.64	-1119.5 -251.57	-1306.1 -293.50

Table **B5-11**. Axial Force in Deteriorated North Truss for Self Weight and HS-20 Trucks

Member ID	Self Weight kN (kips)	1 Truck kN (kips)	2 Truck kN (kips)	3 Truck kN (kips)	4 Truck kN (kips)	5 Truck kN (kips)	6 Truck kN (kips)	7 Truck kN (kips)
1021	218.909	309.974	619.947	929.921	1239.89	1549.87	1859.84	2169.82
	49.19	69.66	139.31	208.97	278.63	348.29	417.94	487.60
1022	55.8876	235.561	471.122	706.682	942.243	1177.8	1413.36	1648.93
	12.56	52.94	105.87	158.81	211.74	264.68	317.61	370.55
1023	191.283	223.457	446.914	670.37	893.827	1117.28	1340.74	1564.2
	42.99	50.22	100.43	150.65	200.86	251.08	301.29	351.51
1024	146.534	180.999	361.999	542.998	723.997	904.997	1086	1267
	32.93	40.67	81.35	122.02	162.70	203.37	244.04	284.72
1025	250.41	306.262	612.525	918.787	1225.05	1531.31	1837.57	2143.84
	56.27	68.82	137.65	206.47	275.29	344.12	412.94	481.76
1026	316.199	352.008	704.017	1056.03	1408.03	1760.04	2112.05	2464.06
	71.06	79.10	158.21	237.31	316.41	395.52	474.62	553.72
1027	248.368	289.704	579.408	869.112	1158.82	1448.52	1738.22	2027.93
	55.81	65.10	130.20	195.31	260.41	325.51	390.61	455.71
1028	160.258	172.202	344.403	516.605	688.807	861.008	1033.21	1205.41
	36.01	38.70	77.39	116.09	154.79	193.49	232.18	270.88
1029	203.285	200.174	400.349	600.523	800.697	1000.87	1201.05	1401.22
	45.68	44.98	89.97	134.95	179.93	224.92	269.90	314.88

Table **B5-12**. Axial Force in Deteriorated North Truss for Self Weight and HS-20 Trucks

Member ID	Self Weight kN (kips)	1 Truck kN (kips)	2 Truck kN (kips)	3 Truck kN (kips)	4 Truck kN (kips)	5 Truck kN (kips)	6 Truck kN (kips)	7 Truck kN (kips)
1030	-416.53 -93.60	-404.20 -90.83	-808.40 -181.66	-1212.61 -272.50	-1616.81 -363.33	-2021.01 -454.16	-2425.21 -544.99	-2829.42 -635.82
1031	-387.74 -87.13	-399.04 -89.67	-798.07 -179.34	-1197.11 -269.01	-1596.14 -358.68	-1995.18 -448.36	-2394.22 -538.03	-2793.25 -627.70
1032	-386.95 -86.96	-399.28 -89.73	-798.55 -179.45	-1197.83 -269.18	-1597.11 -358.90	-1996.38 -448.63	-2395.66 -538.35	-2794.93 -628.08
1033	-452.99 -101.80	-474.73 -106.68	-949.46 -213.36	-1424.19 -320.04	-1898.92 -426.72	-2373.65 -533.41	-2848.38 -640.09	-3323.11 -746.77
1034	-445.23 -100.05	-461.95 -103.81	-923.89 -207.62	-1385.84 -311.42	-1847.78 -415.23	-2309.73 -519.04	-2771.67 -622.85	-3233.62 -726.66
1035	-444.39 -99.86	-476.56 -107.09	-953.12 -214.18	-1429.68 -321.28	-1906.24 -428.37	-2382.80 -535.46	-2859.36 -642.55	-3335.92 -749.64
1036	-379.44 -85.27	-415.48 -93.37	-830.96 -186.73	-1246.44 -280.10	-1661.91 -373.46	-2077.39 -466.83	-2492.87 -560.20	-2908.35 -653.56
1037	-357.86 -80.42	-384.61 -86.43	-769.22 -172.86	-1153.83 -259.29	-1538.44 -345.72	-1923.05 -432.15	-2307.65 -518.57	-2692.26 -605.00
1038	-376.87 -84.69	-398.99 -89.66	-797.97 -179.32	-1196.96 -268.98	-1595.95 -358.64	-1994.94 -448.30	-2393.92 -537.96	-2792.91 -627.62

Table **B5-13**. Axial Force in Deteriorated South Truss for Self Weight and HS-20 Trucks

Member ID	Self Weight kN (kips)	1 Truck kN (kips)	2 Truck kN (kips)	3 Truck kN (kips)	4 Truck kN (kips)	5 Truck kN (kips)	6 Truck kN (kips)	7 Truck kN (kips)
1039	59.38 13.34	225.82 50.75	451.63 101.49	677.45 152.24	903.26 202.98	1129.08 253.73	1354.89 304.47	1580.71 355.22
1040	230.22 51.74	302.16 67.90	604.31 135.80	906.47 203.70	1208.62 271.60	1510.78 339.50	1812.93 407.40	2115.09 475.30
1041	-126.60 -28.45	-181.52 -40.79	-363.04 -81.58	-544.56 -122.37	-726.08 -163.16	-907.60 -203.96	-1089.12 -244.75	-1270.64 -285.54
1042	110.60 24.85	231.67 52.06	463.34 104.12	695.01 156.18	926.69 208.24	1158.36 260.31	1390.03 312.37	1621.70 364.43
1043	-29.97 -6.74	63.62 14.30	127.24 28.59	190.86 42.89	254.49 57.19	318.11 71.49	381.73 85.78	445.35 100.08
1044	-11.77 -2.64	76.48 17.19	152.96 34.37	229.43 51.56	305.91 68.74	382.39 85.93	458.87 103.12	535.34 120.30
1045	-12.68 -2.85	-81.03 -18.21	-162.06 -36.42	-243.09 -54.63	-324.12 -72.84	-405.15 -91.05	-486.18 -109.25	-567.21 -127.46
1046	-28.60 -6.43	68.00 15.28	135.99 30.56	203.99 45.84	271.98 61.12	339.98 76.40	407.98 91.68	475.97 106.96
1047	112.68 25.32	220.99 49.66	441.98 99.32	662.97 148.98	883.97 198.64	1104.96 248.31	1325.95 297.97	1546.94 347.63
1048	-125.16 -28.13	-173.91 -39.08	-347.83 -78.16	-521.74 -117.25	-695.66 -156.33	-869.57 -195.41	-1043.49 -234.49	-1217.40 -273.57

Table **B5-14**. Axial Force in Deteriorated South Truss for Self Weight and HS-20 Trucks

Member ID	Self Weight kN (kips)	1 Truck kN (kips)	2 Truck kN (kips)	3 Truck kN (kips)	4 Truck kN (kips)	5 Truck kN (kips)	6 Truck kN (kips)	7 Truck kN (kips)
1049	233.13 52.39	307.26 69.05	614.52 138.09	921.78 207.14	1229.04 276.19	1536.30 345.24	1843.55 414.28	2150.81 483.33
1050	40.09 9.01	207.22 46.57	414.44 93.13	621.66 139.70	828.87 186.26	1036.09 232.83	1243.31 279.40	1450.53 325.96
1051	201.56 45.30	200.84 45.13	401.67 90.26	602.51 135.40	803.35 180.53	1004.19 225.66	1205.02 270.79	1405.86 315.92
1052	167.46 37.63	178.49 40.11	356.98 80.22	535.47 120.33	713.96 160.44	892.45 200.55	1070.94 240.66	1249.43 280.77
1053	275.91 62.00	301.06 67.66	602.13 135.31	903.19 202.97	1204.26 270.62	1505.32 338.28	1806.39 405.93	2107.45 473.59
1054	339.76 76.35	356.46 80.10	712.92 160.21	1069.38 240.31	1425.83 320.41	1782.29 400.52	2138.75 480.62	2495.21 560.72
1055	277.52 62.37	315.49 70.90	630.98 141.79	946.47 212.69	1261.97 283.59	1577.46 354.49	1892.95 425.38	2208.44 496.28
1056	160.73 36.12	186.02 41.80	372.05 83.61	558.07 125.41	744.09 167.21	930.12 209.02	1116.14 250.82	1302.16 292.62
1057	192.12 43.17	219.64 49.36	439.29 98.72	658.93 148.07	878.57 197.43	1098.22 246.79	1317.86 296.15	1537.50 345.51

Table **B5-15**. Axial Force in Deteriorated South Truss for Self Weight and HS-20 Trucks

Member ID	1 Truck MPa (ksi)	2 Truck MPa (ksi)	3 Truck MPa (ksi)	4 Truck MPa (ksi)	5 Truck MPa (ksi)	6 Truck MPa (ksi)	7 Truck MPa (ksi)
1030	-31.8 -4.61	-47.4 -6.89	-63.1 -9.16	-78.7 -11.43	-94.4 -13.70	-110.1 -15.97	-125.7 -18.24
1031	-30.5 -4.42	-45.9 -6.67	-61.4 -8.91	-76.8 -11.15	-92.3 -13.39	-107.7 -15.64	-123.2 -17.88
1032	-33.5 -4.86	-50.5 -7.32	-67.5 -9.79	-84.5 -12.26	-101.5 -14.73	-118.5 -17.19	-135.5 -19.66
1033	-33.0 -4.78	-49.8 -7.23	-66.7 -9.68	-83.6 -12.13	-100.4 -14.58	-117.3 -17.02	-134.2 -19.47
1034	-32.2 -4.68	-48.6 -7.06	-65.1 -9.44	-81.5 -11.82	-97.9 -14.21	-114.3 -16.59	-130.7 -18.97
1035	-32.7 -4.75	-49.7 -7.21	-66.6 -9.66	-83.5 -12.12	-100.4 -14.58	-117.4 -17.04	-134.3 -19.49
1036	-33.8 -4.91	-51.5 -7.48	-69.2 -10.05	-86.9 -12.61	-104.6 -15.18	-122.3 -17.75	-140.0 -20.31
1037	-28.8 -4.17	-43.6 -6.34	-58.5 -8.50	-73.4 -10.66	-88.3 -12.82	-103.2 -14.98	-118.1 -17.14
1038	-30.0 -4.36	-45.5 -6.60	-61.0 -8.85	-76.4 -11.09	-91.9 -13.33	-107.3 -15.57	-122.8 -17.82
1039	28.9 4.19	51.7 7.51	74.6 10.83	97.5 14.15	120.3 17.47	143.2 20.79	166.1 24.10

Table **B5-16**. Stresses in Deteriorated South Truss for Self Weight and HS-20 Trucks

Member ID	1 Truck MPa (ksi)	2 Truck MPa (ksi)	3 Truck MPa (ksi)	4 Truck MPa (ksi)	5 Truck MPa (ksi)	6 Truck MPa (ksi)	7 Truck MPa (ksi)
1040	43.7 6.35	68.5 9.95	93.4 13.55	118.2 17.15	143.0 20.76	167.8 24.36	192.6 27.96
1041	-25.4 -3.68	-40.3 -5.85	-55.3 -8.02	-70.2 -10.19	-85.2 -12.36	-100.1 -14.53	-115.1 -16.70
1042	34.7 5.03	58.2 8.44	81.6 11.85	105.1 15.26	128.6 18.66	152.1 22.07	175.5 25.48
1043	2.8 0.40	8.0 1.16	13.3 1.92	18.5 2.68	23.7 3.44	29.0 4.20	34.2 4.97
1044	12.3 1.79	26.9 3.90	41.5 6.02	56.0 8.13	70.6 10.24	85.1 12.36	99.7 14.47
1045	-17.8 -2.59	-33.3 -4.83	-48.7 -7.07	-64.1 -9.31	-79.6 -11.55	-95.0 -13.79	-110.4 -16.03
1046	3.2 0.47	8.8 1.28	14.4 2.10	20.0 2.91	25.6 3.72	31.2 4.53	36.8 5.35
1047	33.8 4.91	56.2 8.16	78.6 11.41	101.0 14.66	123.4 17.91	145.8 21.16	168.2 24.41
1048	-24.6 -3.57	-39.0 -5.65	-53.3 -7.73	-67.6 -9.81	-81.9 -11.89	-96.2 -13.97	-110.6 -16.05

Table **B5-17**. Stresses in Deteriorated South Truss for Self Weight and HS-20 Trucks

Member ID	1 Truck MPa (ksi)	2 Truck MPa (ksi)	3 Truck MPa (ksi)	4 Truck MPa (ksi)	5 Truck MPa (ksi)	6 Truck MPa (ksi)	7 Truck MPa (ksi)
1049	44.4	69.6	94.9	120.1	145.3	170.6	195.8
	6.44	10.11	13.77	17.43	21.09	24.76	28.42
1050	25.1	46.1	67.1	88.1	109.0	130.0	151.0
	3.64	6.68	9.73	12.78	15.83	18.87	21.92
1051	16.4	24.5	32.7	40.9	49.0	57.2	65.4
	2.37	3.56	4.75	5.93	7.12	8.30	9.49
1052	14.1	21.3	28.6	35.8	43.1	50.4	57.6
	2.04	3.10	4.15	5.20	6.26	7.31	8.36
1053	23.5	35.7	47.9	60.2	72.4	84.7	96.9
	3.41	5.18	6.96	8.74	10.51	12.29	14.07
1054	24.8	37.5	50.2	62.9	75.6	88.3	101.0
	3.60	5.44	7.28	9.13	10.97	12.81	14.66
1055	24.1	36.9	49.8	62.6	75.4	88.3	101.1
	3.50	5.36	7.22	9.09	10.95	12.81	14.67
1056	14.1	21.7	29.2	36.8	44.4	51.9	59.5
	2.05	3.14	4.24	5.34	6.44	7.54	8.63
1057	16.7	25.7	34.6	43.5	52.5	61.4	70.3
	2.43	3.73	5.02	6.32	7.62	8.91	10.21

Table **B5-18**. Stresses in Deteriorated South Truss for Self Weight and HS-20 Trucks